High Spatial Resolution Diffusion-Weighted Imaging (DWI) of Ischemic Stroke and Transient Ischemic Attack (TIA)

by

Kyle Todd Hafermehl

A thesis submitted in partial fulfillment of the requirements for the degree of

Master of Science

Centre for Neuroscience
University of Alberta

Abstract

Diffusion-weighted imaging (DWI) is the most sensitive imaging technique available to identify ischemic lesions. This magnetic resonance imaging (MRI) technique exploits (non-invasively and in a short scan time) early changes to water mobility caused by metabolic failure of neurons by tagging water molecules and tracking their movement, enabling DWI to detect diffusion restriction (interpreted to indicate infarction in ischemic stroke) within minutes of symptom manifestation. Ischemic stroke and transient ischemic attack are an increasingly diagnosed affliction of the cerebrovascular system causing both death and loss of independence, relying on the utilization of neuroimaging to assist in identification of infarctions and probable etiology in order to initiate the most effective treatment path. But clinical DWI is still obtained using resolution that is insufficient to identify small ischemic lesions in minor ischemic stroke and transient ischemic attack (TIA).

The experiment within this thesis utilized high spatial resolution DWI sequence to detect ischemic lesions present within acute ischemic stroke and transient ischemic attack patients (n = 48). The decreased voxel size (4.7T, 3.4 mm^3; 1.5T, 4.5 mm^3; 3.0T, 3.4 mm^3) and slice thickness (4.7T, 1.5 mm; 1.5T, 2 mm; 3.0T, 1.5 mm) was achieved at the expense of additional time (4.7T, 210 s; 1.5T, 293 s; 3.0T, 259 s) and incorporated into the stroke protocol on 1.5T, 3T and 4.7T magnetic field strength scanners. Ischemic lesions were identified on the high resolution DWI (n = 94) that remained undetected on lower spatial resolution DWI (n = 65) typically utilized on clinical scanners. Undetected ischemic lesions (n = 29) were very small and more often located within the cortex. Ischemic lesions were consistently measured to be smaller in volume and

demonstrated decreased apparent diffusion coefficient values on the high resolution DWI by reducing partial volume effects with adjacent non infarcted tissue.

Improving the spatial resolution of diffusion-weighted imaging sequences and taking advantage of high magnetic fields, improves patient diagnosis and potentially their prognosis by accurate assessment of ischemic lesion patterns and lesion volume and mean diffusivity (MD) estimation. Future work is necessary to combine the high resolution diffusion imaging acquisition parameters used in this thesis with high resolution MRI modalities that evaluate tissue perfusion in order to systematically study transient ischemic attack longitudinally and identify permanent tissue damage.

Preface

This thesis is an original work by Kyle Hafermehl. All figures are original work by Kyle Hafermehl unless otherwise stated. The research project, of which this thesis is a part, received research ethics approval from the University of Alberta Research Ethics Board, Project Name "Magnetic Resonance Imaging Investigation of Cerebrovascular Disease", No. , February 11, 2013.

Acknowledgements

First of course, an enormous thank you is owed to my wonderful supervisor Christian, for granting me this opportunity and teaching me a tremendous amount in such a short span of time. I couldn't begin to quantify how much further my writing skills have advanced because of his meticulous editing skills. I certainly no longer fear the red ink, but rather welcome it as an opportunity to learn. I would also like to take this chance to thank the incredibly busy Dr. Butcher for his help in getting the ball rolling by giving me a starting project to work on and guiding me through the basics in ischemic stroke.

I must also send a huge thank you all of those in Christian's lab, as they were one of the strongest resources he had to offer a student. Two of which I must mention are Robb Stobbe, for his patience and the time he took in teaching me how to operate the scanners, something I never could have imagined doing in my life, as well as helping get my analysis software packages up and running. The second would have to be my office-mate Maria Mora, for teaching me how to operate Matlab and process all of my data as well as providing all of the answers to my many little questions.

A special thanks has to go to all of the patients that, despite many ailments sat through an hour scan to help a masters student with his research project. After volunteering myself for many studies and accumulating many hours inside that tube, I know that it can be an uncomfortable and boring hour, but without this my work surely would not have been possible.

I must send out a thank you to both my family and my girlfriend's family. For they not only supported and loved me, but for maintaining consciousness through multiple practice

presentations while I spilled forth words they could have gone on living without ever hearing. I must also give a special thanks to my future brother-in-law, longtime friend and future lawyer, for assisting in reading through my work and searching for my numerous grammar errors.

The last thank you is a special one, for it belongs to the love of my life and my future wife. For comforting me when things looked grim, for listening to my excited rants, having the patience to listen to my very sporadic ideas and train of thought, and for simply listening to my rampant rants concerning various frustrations and setbacks. She truly showed me the way for she is a spectacular woman. I love her with all my heart, and being loved by her is the best thing I could have ever dreamed of.

Contents

Chapter 1 ..... **1**

Chapter 2 ..... **4**

Strokes **4**

2:1 Definition 4

2:2 Vasculature of the Brain 5

2:2:1 Collateral Blood Supply 10

2:2:2 Regulation of Cerebral Blood Flow and Perfusion Pressure 13

2:3 Ischemic Stroke 15

2:3:1 Etiology of Ischemic Strokes **19**

2:3:2 Pathophysiology of Ischemic Strokes 23

2:4 Imaging Ischemic Strokes 27

2:4:1 Computed Tomography's Role in Ischemic Stroke 28

2:4:2 MRI Role in Ischemic Stroke 30

2:5 Transient Ischemic Attack 33

2:5:1 Transient Ischemic Attack Mimics 38

Chapter 3 ..... **42**

Diffusion-Weighted Imaging **42**

3:1 Diffusion of Water Molecules 42

3:1:1 Measuring Diffusion in the Cerebrum 43

3:1:2 Measuring Diffusion with Magnetic Resonance 46

3:1:3 Production of DWI Images 49

3:2 DWI Role in Pathologies 53

3:2:1 Imaging Artifacts/ Shortcomings of DWI 55

3:2:2 Relevant Literature to Imaging Ischemic Stroke and TIA 58

Chapter 4 ..... **65**

High Spatial Resolution Diffusion-Weighted Imaging in Patients with Acute Ischemic Stroke **65**

Abstract **65**

4:1 Introduction 66

4:2 Materials and Methods 68

4:2:1 Magnetic Resonance Imaging Protocol 68

4:2:2 Patients and Inclusion Criteria 71

4:2:3 Data Analysis 71

4:3 Results 72

4:4 Discussion 89

4:5 Conclusion 95

Chapter 5 ..... **97**

Concluding Remarks **97**

Bibliography **101**

List of Figures:

Figure 1 Inferior View of the Arteries at the Base of the Brain.... 8
Figure 2 Blood Supply to the Anterior, Lateral and Posterior Portions of the Cerebral Hemisphere. 12
Figure 3 Illustration of a Middle Cerebral Artery Occlusion Resulting in Infarction 15
Figure 4 Cerebral Blood Flow (CBF) Threshold Levels of a Neuron 24
Figure 5 Layers of the Cerebral Cortex.... 44
Figure 6 Pulsed Gradient Spin Echo Sequence. 48
Figure 7 Construction of DWI Images.... 50
Figure 8 Apparent Diffusion of Water in a Biological System.... 52
Figure 9 Conventional and High Spatial Resolution Images from Three Separate Patients Imaged at 1.5T, 4.7T and 3.0T.... 74
Figure 10 Superior Anatomical Detail Through Thin Slice DWI of Ischemic Stroke Imaged at 1.5T 75
Figure 11 Conventional and High Spatial Resolution DWI in Acute Ischemic Stroke Patient Imaged at 4.7T. 76
Figure 12 Superior Lesion Characterization with High Spatial Resolution in Acute Ischemic Stroke Imaged at 1.5T.... 77
Figure 13 Conventional and High Spatial Resolution DWI in Acute Ischemic Stroke Patient Imaged at 4.7T 78
Figure 14 Conventional and High Spatial Resolution DWI in Acute Ischemic Stroke Patient Imaged at 3.0T 79
Figure 15 Small Ischemic Lesion Identification Improved Using Isotropic In-plane Resolution Imaged at 4.7T.... 82
Figure 16 Superior Imaging of Small Ischemic Lesions within the Infratentorial Region Using High Spatial Resolution Imaged at 4.7T.... 83
Figure 17 Conventional and High Spatial Resolution DWI in Acute Ischemic Stroke Patient Imaged at 3T.... 85
Figure 18 Conventional and High Spatial Resolution DWI of Transient Ischemic Attack Patient Imaged at 1.5T.... 86
Figure 19 Identification of a Small Ischemic Lesion in a TIA Patient Using High Spatial Resolution DWI Imaged at 1.5T 86
Figure 20 Conventional and High Spatial Resolution DWI of TIA Patient Imaged at 1.5T.... 87
Figure 21 Conventional and High Spatial Resolution Color Fractional Anisotropy Map at 3.0T. 90

List of Tables

Table 1 : Clinical Symptoms of TIA vs. TIA Mimics. 41
Table 2 : Common Diffusion-Weighted Imaging Parameters Utilized in Acute Ischemic Stroke and Transient Ischemic Attack 60
Table 3 : DWI Sequence Parameters 69
Table 4 : Measurements of DWI Lesions Detected Using High and Conventional Spatial Resolution at 1.5T, 3T and 4.7T in 48 Patients with Ischemic Stroke or TIA..... 80
Table 5 : Ischemic Lesions Identified on Both Scans from 4.7T Subjects (n = 17)..... 81
Table 6 : Ischemic Lesions Identified on Both Scans from 1.5T Subjects (n = 9)..... 84
Table 7 : Ischemic Lesions Identified on Both Scans from 3.0T Subjects (n= 3)..... 84
Table 8 : Exclusive Lesions Detected in Acute Ischemic Stroke and Transient Ischemic Attack (TIA) Patients Using High Resolution DWI..... 88

List of Abbreviations

ACA	Anterior cerebral artery
ADC	Apparent diffusion coefficient
ASL	Arterial spin labelling
ATP	Adenosine tri-phosphate
CBF	Cerebral blood flow
CBV	Cerebral blood volume
CSF	Cerebral spinal fluid
CT	Computed tomography
CTA	Computed tomography angiography
CTP	Computed tomography perfusion
DWI	Diffusion-weighted imaging
EPI	Echo-planar imaging
FLAIR	Fluid attenuated inversion recovery
GM	Gray matter
ICA	Internal carotid artery
MCA	Middle cerebral artery
MRA	Magnetic resonance angiography
MRI	Magnetic resonance imaging
PCA	Posterior cerebral artery
PET	Positron emission tomography
PWI	Perfusion-weighted imaging
SWI	Susceptibility-weighted imaging
TIA	Transient ischemic attack
t-PA	Tissue plasminogen activator
WM	White matter

Chapter 1

Magnetic resonance imaging (MRI) has become increasingly important in the evaluation of healthy brain structure and function. Research using MRI has led to a tremendous amount of progress to the understanding of the human brain and the numerous cerebral diseases that afflict it. Now a vital imaging modality with increased accessibility, MRI has come to be routinely exploited for the wealth of information it yields in the clinical setting to assess both acute and chronic pathologies. The noninvasive nature of MRI furthermore adds to its unique benefits, imposing no risks provided volunteers and patients are screened properly.

Conventionally, MRI was used to image structural features because of its superior image contrast between tissue types and pathologies through the exploitation of distinct longitudinal and transverse relaxation times (T1 and T2 respectively). However, the flexibility in MRI allows for the alteration of acquisition parameters, permitting the isolation of specific properties of the brain that may be of interest: magnetic resonance angiography (MRA) examines the major arteries traversing through the neck and into the cerebral cortex for extent of stenosis, occlusions or aneurysms; magnetic resonance spectroscopy creates a relative concentration estimate of cerebral metabolites, lending insight into neurocognitive disorders that cause impairments through the disruption of normal neurotransmitter concentrations (e.g. disrupted serotonin, norepinephrine and dopamine levels associated with depression); functional MRI determines how the healthy brain functions allowing for the identification of abnormal brain activity in neurocognitive disorders (e.g. schizophrenia, bipolar disorder, depression); diffusion tensor

imaging tracks water movement along tracts in the brain, which assesses cortical connections and how these white matter (WM) tracts change with age and various disorders (e.g. degeneration of WM tracts in multiple sclerosis); perfusion and diffusion weighted imaging (PWI and DWI, respectively) can be utilized to investigate physiological aspects of the brain with particular utilization during stroke assessment. This list, however, is far from exhaustive, as advances in MRI continue to lead to both the improvement and introduction of new techniques to probe the mysteries of the human brain.

Stroke is a debilitating vascular disease that is segregated into two types to describe the specific manner in which normal blood flow is disrupted to the brain. For both types it is necessary to determine the extent of neurological tissue damage as well as the underlying pathological mechanism that initiated the event. Because of a stroke patient's neurological instability and the need to initiate treatment rapidly, MRI sequences in clinical settings are optimized to reduce scan time, limiting the signal and resolution available. We suspect that these clinical MRI sequences with low spatial resolution, specifically the DWI sequence utilized in stroke assessment, are potentially limited in their diagnostic yield because of a large degree of partial volume effects and low anatomical coverage using thick slices, limit their accuracy for the identification and characterization of small abnormalities. We hypothesize that by increasing the spatial resolution of DWI sequences when assessing acute ischemic stroke patients, the observed number of ischemic stroke lesions and measurement accuracy of the lesions characteristics will increase relative to conventional clinical DWI sequences.

This thesis addresses this issue and attempts to provide insight into the pathology of acute ischemic stroke and transient ischemic attack (TIA) by improving spatial resolution of DWI by going beyond conventional clinical DWI parameters and previous work implementing thinner

slice DWI. This thesis is organized into 5 chapters: Chapter 2 will introduce the important aspects of ischemic stroke and TIA while Chapter 3 will discuss the biophysical principles of the methodology utilized throughout and its potential limitations within the clinic. Chapter 4 will outline the experiment performed to address the issue of limited spatial resolution in clinical DWI parameters to diagnose ischemic stroke patients. The final chapter evaluates the information gained and provides concluding remarks on what was learnt.

Chapter 2

Strokes

2:1 Definition

Strokes are defined as a sudden disruption in blood flow to the brain, caused by either the occlusion (ischemic stroke) or rupture (hemorrhagic stroke) of blood vessels carrying oxygen and nutrients. Extent of disruption to blood flow, quality of collateral blood flow, metabolic demand of the specific tissue and the period of time blood flow is disrupted determine the extent of damage to the brain. Resulting neurological symptoms are attributed to the specific location of damaged tissue within the brain from either the lack of blood flow or the direct exposure of neurons to cytotoxic blood. Strokes are the fifth leading cause of death in the world and the leading cause of long term disability, with one Canadian experiencing a stroke every 10 minutes[1], costing Canada 3.6 billion dollars per year alone[2]. The greatest burdren caused by stroke does not lie in the mortality like cancer and coronary heart disease, but instead in the resulting chronic disability[3]. The vasculature of the brain will be discussed first followed by a discussion on the etiology, pathophysiology and neuroimaging of stroke.

2:2 Vasculature of the Brain

Strokes are an affliction of the cerebrovascular system, the reason strokes are commonly referred to as a cerebrovascular disease, and as such it is important to consider which arteries supply specific regions of the brain so that ensuing neurological symptoms can assist in identification of where an occlusion may reside and where it originally came from.

The cerebral circulation is an enormously vast and complex system largely composed of three major arteries, the middle cerebral arteries (MCA), anterior cerebral arteries (ACA) and the posterior cerebral arteries (PCA) which branch off into smaller arteries, arterioles and eventually into a single celled layer of endothelial cells. These neurovascular systems are responsible for providing the oxygen, glucose and metabolites essential for aerobic metabolism within the neurons of the brain, while simultaneously carrying away metabolic waste. A detailed account of the cerebral circulation system is described by Sheldon[4]. Blood is directed to the brain through an anterior system and a posterior system but anastomose at the base of the brain to form the circle of Willis. The anterior circulation is supplied off of the common carotid arteries which are branches arising from the aortic arch just before the left subclavian artery on the left side of the body, and off of the brachiocephalic artery to the right of the heart. The common carotids continue up through the neck and bifurcate at the fourth cervical vertebrae, giving rise to the external carotids which supply much of the face and neck, as well as the internal carotid arteries (ICA), which supply 80% of the blood to the brain. The posterior circulation is composed of the two vertebral arteries which run rostrally along the medulla and fuse at the pons forming the basilar artery to supply the remaining 20% of the total blood traversing through the brain.

The ICA ascends each side of the neck, reaching into the subarachnoid space at the base of the brain. The ophthalmic artery is the first branch off the ICA and travels along the optic nerve, supplying nearby structures on its way to the orbit. Disrupted flow through the ophthalmic artery can result in ocular ischemic syndrome causing transient or permanent monocular blindness. Before bifurcating into the MCA and ACA, the ICA gives rise to the smaller anterior choroidal artery and posterior communicating artery. The anterior choroidal artery is a thin artery, making it susceptible to cerebrovascular accidents which can potentially be significant because it supplies deep structures such as the internal capsule, amygdala, hippocampus, medial portion of basal ganglia, pituitary gland and thalamus.

The first major branch off the ICA, the ACA, begins to run medially until it reaches the longitudinal fissure, at which point it begins to arch posteriorly to supply the medial portion of the frontal and parietal lobes. The ACA is commonly segmented into three components based upon distance from bifurcation off the ICA. A1 is the origin of the ACA, beginning at the ICA and running until it gives rise to the anterior communicating artery. A2 continues on from the anterior communicating artery passing anterior to the genu of the corpus callosum, forming the origin of the first major branch known as the callosomarginal artery, while the A3 segment continues on as the second major branch labeled as the pericallosal artery. One of the largest perforating branches derived from the ACA has it origin off the A2 segment and is known as the medial striate artery, or the recurrent artery of Heubner, which is responsible for supplying the head of the caudate nucleus, paraterminal gyrus, anterior portion of the lentiform nucleus and anterior limb of the internal capsule. Another important artery considered to be derived from the ACA is the medial lenticulostriate arteries which run to supply the globus pallidus and medial portion of the putamen. Occlusions of the ACA often result in contralateral motor and

somatosensory deficits of the legs, because the precentral and postcentral gyri extend onto the medial surface of the frontal and parietal lobe which is primarily supplied by the ACA.

The second major branch off the ICA is the MCA and is primarily responsible for supplying most of the lateral surface of both cerebral hemispheres. The MCA can be considered to be segmented into four components; M1 which begins at the origin of the MCA, travelling horizontally until a bifurcation, creating two M2 segments which form a hairpin bend at the circular sulcus of the insula and continue on as the M3 segments until they emerge from the sylvian fissure and continue onto the convex surface of the hemisphere as the M4 segments. Clinical significance of this artery is in part due to the fact that most of the blood supplied to the precentral and postcentral gyrus as well as part of both the internal capsule and basal ganglia is derived from the MCA, while also being the most commonly occluded artery causing stroke[5]. Occlusions frequently result in major motor and somatosensory deficits just as occlusions of the ACA making it difficult in certain circumstances to discern the likely afflicted cerebrovascular territory afflicted. Occlusions of the MCA can also afflict language production and understanding if blood flow is interrupted to the language centers within the language dominant hemisphere. There are small lateral groups of lenticulostriate arteries that branch off the proximal M1 segment of the MCA and penetrate directly from their origin into the brain to supply lateral portions of the putamen and external capsule while also providing blood to the upper portion of the internal capsule, while the insula is supplied by direct branches off the MCA. Small vessel disease refers to atherosclerosis within these lenticulostriate arteries and cause lacunar infarcts.

Many other small, perforating arteries exist to route blood from arteries at the base of the brain to supply blood to deep cerebral structures including the corona radiate, hypothalamus, basal ganglia and internal capsule (**Figure 1**) [5]. These thin and narrow-walled vessels are

frequently involved in strokes and are clinically problematic because despite their size, because infarction of the structures they supply result in deficits of similar magnitude to those caused by large expanses of damaged cortex.

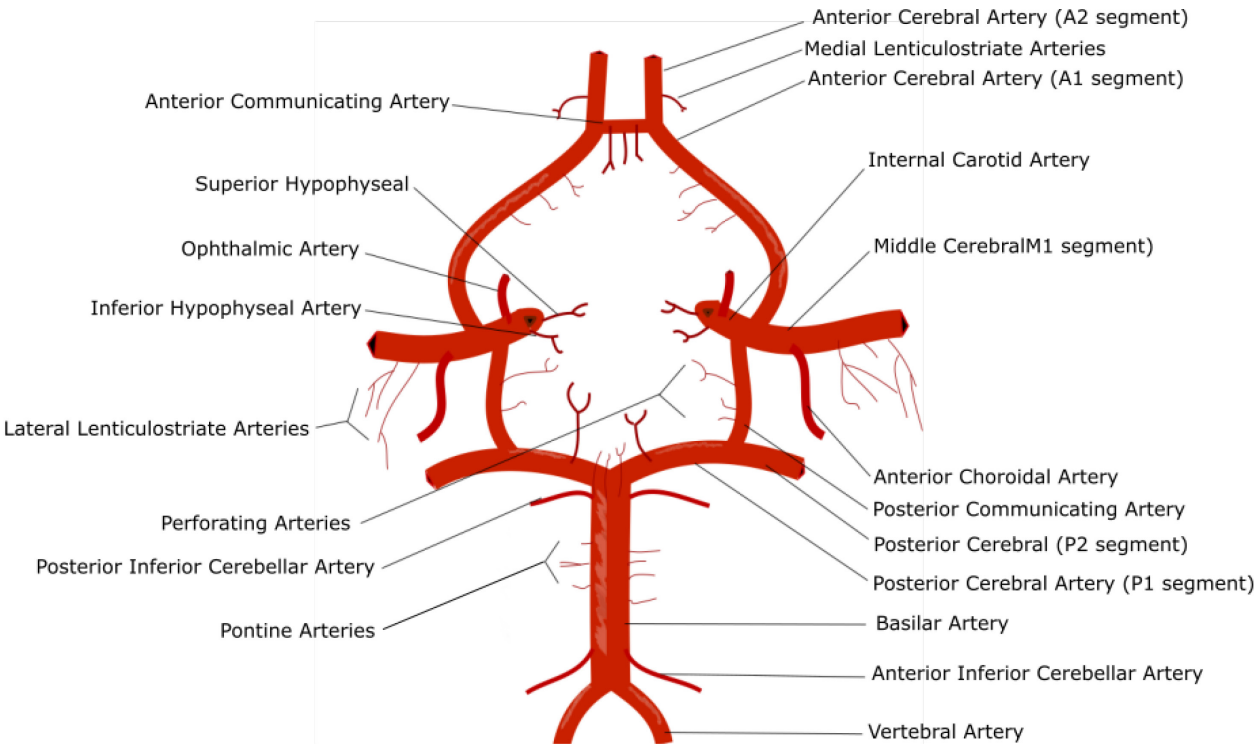

Figure 1 Inferior View of the Arteries at the Base of the Brain –The connection between the anterior circulatory and posterior circulatory system is accomplished through the anterior and posterior communicating arteries which together form the circle of Willis. Many small perforating arteries branch from larger arteries at the base of the brain to supply deep cerebral structures. The major perforating arteries are the medial lenticulostriate arteries off the ACA, the lateral lenticulostriate arteries off the MCA, the superior hypophyseal artery which runs to supply the adenohypophysis portion of the pituitary gland, and the inferior hypophyseal artery which supplies the neurohypophysis portion of the pituitary.

Prior to the formation of the basilar artery, the two vertebral arteries feed three smaller arteries and small penetrating arteries which project to the medulla. Two of these arteries supply the anterior and posterior upper portions of the spinal cord while the third is identified as the posterior inferior cerebellar artery. As the name suggests, it delivers blood to the inferior and

posterior surface of the cerebellum as well as the inferior vermis. In addition to this, the posterior inferior cerebellar artery continues on to curve around the brainstem, reaching the lateral medulla and choroid plexuses within the fourth ventricle. Pontine arteries off of the basilar artery provide the remainder of the circulation supplied to the pons. Occlusion of pontine arteries can cause vertigo and ipsilateral deafness since these arteries often reach the inner ear.

The two PCAs are the major bifurcations of the basilar artery at the level of the midbrain. There are numerous branches before the bifurcation with two explicitly labeled as the anterior inferior cerebellar artery and the superior cerebellar artery. The anterior inferior cerebellar artery supplies the anterior and inferior portions of the cerebellum as well as the caudal pons, while the source of blood for the superior surface of the cerebellum is through the superior cerebellar artery and also runs to supply the caudal midbrain and rostral pons. The PCA, like the ACA and MCA is segmented into four components and runs a course around the midbrain, spreading out to supply medial and inferior surfaces of the occipital and temporal lobes. P1 forms the origin of the PCA, beginning after the termination of basilar artery and runs until reaching the posterior communicating artery within the interpeduncular cistern. The P2 is sub-segmented into anterior and posterior portions but anastomose upon reaching the crural cistern and ambient cistern respectively. P3 is the segment that lies within the quadrigeminal cistern and branches into P4, also known as the calcarine artery, laying within the calcarine fissure and sending branches to both the cuneus and lingual gyrus. Branches are sent out along the way to supply the rostral midbrain and portions of the diencephalon. Disruption of blood flow through the calcarine artery can cause homonymous hemianopia. Many arteries derived from the PCA branch to supply blood to the important relay station of the brain known as the thalamus. These arteries include the paramedian thalamic-subthalamic arteries, inferolateral, and posterior choroidal arteries.

Posterior choroidal arteries also run to provide blood to the choroid plexus of the third and lateral ventricle to maintain cerebral spinal fluid production. An occlusion within the PCA causes deficits in visual fields and symptoms referable to the midbrain and diencephalon. Cortical, central and circumferential arteries, also known as penetrating arteries, branch off of the PCA, MCA and ACA to course lateral and medial aspects of both hemispheres. From these, smaller terminal branches arise and penetrate at right angles with longer ones penetrating deep enough to supply the subcortical WM.

2:2:1 Collateral Blood Supply

Normal blood supply to the brain can be considered to be divided into the anterior two thirds of the brain portion (i.e. the ICA) and a remaining posterior thirds portion (i.e. basilar artery), but these two systems are not separate and the brain possess the capacity to form collateral channels in the event of an occlusion. These collateral channels are essential to maintain a degree of perfusion sufficient enough to maintain normal cellular function following occlusions, as it extends the time through which functional recovery can occur through intervention. While these collateral channels are more efficiently established in the event of gradual occlusions rather than sudden events, the brain does have various mechanisms to establish collateral flow in different areas. Unfortunately, there is a large degree of inter-subject variability when considering the vasculature of the brain. In some extreme circumstances, certain segments may be hypoplastic or absent all together, limiting the degree of potential for collateral flow in a significant proportion of the population.

A cerebrovascular structure capable of providing collateral blood supply that is found to be extremely variable in both its components and branches[6], is established through the circle of Willis. Two communicating arteries make up the circle of Willis, the posterior communicating artery and the anterior communicating artery which connect the ICA to the PCA and the two branches of the ACA within each hemisphere respectively (**Figure 2**). Normally, little blood passes through these communicating arteries due to differences in arterial pressures. Should one of the major arteries become occluded, a difference in pressure is established, shunting blood through the circle of Willis, and thus perfusion may be maintained through anastomotic flow in communicating arteries, possibly minimizing or even preventing neurological damage. The circle of Willis and main cerebral arteries give rise to small central and cortical branches. These central branches penetrate perpendicularly into the basal brain and perfuse the basal ganglia, internal capsule and diencephalon.

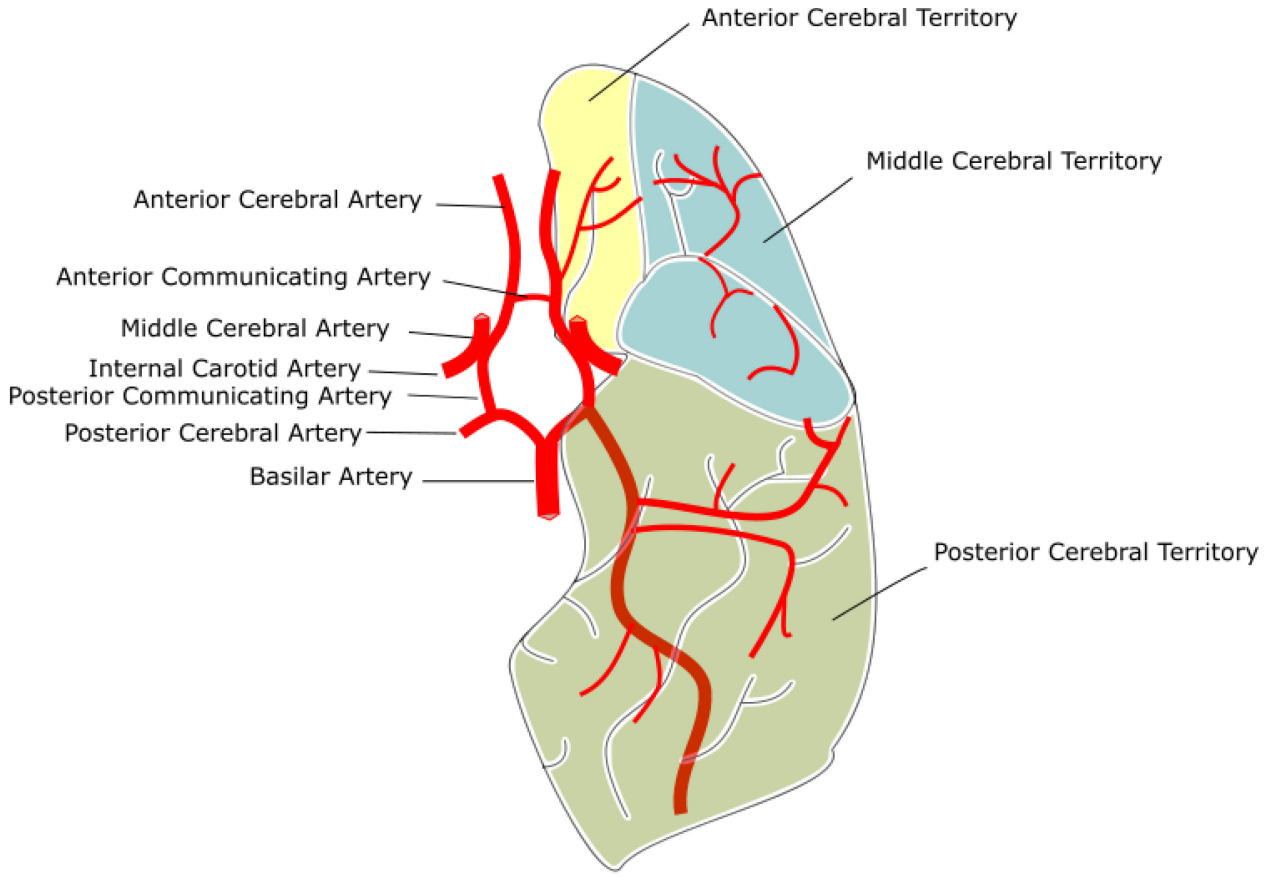

Figure 2 Blood Supply to the Anterior, Lateral and Posterior Portions of the Cerebral Hemisphere -The three major constituents of the arterial system form cerebral artery territories with known neurological deficits allowing infarction zones to be approximated. These arterial zones form a watershed but in the event of an occlusion at these arterial borders, some collateral blood flow may form from neighbouring territories to maintain perfusion.

Anastomoses can occur between various cerebral branches in the event of an occlusion with many well established locations documented to anastomose. The carotids have several recognized anastomoses that can develop in the event of an occlusion within the common and internal carotid arteries. These include branches between the subclavian artery when the common carotids are obstructed, branches of external carotid artery can direct blood flow into the orbit and anastomose with the ophthalmic artery should significant stenosis or obstruction occur

within the internal carotids with blood potentially reaching the MCA, ACA and PCA. Several meningeal branches from the ICA, external carotid artery and vertebral arteries can even anastomose with each other. Other common anastomosis include muscular branches of the vertebral artery within the neck, receiving blood from occipital and ascending pharyngeal branches of the external carotid artery or from deep and ascending cervical arteries, perforating precapillary beds at the base of the brain can anastomose to supply the basal ganglia, while the anterior choroidal artery has the potential to anastomose with the posterior choroidal artery. The leptomeningeal branch is an important collateral pathway that can be utilized when the circle of Willis is inadequate and develops at the surface of the brain between cortical branches of the ACA, MCA and PCA. Arterioles and capillaries do possess the potential to anastomose between terminal branches but do not likely maintain the extent of collateral flow that major collateral channels provide (e.g. circle of Willis). However, together these potential sources of collateral flow assist in maintaining an adequate level of perfusion to prevent cerebral blood flow (CBF) from dropping below the threshold level to cause infarction during cerebrovascular stenosis and occlusion, providing the therapeutic window necessary to save cerebral tissue.

2:2:2 Regulation of Cerebral Blood Flow and Perfusion Pressure

The current understanding of the underlying pathophysiology of acute ischemic stroke was largely gained through the investigation into the relationship between cerebral blood flow and metabolism[7]. Through positron emission tomography (PET) imaging, cerebral blood flow, cerebral blood volume (CBV) and cerebral energy metabolism, were found to be coupled and consistently higher in GM than WM[7]. This led to the conclusion that the oxygen extraction

fraction (conversion of oxyhemoglobin to deoxyhemoglobin) is fairly similar throughout the expanse of the brain[8]. Aging brains demonstrate a gradual decrease in CBF, CBV and cerebral metabolism but maintain coupling, making oxygen extraction fairly constant through the aging process[9].

The healthy brain attempts to maintain a constant CBF through a process called autoregulation[10], by attempting to balance cerebral perfusion pressure and cerebrovascular resistance. This is accomplished through manipulation in the degree of cerebrovascular resistance. When systemic blood pressure begins to drop, small cerebral blood vessels begin to undergo vasodilation within seconds, increasing the blood volume and as such, maintaining CBF. Autoregulation in healthy adults is able to maintain a constant CBF across a range of systemic blood pressures from 50 to 170 mmHg, but becomes less effective in the elderly and as such, postural hypotension is more likely to result in symptomatic ischemia[11]. In the event of an obstruction to blood flow, vasodilation becomes maximal and cerebral blood pressure begins to fall resulting in decreased CBF, but metabolic activity can be maintained by increasing the oxygen extraction fraction creating the scenario known as “misery” perfusion or oligemia. As perfusion pressure continues to drop, oxygen extraction fraction becomes maximal and eventually, metabolic activity can no longer be maintained resulting in ischemia and eventually permits the visibility of structural abnormalities when utilizing certain MRI sequences and contrasts.

2:3 Ischemic Stroke

Ischemic strokes are the more common of the two types of strokes and will therefore be the focus of discussion for this thesis, accounting for 85% of all stroke occurrences while subarachnoid hemorrhage (5%) and intracerebral hemorrhage (10%) constitute the remaining 15%[12]. Cerebral tissue becomes ischemic once proper blood flow falls below the threshold for normal physiological function, occurring when the vessel supplying the tissue becomes blocked or restricted (**Figure 3**). Ischemia can be defined as a decrease in CBF, or oligemia that is associated with a loss of neuronal function, while infarction is cell death resulting from ischemia.

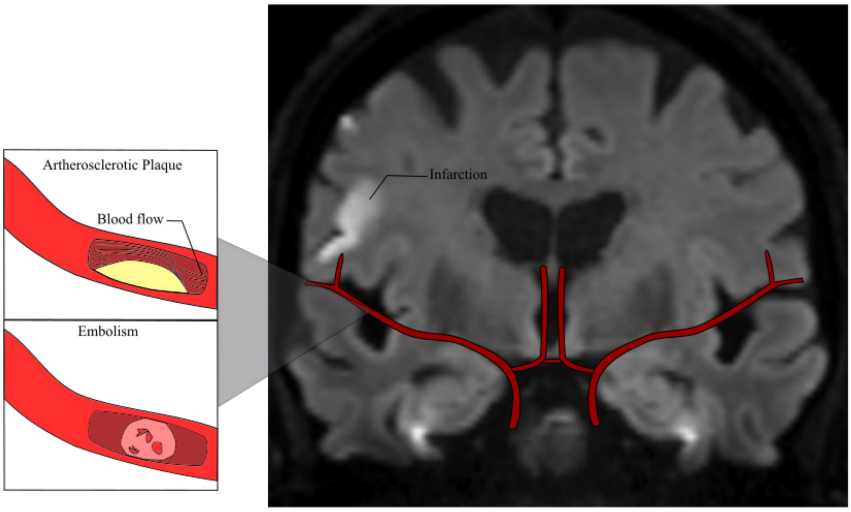

Figure 3 Illustration of a Middle Cerebral Artery Occlusion Resulting in Infarction – Arteries can become occluded or restrict blood flow under a variety of circumstances, with the two most common being illustrated. When blood flow is diminished to a tissue, infarction can ensue.

Neurons possess different thresholds for drops in CBF before neuronal functionality is lost, based upon their metabolic rates (e.g. the hippocampus is a very metabolically active tissue that demands higher rates of CBF). Ischemic strokes can be classified into subtypes based upon their suspected cause, which includes; cardioembolic, large-artery atherosclerosis, small-vessel

occlusion (i.e. Lacunar), or stroke of other determine etiology (e.g. non-atherosclerotic vasculopathies, hematologic disorders or hypercoagulable states) [13]. However, 20 – 33% of ischemic strokes are labelled as cryptogenic strokes, because no underlying cause can be determined despite thorough vascular, cardiac and serologic evaluation[14].

There are several risk factors associated with increased incidences of ischemic strokes, including age, male, hypertension, diabetes mellitus, valvular heart disease, chronic kidney disease, inflammatory disorders, dyslipidemia, previous stroke, sleep apnea, leukoaraiosis, low HDL levels, hypercholesterolemia, alcohol consumption and tobacco use[15]. Age still remains to be the strongest risk factor known for both ischemic stroke and primary intracerebral hemorrhage with an estimated 25 times higher incidence rate in those aged 75-84 over those aged 45-54[15]. Leukoaraiosis, also known as WM hyperintensities because of the bright appearance of WM on T2 weighted brain images, is thought to possibly be caused by WM infarctions and are commonly associated within elderly populations that have experienced a recent ischemic stroke[16]. Evidence suggesting that leukoaraiosis is a vascular disorder comes from its association with aggressive small vessel cerebrovascular pathologies such as cerebral amyloid angiopathy. These affected vessels induce ischemia in deep WM through chronic hypoperfusion and simultaneous disruption of the blood brain barrier, putting these patients at risk of bleeding when administered anticoagulants[17]. Because of this, it is thought to be a strong risk factor for increased incidents of both ischemic and hemorrhagic stroke[18]. Recent studies have linked mutations in the FOXC1 gene, a developmental transcription factor required for formation of the eye and required for support of angiogenesis, to be linked to cerebral small vessel disease, suggesting that WM hyperintensities and stroke may have a congenital component[19].

The primary goal in stroke management is to reduce brain injury and to promote patient recovery following the stabilization and initial assessment of the patient. This is achieved through treatment focused on restoring blood flow to the hypoperfused tissue by removing or reducing the size of occlusion, usually through thrombolytic medication, which must be administered as quickly as possible to negate the neurological deficits, followed by treatment of the source in order to minimize the risk of reoccurrence. Each passing minute tissue remains hypoperfused, more neurons proceed to infarction, creating the aphorism "time is brain". Intra venous recombinant tissue plasminogen activator (t-PA), specifically alteplase, a naturally occurring enzyme within the body capable of catalyzing the conversion of inactive proteases into the active serine protease, plasmin, to actively dissolve fibrin clots, is the only thrombolytic medication available during the hyperacute phase of ischemic stroke. But t-PA is limited to a 4.5 hour window of peak effectiveness following symptom onset[20] with higher success rates of recanalization the earlier it is administered[21]. After which, the risk of hemorrhagic complications and death outweighs the limited functional increase in neurological function following administration. There are many other factors that preclude use of IV t-PA because of the risk of hemorrhagic complication, as dictated by the 2013 American Heart and Stroke Association guidelines[22]. These include evidence of intracranial hemorrhage, severe uncontrolled hypertension, recent head trauma or stroke within the last three months, severe hypoglycemia or other stroke mimics, minor stroke (defined as NIHSS ≤4) especially if symptoms are rapidly resolving unless persistent symptoms will cause limitations in the patient's life, severe strokes (typically defined as ≥20, and recent major surgery (e.g. coronary artery bypass). However, devices and other medications exist that operate outside this therapeutic window or when a patient is ineligible for t-PA and are shown to be effective in acute management of stroke and

reduction of neurological deficits. These include endovascular recanalization using stent retrievers[23, 24], other intravenous thrombolytic agents such as desmoteplase[25] or intra-arterially administered tirofiban combined with urokinase thrombolytics[26].

Common interventions to reduce the risk of future strokes include endarterectomy to surgically remove large formations of plaque within the carotid arteries when stenosis exceeds 50%, or a treatment regime of intravenous and oral antiplatelets, and anticoagulants to prevent fibrin clots from forming off a thrombus or from cardiac sources. Anticoagulants and antiplatelets work by interrupting the process through which fibrin blood clots are formed, in contrast to thrombolytic medication which works through direct fibrinolysis by activating plasminogen and converting it into plasmin, the active component that degrades fibrin into soluble fibrin products[27]. Even the use of aspirin can moderately reduce the risk of recurrent stroke. Emerging medications and innovative response strategies such as ambulances equipped with brain imaging technologies are in constant development in order to combat the rapidly developing epidemic of ischemic stroke nationwide.

There are four distinct phases characterizing ischemic stroke based upon the approximate time from symptom onset, while precise timings are variable and subject to debate[28-30]. The first phase, which is arguably the most important as patients still remain eligible within the narrow window to receive thrombolytics, is the hyperacute phase which describes patients still within the first 6 hours from the time they were last known to display no neurological deficits. As the patient progresses into the acute phase (6-24 hours after symptom onset), it is imperative to accurately establish the presence of any hypoperfused, yet viable tissue before it proceeds to infarction, as the expansion of the ischemic core can be temporally variable, enabling some

patients to retain a viable penumbral zone with salvageable tissue during the acute phase[31]. While perfusion imaging techniques such as PET, CTP, PWI and ASL exist to accomplish this, other techniques such as mean diffusivity (MD) thresholding has demonstrated potential in predicting tissue fate through measurement of intermediate MD values[32]. This technique relies on the MD maps created from diffusion imaging (discussed in Chapter 3) to predict the quantity of salvageable tissue. This involves isolating the amount of tissue with intermediate values of MD by setting a threshold for MD lower than the MD within healthy tissue and subtracting tissue containing severely reduced MD values (i.e. infarct core). Patient management focus shifts during the late acute phase and as they transition into the subacute phase (1 – 7 days) to functional recovery[33], as the penumbral zone is no longer likely to be present or salvageable at this time[34] and thrombolytics such as t-PA are no longer effective at dissolving clots. The chronic phase describes patients beyond the subacute phase and typically involves rehabilitation to recover from any persistent neurological deficits.

2:3:1 Etiology of Ischemic Strokes

There are multiple mechanisms through which normal CBF can be disrupted to the extent that it can induce ischemia and infarction. Ischemia is due to low blood perfusion of the cerebral tissue, therefore under any hypotensive situations (e.g. heart failure, blood loss, obstructed blood flow, postural changes, etc.) some tissue may become inadequately perfused and proceed to infarction. Less common mechanisms causing reduction in systemic pressure include: vasospasms, occlusions of the venous system and hemorrhaging acting through constriction of the vessels supplying the brain. The most common cause of major artery occlusion involves the narrowing of major or cortical arteries by greater than 50%, induced by atherosclerosis which

markedly reduces blood flow. Atherosclerosis causes the gradual hardening of the arteries and luminal stenosis through a pathological process in which calcified lipid deposits accumulate circumferentially along the innermost layer of the vessel wall. These atherosclerotic plaques typically form at daughter vessels of major bifurcations such as the internal carotid arteries after the bifurcation at the common carotids. Plaques induce an immune response causing influx of macrophages and eventually lead to the rupture of the endothelial layer. Atherosclerotic plaques also introduce turbulent blood flow thereby creating shear stress which can damage the endothelial wall and result in endothelial lesions. Both shear stress and plaque rupture result in platelets responding through aggregation and the formation of a fibrin clot known as a thrombus. Thrombi can form anywhere there is stress on the endothelial wall and cause significant restrictions in flow, making thrombosis within extracranial and intracranial arteries another common cause of ischemic strokes and TIA.

Emboli are mobile pieces of particulate matter that act as travelling clots. When platelet aggregates are mobilized or have dislodged from their source, they become known as an embolus which travel along the arteries until the vessel diameter narrows to the point that the emboli is restricted and cannot proceed any further, creating an obstruction to blood flow. Embolic strokes cause a third of all ischemic strokes and have a range in severity based upon the size of particulate as well as the specific artery the emboli becomes lodged in. Microemboli often cause lacunar infarcts, minor strokes and TIA once they become lodged within thin diameter vessels such as small penetrating arteries (e.g. lenticulostriate arteries causing lacunar stroke) and small cortical arteries. Multiple sources can give rise to an embolus, making it important to discern where an embolus originated because it dictates the prevention strategy of recurrent strokes. Emboli arise from blood clots formed in the heart (cardioembolic), lungs (pulmonary emboli),

peripheral circulation and thrombi formed from atherosclerotic lesions within the cranial arteries (artery-artery emboli or thromboembolism) due to shear stress.

Cardioembolic strokes are one of the most common sources of emboli and are a symptom of cardiac dysfunctions that enable platelet aggregation, which subsequently travel cranially and induce infarction. This is because general failure of the heart prevents complete ejection of blood from the ventricles or atrium, resulting in clotting and can subsequently become mobile by the aggressive contraction of the cardiomyocytes forming multiple emboli. Incomplete ejection will occur through a variety of failures including: atrial fibrillation, fibrosis, chamber dilation, mechanical dysfunction within the left atrial appendage, valvular heart disease, ventricular cardiopathy and impaired myocyte function[35]. Atrial fibrillation has been documented to be strongly associated with stroke[36-38], as the dysrhythmia induces a thrombus that subsequently breaks apart and mobilizes multiple minute emboli, and continue on to cause occlusions in multiple arterial territories. The risk of ischemic stroke has been estimated to be 3-5 x larger following the onset of atrial fibrillation and it is biologically plausible to assume that there is a causal relationship[37, 38]. However, a recent study suggests that the relationship between atrial fibrillation and stroke may be more complex than a simple causal relationship[39].

Carotid artery dissection is a less frequent cause of stenosis but can also be a potential source of emboli. Dissection within the carotid arteries can occur both spontaneously or through traumatic injury to the head or neck and consequently has the potential to induce infarction[37]. This makes dissection a potential pathological mechanism for ischemic stroke in the younger and healthier demographic. Whether traumatic or hereditary, both introduce shear stress on the arterial lining and lead to a tear in the intima of the carotids creating a void through which blood

can flow. This can lead to a partial or complete occlusion and introduces a potential source of a thrombus that can subsequently be mobilized and occlude intracranial arteries.

Cerebral small vessel disease has diffuse, cerebrovascular consequences, including cognitive impairment aggravating or causing dementia in the elderly, leukoaraiosis, lacunar infarcts, microbleeds and hemorrhaging[41, 42]. As the name implies, small arteries, arterioles, capillaries and venules of the brain are afflicted with damage to the endothelial layer causing reduced blood flow or weakness which permits permeability of blood. Common forms include age and hypertensive related disease, atherosclerosis or cerebral amyloid angiopathy. When regarding lacunes and leukoaraiosis, small vessel disease is referred to as microangiopathic brain lesions and constitute a fifth of all ischemic strokes[43, 44]. Lacunar strokes are an important subset of ischemic stroke caused by small vessel disease that results in small infarcts typically ranging from 2 – 20 mm in diameter[43]. Lacunar infarcts occur as a result of occlusions contained within the small perforating arteries supplying the subcortical areas of the brain and usually leave a third of patients dependent on assistance from others because the afflicted regions (e.g. basal ganglia) of the brain cause severe motor deficits[44]. Because of the distinct motor and sensory symptoms with the former being the most frequent, lacunar strokes are clinically recognized and defined as displaying lacunar syndromes which typically include persistent or transient motor hemiparesis or hemiplegia afflicting the face, arm and leg, ataxic hemiparesis including weakness and clumsiness, dysarthria, pure sensory or mixed sensorimotor stroke. These syndromes are highly predictive of small lesions within the corona radiata (ataxic), internal capsule (motor), thalamus (sensory stroke), cerebral peduncle or pons (dysarthria) which are more often detected on MRI than CT.

2:3:2 Pathophysiology of Ischemic Strokes

There are typically two zones of affected tissue during the hyperacute phase of an ischemic stroke (0 - 6 hours after symptom presentation), defined by the degree of CBF supplying the tissue; the ischemic core, or infarct, is characterized by complete depletion of ATP reserves resulting in ionic disruption and metabolic failure leading to cell death within minutes, while tissue within the penumbra zone remains viable for a limited time frame but remains both metabolically and ionically challenged causing the recruitment of active cell death mechanisms. The degree of drop in CBF required to induce either ischemia or infarction is dependent on both the tissue and the cell type. Typically, neurons (e.g. CA1 neurons of the hippocampus) and oligodendrocytes are more vulnerable to cell death than astroglial or endothelial cells. Grey matter with higher metabolic rates depicts this enhanced sensitivity to decreases in CBF relative to the low metabolic rates characteristic of WM. On average, the CBF to all grey matter is approximately 50 - 60 ml/100 g/min, and in the event of even a moderate drop of 10 – 20 ml/100 g/min begins to induce electrical failure resulting in gradual loss of proper neuronal functions (**Figure 4**).

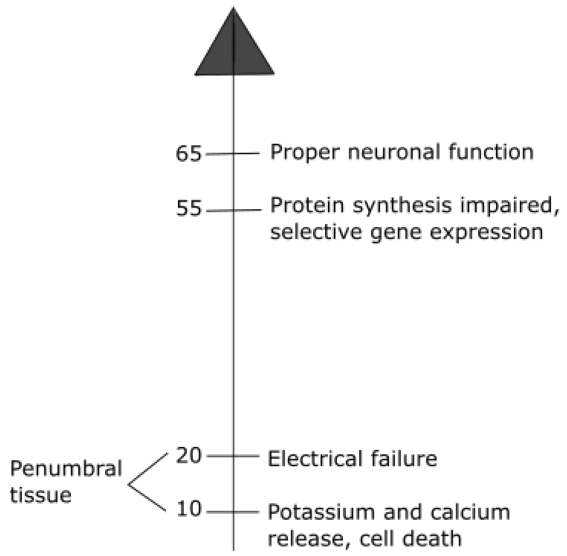

Figure 4 Cerebral Blood Flow (CBF) Threshold Levels of a Neuron – CBF is maintained at a constantrate through autoregulation to sustain proper neuronal function and is measured in mL of blood delivered per 100 g of brain tissue per minute. Moderate decreases in flow to brain tissue causes the neurons to halt synthesis of proteins and promotes selective gene expression, preserving energy for survival of the neuron. Further decreases in CBF leads to electrically silent neurons, while a further reduction in CBF will result in failure of sodium/potassium pumps causing necrosis and infarction.

Modified from Astrup J, et al[45].

This tissue would be considered temporarily salvageable if flow is not diminished any further, separating it from the infarct core and is typically known as the penumbra zone as it usually surrounds the infarct core. A further decrease in CBF or prolonged period of low CBF will cause a loss of membrane structural integrity and the tissue ultimately proceeds to infarction.

The pathophysiology of the infarct core follows necrotic pathways that do not result in the expenditure of energy, as the cells' energy reserves have been exhausted. Upon depletion of energy stores, the ATP dependent sodium/potassium pumps begin to fail, resulting in an ionic imbalance causing neurotransmitter release and inhibition of neurotransmitter reuptake. Glutamate concentrations at the synaptic cleft begin to rise, binding to and activating membrane receptors leading to glutamate toxicity, promoting excessive calcium influx, thus activating phospholipases and proteases causing degradation of membranes and proteins essential to the

integrity of the cell[46, 47]. Free radical species are generated by the action of phospholipases causing lipid peroxidation and membrane damage creating a cascade of inflammation and apoptosis in surrounding tissue[48]. The excessive release of glutamate and potassium ions from the ischemic core can induce depolarization and subsequent repolarization of neurons in the neighboring penumbral tissue, causing repetitive de- and repolarization. This may exacerbate the energy failure within the penumbra zone and propagate the expansion of the ischemic core.

As an excessive amount of sodium begins to enter the cell due to the failure of the sodium/potassium pumps, an influx of water ensues and begins to accumulate intracellularly, causing swelling, beading and edema. This increases the local hydrostatic pressure and can potentially compromise blood flow further, but more importantly has the potential to induce mass effect which leads to brain shifting and eventually brain herniation, often causing death within the first week. Evidence suggests that the energetic failure of the sodium/potassium pumps is the physiological mechanism necessary for DWI detection of stroke[49], as this causes the cell swelling and beading thought to restrict water movement both intracellularly and extracellularly.

In contrast, the penumbra typically displays apoptotic-like pathways which consist of both caspase dependent and caspase independent pathways. These apoptotic pathways maintain plasma and mitochondrial membranes until late in the process as DNA is cleaved and autolytic pathways begin. This is because cells are preferentially induced to undergo apoptosis rather than necrosis in order to minimize the inflammatory responses but require energy to activate these pathways. Recent innovations have highlighted prospective therapies in neuroprotection through experimental models involving caspase inhibitors, preventing expansion of the infarct core[50]. As infarcted tissue enters the chronic phase, dead tissue is removed by microglia, replacing the

infarcted tissue with a fluid filled space which can be easily identified using neuroimaging (e.g. fluid attenuated inversion recovery, FLAIR).

The rapid cell death of neurons caused by lack of blood flow resulting in apoptosis and cytotoxicity are the primary causes of damage, however, evidence suggests cell damage is also induced by the presence of reactive oxygen species[51] through a variety of injury mechanisms including inflammation[52], mitochondrial inhibition, calcium overload and reperfusion injury[53]. Following the degradation of cellular and nuclear membranes during necrosis, microglia cells are activated by cellular debris and DNA fragments, transforming microglia cells into active phagocytes. This is followed by the release of cytotoxic molecules and pro-inflammatory cytokines such as tumor necrosis factor alpha, interleukin-1 and interleukin 6[54]. Thus, targeting oxidative damage and inflammation through therapeutic approaches have been proposed as a neuroprotective technique in acute ischemic stroke[55-60]. However, despite the damage induced by inflammation, microglia may be responsible for releasing neuroprotective molecules including insulin-like growth factor 1 and other active growth factors[56].

Following ischemia, the ultimate goal in intervention is to restore blood flow to the hypoperfused tissue in an effort to reduce the amount of cerebral tissue damage. Paradoxically, in effort to save brain tissue from infarction, it has been frequently observed that following restoration of circulation, there is an increase in inflammation and oxidative damage[61]. This inflammatory response to oxygenation is believed to be a result of activated endothelial cells within the microvasculature that were altered by the ischemia and produce oxygen radicals rather than nitric oxide[61]. This apparent reperfusion injury is placing the tissue at further risk of necrosis and limits functional recovery in a percentage of the ischemic population. While exact mechanisms are still under investigation, the susceptibility of the endothelial cells to oxygenation

following ischemia seems to be enhanced by a history of hypertension, hypercholesterolemia and diabetes[61]. In addition to a reperfusion injury risk following a period of hypoxia induced by occlusion, there is a chance that the blood brain barrier may have lost some of its integrity as a result of the ischemic conditions[62, 63]. In this situation, patients that receive recombinant t-PA, are at risk of hemorrhagic transformation, significantly increasing the chance of morbidity and failure to regain functional independence following the ischemic stroke. This population constitutes 8.8 - 11% of the patients that are eligible to receive thrombolytic medication[63] and are a significant cause of concern when administering thrombolytic medications.

2:4 Imaging Ischemic Strokes

Through the use of neuroimaging, great advances have been achieved in the understanding of the pathology while simultaneously enhancing both acute stroke management and the secondary prevention of ischemic strokes. There are several different neuroimaging modalities available in the repertoire for assessment of acute ischemic stroke patients that will be discussed below, however, the underlying goals are consistent independent of the techniques employed. Initially before progressing to establish evidence of a vascular origin associated with symptoms, intracranial hemorrhage must be ruled out as the cause of symptoms and is typically accomplished through computed tomography (CT). This is followed by identification of the ischemic lesion corresponding with the clinical symptoms while excluding other possible non-ischemic origins. Ischemic lesions identified in this way have been documented to represent distinct patterns that dictate the prognosis of ischemic stroke patients, making it pivotal to assess stroke patients using neuroimaging techniques. This usually includes the simultaneous estimation

of the extent of damage and to identify the benefit to risk ratio of recanalization interventions, accompanied by vascular imaging to ascertain the underlying vascular mechanism of the event, and guide endovascular techniques to open up the occluded artery and reduce the risk of recurrence. While neuroimaging is pivotal in these roles, additional tests exist to assist in the thorough assessment of ischemic stroke patients. These often include electrocardiograms to evaluate the heart for failures that might be forming emboli causing intracranial occlusions, while urine and blood sampling may isolate potential markers indicating stroke mimics such as infections or hypoglycemia causing manifestations of stroke like symptoms. The two most pivotal technologies used routinely in hospitals for the assessment of ischemic stroke remain CT and MRI. While the superiority of MRI is strongly supported, CT is still commonly utilized in stroke assessment. The ultimate goal remains unobscured, to administer thrombolytics as quickly and safely as possible, which ultimately requires the assistance of neuroimaging.

2:4:1 Computed Tomography's Role in Ischemic Stroke

Currently, CT is the more frequently utilized method of imaging ischemic stroke and TIA during the hyperacute and acute phase in most places in the world, including Canada. This is not because CT is superior in imaging infarcted tissue, but rather because of availability, rapid acquisition and suitability for patients with pace makers or any other contraindications to use MRI[64]. Larger infarct volumes are often detected as hypodense brain tissue, permitting CT to detect safety contraindications to interventions as large quantities of infarcted tissue are more susceptible to hemorrhaging upon thrombolytics administration[65]. Although non-contrast CT is not ideal in identifying infarctions within the hyper acute phase or the acute phase as changes can

be subtle or nonexistent[66], it is the most readily available and effective choice in ruling out hemorrhaging or other gross lesions that contraindicate use of thrombolytic therapies[66]. As time progresses through the acute and into the subacute phase (1-7 days following symptom onset), CT accuracy in detecting the edema and mass effect associated with ischemic strokes improves.

CT perfusion (CTP), is establishing itself as important adjunct to CT, which is employed to delineate tissue with disrupted blood flow through the injection of an iodinated contrast material. When CT is unable to see an ischemic region, CTP may reveal an area of diminished CBF, decreases in CBV, and declines in perfusion pressure measured by the calculated mean transit time, effectively differentiating penumbra and irreversibly damaged tissue[67]. Although CTP has not been found to be able to identify the infarct core as accurately as MRI, CTP has improved CT success of accurate stroke assessment[67].

After diagnoses of infarction, the next step is to identify the vessel involved using CT angiography (CTA), an alteration to CT that allows a three dimensional reconstruction of cerebral vasculature (both the arterial and venous system). Large occlusions within the major arteries can be identified using CTA with a high degree of accuracy[68], guiding endovascular intervention and implanting stents. It can also be used to give an idea to the extent of microvascular hypoperfusion and exclude those that are not eligible for aggressive recanalization procedures and identify aneurysms. Recent studies have debunked the common fear that injection of two contrasts for combined CTA and CTP would increase the risk of contrast induced nephropathy and were shown to be no different in toxicity to single exposure to iodinated contrast agents[69]. Safe utilization of combined CTA and CTP serves to enhance CT's diagnostic merit.

2:4:2 MRI Role in Ischemic Stroke

MRI has multiple techniques to acquire images with greater anatomical detail, enhanced differentiation between tissue types, as well as angiographic, spectroscopic and perfusion information. Using these techniques, MRI has increased accuracy and specificity over CT in detecting infarctions and other brain diseases that mimic stroke (e.g. neoplasms, infections and inflammatory diseases) [70]. MRI does not use radiation and echo-planar imaging (EPI, a fast MRI technique capable of acquiring all spatial encoding information after a single radio frequency pulse) based protocols, can be used to achieve 6 minute stroke protocols, reducing the difference in scan times between MRI and CT[71]. However, many imaging sequences utilized in MRI remain slow and the compatibility of a patient to undergo MRI requires thorough screening preventing wide spread use of MRI for stroke assessment, and as such, MRI has most commonly benefited decision making during the hyper acute and acute phases of strokes, when CT is at the lowest efficiency in detecting ischemic events and while the patient is still within the narrow reperfusion window that will possibly yield a clinical benefit.

MRI has four commonly accepted and routinely utilized modalities to localize cerebral ischemia to anatomical structures and are commonly utilized in assessment of ischemic stroke. The first is the application of diffusion-weighted imaging (DWI), which detects infarction within minutes of a drop in CBF significant enough to cause failure in the sodium/potassium pumps [72, 73]. Cytotoxic edema develops as a result of the net shift of water into the intracellular compartments causing neuronal and dendritic beading which involves the enlargement and constrictions of neuronal membranes[74]. This explains the decreases in diffusion through introduction of new barriers and creates the apparent decrease in MD, replacing the previous

conception that only cell swelling causes the decrease in MD and also potentially explains the greater change in MD within WM compared to GM[75]. Because of the restriction in diffusion, the water signal in ischemic tissue is not attenuated as much by the diffusion gradients (method to be discussed in greater detail in Chapter 3), allowing ischemic lesions to be detected as hyperintensities on DWI images. Modifications to diffusion coefficients can be detected with a high degree of accuracy and within minutes of infarction, making DWI the most appropriate choice for clinical confirmation that symptoms are a result of a neurovascular accident and assist in localization of the occlusion, despite the low anatomical resolution DWI achieves[76].

The second technique commonly employed is FLAIR. FLAIR permits excellent tissue differentiation by observing T2 prolongation while also suppressing CSF, making FLAIR optimal to identify previous lesions in which infarcted tissue has been cleared by microglia and other non-vascular diseases that may mimic stroke (e.g. multiple sclerosis). FLAIR is a T2-weighted sequence but can more easily identify cerebrovascular related hyperintensities than normal T2 images and T1 images in the acute/subacute phase[77] because FLAIR eliminates the bright signal caused by CSF. During the acute phase, ischemia and infarction are very apparent on FLAIR as edema continues to build. The transition into the chronic phase (1 month post-ictus) appears as distinct areas of tissue loss on FLAIR as the edema resolves.

Third is magnetic resonance angiography (MRA), which assists in localization of the source causing the reduction in blood flow by detecting and characterizing the presence and degree of stenosis whilst able to identify the existence of emboli or aneurysms. This is achieved by creating a three dimensional reconstruction of cerebral vasculature using MRI with either flow-dependent or flow-independent methods. Generally, CTA is capable of better contrast,

resulting in increased plaque characterization over MRA when evaluating coronary artery disease in both medium and large vessels; while contrast agents implemented to enhance tissue distinction are typically found to be less toxic than those for CTA[67]. While MRA may not specifically identify stenosis in penetrating arteries and arterioles as there is insufficient signal to map these small arteries, MRA may still identify atherosclerotic lesions giving rise to emboli that result in minor and transient stroke symptoms as well as other abnormalities such as aneurysms, occlusions, venous thrombosis and dissections. Identification of vascular diseases within the arteries supplying the brain through MRA enables assessment of which interventions will best suit the circumstances in order to maximize the reduction in future recurrence risk.

An extremely useful technique that has arisen recently to assist in identification of hemorrhaging and microbleeds before administration of thrombolytics is susceptibility weighted imaging (SWI). By exploiting the known susceptibility differences of tissues through the use of phase imaging, enhanced contrast images are created with a distinct sensitivity to venous blood, hemorrhage and iron storage. High resolution SWI can be used to image microbleeds which may reveal patients posing greater risk of intracranial hemorrhage upon receiving thrombolytics and anticoagulants[78, 79]. SWI may yet prove that microbleeds are not always silent and possibly account for a number of TIA mimics[80].

The fourth and perhaps the most pivotal development in clinical stroke assessment has been the introduction of DWI in combination with PWI to delineate salvageable and severely hypoperfused tissue[81, 82]. It is worthy to note that PET remains the “gold standard” imaging modality to detect the penumbra zone, but radiation exposure, complex logistics and costs exceeding those of MRI limit its application[83] while new MRI scanners are incorporating PET. The status of cerebral perfusion can be estimated by exploitation of an IV contrast bolus during

MRI that decreases the T2 relaxation time of water protons through its paramagnetic effects as it travels through brain tissue. The CBF, CBV, mean transit time, time to peak and time of arrival can then be derived to delineate potentially salvageable penumbral tissue from infarct core. It is currently speculated that lesions appearing on DWI represent irreversibly damaged tissue, so upon PWI depiction of larger areas of hypoperfused tissue not seen on DWI, it is interpreted to reflect an estimate of the tissue that is destined to proceed to infarction should reperfusion not occur[84]. Through the application of both DWI and PWI, it is possible to predict the degree of hypoperfused areas thought to be at risk of proceeding to infarction by evaluating the degree of perfusion-diffusion mismatch, enabling an accurate assessment of whether or not it is worth the risk to proceed with aggressive interventions. Advances in perfusion imaging currently seek to replace PWI and the use of its invasive contrast agents by measuring perfusion with sequences that label blood without the injection of tracers (e.g. arterial spin labeling, ASL). ASL does not rely on an invasive contrast agent, can selectively label individual vessels in order to determine their contribution to the overall blood supply and resolution can be enhanced further than traditional dynamic susceptibility contrast-based techniques[85], increasing accuracy of identifying perfusion deficits[86].

2:5 Transient Ischemic Attack

Transient ischemic attack is commonly known by the public as a warning stroke. TIA is a significant public health concern with an incidence of 68 Canadians a year being diagnosed per 100 000 people in 2004[87]. In the United States, nearly half of the population will report a brief episode of transient neurological symptoms at some point in their life[88] and is in fact often a

predictor of stroke, preceding ischemic strokes in 23% of the cases[89]. This translates to roughly 200,000 to 500,000 TIA diagnoses by clinicians a year in the US alone, while it is speculated 300,000 to 700,000 people do not seek medical attention for their transient focal loss of brain function[90].

A TIA is thought to be caused by minute emboli arising from similar mechanisms that cause ischemic strokes or in situ occlusion of small perforating arteries. Associated symptoms are only temporary because occlusions are thought to be lysed by normal body mechanisms or collateral blood flow restores sufficient perfusion to the ischemic tissue before infarction occurs[91]. The degree of permanent damage after occlusion is dependent upon the time required to dissolve the emboli or the degree of perfusion collateral blood flow maintains. The previous definition set out by the World Health Organization characterizes TIA as the sudden onset of clinical neurological deficits that dissipate in less than 24 hours without a clear nonvascular cause, a time based definition founded upon the transient nature of focal ischemic symptoms[92]. Diagnosis by a clinician requires their best judgment as to whether the patterns of signs and symptoms are elicited by a specific arterial zone. However, most do not receive medical attention until after their symptoms have resolved, in fact, it is estimated that only 0-7 % could ever be examined at the peak of their symptom manifestation[93, 94]. This is because the majority of TIA symptoms never exceed 10 minutes[95]. Often, many patients recall vague details of their transient loss that is not enough to enable localization of an afflicted arterial zone. This makes TIA a diagnostic dilemma that could have a significant false-negative diagnostic rate when based upon clinical judgement alone[96-98]. Early and accurate diagnosis is essential as despite symptoms being transient in nature, patients diagnosed with TIA are at a high risk of secondary strokes[73, 99].

The notion that TIA symptom manifestation and subsequent dissipation did not have any permanent effect on cerebral tissue was held until significant advances in neuroimaging changed the perception of the disease. DWI (Chapter 3) revealed permanent damage at the tissue level in a portion of the population, demonstrating that the clinical event was not necessarily transient. These instances of permanent cerebral infarction on DWI were observed in a range of 21 – 67 % of patients with the diagnosis of TIA, creating uncertainty in what is occurring in the other one to two thirds of the population[100]. Ischemic lesion damage confirmed in a portion of the population directed the proposition of a tissue based definition by the TIA Working Group[101]. In order to be classified as a true TIA, a patient must demonstrate a brief episode of neurologic dysfunction that can be localized to a specific arterial zone and does not possess evidence of acute infarction as officially re-defined by the American Heart and Stroke Association in 2009[102]. Those that are associated with brain infarction are classified as minor acute ischemic stroke and receive appropriate intervention to decrease the risk of recurrent stroke despite their transient neurological events. Following the implementation of a tissue based definition of TIA, the incidence of stroke increased by 7% while reducing incidence of TIA by an estimated 33%[103]. TIA infarcts are most often very small penetrating infarctions but can be larger when found in relatively silent brain regions; because of this, TIA infarcts have been called `footprints` of infarction[93]. This suggests that both volume and the presence of infarcts determines whether or not a complete and rapid recovery will occur or not, accounting for the transient nature of TIA.

The reclassification of TIA to a tissue based diagnosis, does not alter the clinical significance of TIA without infarction, as patients diagnosed with TIA are at high risk of stroke[73, 99, 104]. The risk of ischemic stroke for patients diagnosed with TIA is similar to occurrences of recurrent stroke in ischemic stroke patients within the first two days of symptom

manifestation and is highest within hours of TIA, with the risk estimated to be 12% within the first week and exceeding 21% within the first month[99]. Nearly two thirds of recurrent strokes occur in the first 48 hours of initial transient ischemic event[105]. Because of this high risk in TIA, treatment involves rapid identification of the source of occlusion in order to minimize the risk of reoccurrence. It has become essential to identify TIA patients with a lesion as quickly as possible, as the risk of recurrent stroke can be reduced by up to 80% should they receive urgent and efficient intervention therapies while they`re still within the treatment window[106]. The 7-day risk of recurrent stroke is even believed to be higher in TIA with confirmed infarction than ischemic stroke[106]. The short term prognostic estimates have caused some to call for the creation of ischemic syndrome classes that identify their prognostic differences[107]. These categories would prevent changing diagnosis of TIA patients found to have cerebral infarction to ischemic stroke, but rather transient symptoms with infarction[107, 108] as they are the most unstable amongst the three phenotypes.

Managing the risk of subsequent stroke in TIA patients both with and without evidence of permanent cerebrovascular tissue damage initially focuses on controlling the risk factors to prevent recurrence (e.g. addressing hypertension, glycemic control, treating dyslipidemia with statin therapies, etc.). The frontline medication for prevention of subsequent stroke for non-cardioembolic TIA is considered to be aspirin, which has been shown to be effective in reducing the risk of stroke and TIA[109] while other antiplatelets can also be administered. Aspirin does not treat the source of the primary event, only prevent the formation of subsequent clots. Anticoagulants such as warfarin can be given to TIA patients presenting with evidence of a cardioembolic source. However, identifying TIA patients with small volumes of permanent tissue damage not only alters their diagnosis to that of minor ischemic stroke, but also the

approach to their therapeutic management. These patients are at a greater risk of subsequent stroke, especially if evidence of intracranial vessel occlusion is established[106]. Identifying small ischemic lesions using MRI warrants the immediate hospitalization of TIA patients for complete diagnostic evaluation in order to search for the specific underlying etiology and begin the most appropriate preventative treatment. For example, identifying TIA patients with atherothrombotic disease either extracranially or intracranially may sanction carotid endarterectomy or the use of endovascular therapies. Thrombolytics are only administered if the hospitalized TIA patient develops a stroke within the first 24 – 48 hours after diagnosis because of their rapidly resolving symptoms and risk of hemorrhagic transformation, making it imperative to identify an ischemic lesion in order to retain a TIA patient for careful monitoring.

An intriguing subclass of TIA has been distinctly identified as capsular warning syndrome, which is often used to describe reoccurring lacunar TIAs. Symptoms are transient but occur in multiple instances within a single day. Cerebral small vessel disease of one of the lenticulostriate arteries is presumed to be the mechanism while atherosclerotic disease of the MCA and emboli from the heart may have a role as well[110-114]. Capsular warning syndrome, like TIA is associated with high risk of subsequent stroke with a reported lacunar stroke risk of up to 40% within 10 days, exceeding that of regular TIA[114]. Such patients are typically treated with antithrombotic agents, however the resolution of capsular warning syndrome TIAs caused by stenosis of the MCA using intracranial angioplasty instead of thrombolytics has been reported to be successful[113]. This subclass of TIA is important, because like TIA, they may have small infarctions that are invisible on current DWI with low spatial resolution.

2:5:1 Transient Ischemic Attack Mimics

As briefly eluded to previously in this chapter, the true difficulty in diagnosis of TIA is based upon the overall judgment call made by the physician overseeing the patient. They must consider the symptoms and onset times that are often recalled either by the patient or those that witnessed the initial manifestation as they typically resolve within the first 10 minutes[95], and then attempt to make a definitive diagnosis of transient cerebrovascular disease as the most likely culprit causing previous symptoms in order to begin any efficient form of intervention. However, there are potentially other sources that afflict cerebral tissue that mimic stroke neurological deficits that are difficult to clearly ascertain an afflicted arterial territorial zone (e.g. isolated vertigo, dysarthria or hemisensory disturbance) [91]. Adding to these complications, TIA are but one of the many causes that induce transient focal neurological attacks. These are referred to as TIA mimics and can be difficult to rule out, but are important to be aware of in order to try and distinguish from cerebrovascular disease as they have distinct etiologies and prognosis, while TIA has a distinct risk of future stroke should they not receive early intervention making early, differential diagnosis paramount. TIA mimics are the source of disagreement amongst clinicians when making a definitive diagnosis of TIA, highlighting the necessity to create more effective neuroimaging techniques to account for a number of MRI negative TIA[111-113, 96-98, 115, 116].

Multiple sclerosis rarely presents with stroke like manifestations but there are cases where the patient presents with rapid initial progression of aphasia, deafness or hemiplegia, resembling TIA or minor stroke[117-119]. In these cases, authors report using DWI to differentiate as multiple sclerosis lesions occasionally appear hyperintense on b1000 images but have no

corresponding reduction in MD. The concerns with using DWI to differentiate between pseudostroke form of multiple sclerosis and stroke is the reports of neuroradiologic diversity in MS lesions, as there are case reports of recent multiple sclerosis lesions presenting with reduced MD[120]. Gass et al proposed that MD may be reduced in recent multiple sclerosis lesions because of inflammatory cytokines inducing mitochondrial dysfunction, resulting in cytotoxic edema[121], while it has also been speculated that pathogenesis of multiple sclerosis should be considered to be a result of vascular injury and would mimic ischemic lesions in the acute phase[122, 123]. The absence of elevated levels of immunoglobulin G within blood serum and no prior indications of temporal or spatial dissemination abnormalities are considered to be essential clinical evidence in order to confirm cerebrovascular accidents in patients presenting with stroke like multiple sclerosis[124].

While microbleeds have been found to be associated with TIA and ischemic stroke in 24% of the cases[125] and are a key marker of cerebral small vessel disease[35], microbleeds have also been speculated to be a potential TIA mimic or potentially suggest that TIA may not have to be ischemic in nature as it has been postulated that not all microbleeds are neurologically silent[126, 127]. The small degree of hemorrhaging and accompanying edema caused by the minute disruption in the vascular wall can cause both disruption and compression of adjacent cerebral tissue resulting in neurological dysfunction. Small amounts of blood escaping the endothelial layer may potentially clot and be cleared by the body or hypertensive conditions may be controlled causing neurological deficits to dissipate.

Detecting the presence of cerebral microbleeds causes some clinicians to hesitate when considering administration of anticoagulants or thrombolytics, as impairing platelet function may

aggravate the situation, putting patients presenting with microbleeds at risk of intracranial hemorrhage and an agreement as to whether or not this risk exists has not been fully established[128]. These patients are especially at risk if they present with WM hyperintensities as they may have cerebral amyloid angiopathy which further increases risk of hemorrhaging[35]. While numerous studies have searched for a connection between atherothrombotic or cardioembolic stroke with microbleeds and increased incidences of hemorrhagic transformation, the relationship has continued to prove to be controversial and convoluted[129, 130]. Thus, identification of microbleeds either causing the transient ischemic symptoms or the association of microbleeds with TIA is important before initiating intervention.

Complicated migraine without headache and partial seizures are considered to be the more common forms of TIA mimics but are ordinarily differentiated from TIA based upon the time course of the symptoms[35], as TIA symptoms typically display a spontaneous and sudden onset rather than a gradual progression or spreading. However, the symptoms, risk factors of cerebrovascular disease and vague onset recollection may convolute the decision making process, particularly when MRA and DWI images or other neuroimaging tests come back without revealing any abnormalities[131]. Symptoms more commonly associated with TIA are often negative presenting rather than positive, assisting in differential diagnosis and are depicted in Table 1 with their respective frequencies.

Table 1 : Clinical Symptoms of TIA vs. TIA Mimics Table from Transient Ischemic Attack: Part I. Diagnosis and Evaluation[132].

Clinical Symptom	Percentage of TIA Mimics	Percentage of TIAs
Unilateral paresis	29	58
Memory loss/cognitive impairment	18 - 26	2 - 12
Headache	15 - 23	2 - 36
Blurred vision	22	5
Dysarthria	13	21
Hemianopia	4	4
Transient monocular blindness	0	6
Diplopia	0	5

Seizures have also been documented to appear as a stroke, demonstrating sudden onset neurological symptoms with accompanying perfusion deficits[133]. This makes differential diagnosis difficult, as the only marker of seizure is the atypical vascular territories afflicted with perfusion deficits following cerebral hyperactivity. There remain to be many other potential TIA mimics to be aware of when diagnosing TIA. These include: syncope, anxiety related, transient global amnesia, bells palsy, subdural hematoma, intracerebral hemorrhage, brain tumors (e.g. meningioma, hemorrhagic melanoma metastasis and multiple cerebral metastases)**,** cervical disc disease, multiple sclerosis, cerebral venous thrombosis, hypoglycemia, drugs, and compression disorders[35].

Chapter 3

Diffusion-Weighted Imaging

3:1 Diffusion of Water Molecules

Robert Brown was acknowledged in 1828 to be the first to describe the random, yet constant motion of water molecules (through his observation of the random movement of pollen-grains when submersed within water) when at a temperature above absolute zero (i.e. > -273.15 °C). This molecular phenomenon is thermally driven and is now commonly referred to as Brownian motion in honor of Brown's observations. If it were possible to specifically monitor an individual molecule of water amongst many others over time, the longer we observed this molecule, the further it would be perceived to have traveled in a seemingly random path. However, there is an equal probability of this molecule traveling in any direction; therefore the average displacement over time would have to remain equal to zero. It is through the contribution of Albert Einstein that permits us to mathematically describe Brownian motion on the order of 10 microns, with the degree of movement each water molecule experiences being approximated by solving for the diffusion coefficient *D*. The displacement of water in one dimension over time (t) is given by:

$$\text{Displacement} = \sqrt{2D\text{t}} \qquad (2.1)$$

Diffusion is random and therefore *D* is directionally independent, or termed to be isotropic in nature. Recall that diffusion is thermally driven, making the magnitude of *D* at least partially dependent on temperature, but can also be attributed to the size of the molecule in question while also considering the viscosity of the solvent or medium in which the molecule is located. Because the primary constituent of the solvent for water molecules in mammal bodies is water, the proper terminology to describe the diffusion of water in tissue is self-diffusion and considered to be at body temperature (i.e., 37°C), making *D* in free water roughly equal to 3.04 x 10^{-3} mm^2/s. Throughout the remainder of this thesis, use of the term diffusion, refers to the self-diffusion of water molecules.

3:1:1 Measuring Diffusion in the Cerebrum

As one might suspect, water contained within a biological system does not behave in the same manner as in a petri dish full of water, as water cannot freely diffuse without interaction with other structures and molecules. There are many semi-permeable extracellular and intracellular barriers to take into consideration when evaluating diffusion including cellular membranes, cytoskeletons and organelles that cause diffusion to deviate from free isotropic diffusion. Hence the term apparent diffusion coefficient (ADC) used to describe the net effect of this restriction on water diffusion that is time dependent in tissue. When the diffusion of water is directionally dependent, it is considered to have adopted anisotropic diffusion. It is relevant to consider the physiological makeup of the four major tissue types when considering water diffusion in the brain:

Gray matter (GM) comprises the cerebral cortex which spans the surface of the cerebral hemispheres and the cerebellum, as well as the subcortical nuclei (e.g. thalamus, basal ganglia). The GM is differentiated into six horizontal layers consisting of neuronal bodies that connect to form cortical columns (**Figure 5**), which also contain glial support cells with the most abundant being the astrocytes (also the most abundant cell throughout the entire cerebrum). There are more than 100 000 million neurons within the GM corresponding to a width of only 1-5 mm yet composes 45% of the total volume in the adult brain[134]. This creates a relatively high degree of complexity within the tissue and often resembles a relatively more isotropic diffusion environment.

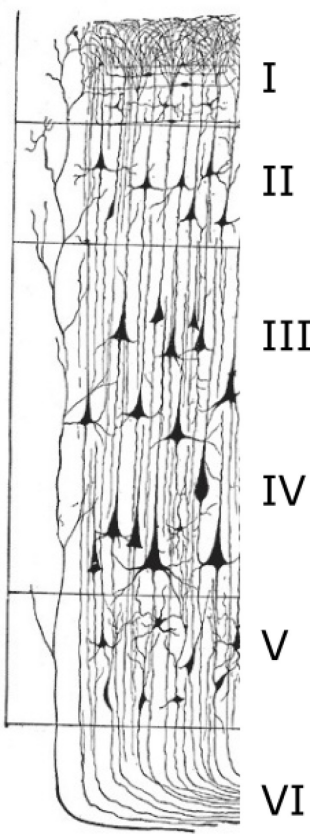

Figure 5 Layers of the Cerebral Cortex – Representation of the six cortical layers from the visual cortex. Layers 1-6 contain the cell bodies of the neurons within the brain and lack myelin, resulting in the gray color owing to the name. The high degree of complexity resulting from dendrites and cell bodies is clearly shown and accounts for the relative lack of anisotropic diffusion. Following the sixth layer, the WM tracts exit carrying the information from the cell bodies to other portions of the brain and demonstrate the highly ordered structure, creating the anisotropic diffusion detected by diffusion sensitizing gradients.

Modified from Grays Anatomy[135]

White matter (WM) is highly organized tissue composed of axons and oligodendrocytes that provides connections to and from the cerebral cortex and subcortical regions to both proximal and distal portions of the brain and body. A single oligodendrocyte can sheath one or multiple axons in myelin, creating the white appearance owed to the high fat content in myelin and acts to speed the conduction velocity of action potentials. The myelinated axons comprise up to 35% of the

volume in the adult brain and spans up to 118000 km [136]. The high degree of organization of axonal bundles within the brain creates a relatively anisotropic environment.

Cerebral spinal fluid (CSF) is created by the choroid plexus within the ventricles of the brain, and bathes the brain and spinal cord. CSF typically occupies a total volume of only 150 mL, representing 10% of the total brain volume and is 99% water. CSF largely reflects blood plasma, as it is created from blood supplying the choroid plexus with the exception of being nearly protein free and possessing elevated electrolyte levels. Due to the continuous flow and the majority of the contents being water, CSF reflects a largely isotropic diffusion environment and as such *D* would be closer to that as in free water (3.0×10^{-3} mm^2/s).

Blood comprises the final 10% of the total brain volume, supplying both the primary energy molecule (i.e. glucose) and final electron acceptor (i.e. oxygen) for neuronal metabolic demand in the brain. 15-20% of the total cardiac output is sent to the brain because of its high metabolic demand, despite its small weight relative to the rest of the body.

Axonal membranes act to impart the greatest restriction to diffusion and create anisotropy in the brain[137] with even further restriction imparted by the less permeable lipid bilayer of myelin sheaths. While the GM is organized into layers and columns of neuronal bodies, the dendrites are tangled and act to reduce the coherency of the architecture in a seemingly random fashion. For this reason, the cortex tends to clearly and consistently demonstrate less anisotropy then the organized fasciculi or bundles of myelinated axons within the WM. Overall, a small degree of anisotropic diffusion is indeed present in GM [138-140] and to a much larger extent within WM, however MD values are similar (GM = 0.8-1.0 x $10^{-3}$$mm^2/s$, WM = 0.67 - 0.88 x 10^{-3} mm^2/s), while being primarily isotropic in the ventricles containing CSF creating distinct tissue contrast when conducting MRI experiments[141-144].

3:1:2 Measuring Diffusion with Magnetic Resonance

The spin-echo was first described by Hahn in 1950[145], shortly after the first paper measuring *D* in water samples using quantitative T2 measurements belonged to Carr and Purcell[146]. Introduction of the pulsed gradient spin-echo (PGSE) sequence came about in the sixties through the work of Stejskal and Tanner[147] and thus facilitated the quantitative measurement of molecular diffusion coefficients. In 1973, the first 2D MRI images were generated through the application of gradients to the MR technique by Paul Lauterbur, which was shortly followed by production of 3D MRI images[148, 149]. While the first diffusion images were presented by Denis Le Bihan in 1985[150], it wasn't until the echo-planar imaging (EPI) technique was developed by Peter Mansfield that MRI images could be acquired in a seconds rather than hours[151] enabling the eventual transition to practically and safely study the diffusion of water molecules in human subjects through the combination of EPI and diffusion[152].

The basic concept behind measuring diffusion using DWI is to encode the spatial position of water molecules (spins) at $t = 0$, invert the spin phase with a 180 degree radiofrequency (RF) pulse, and decode the spin position after allowing time for water molecules to diffuse (Δ). Encoding and decoding the spatial position is accomplished through the use of magnetic field gradients. This specifically works through a spin-echo technique, which initially places the net magnetization in the *x, y* plane with zero-phase through the use of a 90° RF pulse, at which point a magnetic field gradient is turned on with an amplitude of *G* and for a duration of δ. This gradient acts to impart a phase shift to the spins according to their current spatial position and the strength of the gradient. By applying a 180° RF pulse at this time, the phase shift of the spins becomes reversed to that of which the first gradient induced, otherwise the second gradient must

be applied in the opposite direction as it was when the method was initially produced. Application of a second magnetic field gradient also with amplitude *G* for duration of δ after an allotted time period Δ (diffusion time), forces spins to re-gain their original phase if they have not deviated from their original encoded spatial position. For spins that have deviated during the time period between the application of the two gradients (i.e. diffusion), the spins will be subjected to a different magnetic field strength than that which it was originally subjected to and does not completely return the spin to its original phase, causing an attenuation of the measured MR signal[153]. A spin that undergoes a larger displacement (i.e. a hydrogen molecule within an isotropic environment) will experience a greater phase shift, resulting in increased attenuation and will appear lower in signal intensity (e.g. CSF). A basic wave form of the diffusion technique can be seen in Figure 6.

The sensitivity to diffusion using a PGSE sequence can be modified by altering characteristics of the sequence. One such alteration is through the application of larger gradient amplitudes through the use of stronger gradient coils (i.e. increase *G*). Larger amplitudes of G increase the amount of phase change detected because less motion is required to experience a different magnetic field. Another alternative lies in modification of the amount of time spins are allowed to diffuse before application of the second magnetic field gradient, which serves to increase the probability for the spins to de-phase. PGSE sensitivity to diffusion can be expressed as:

$$b = \gamma^2\delta^2G^2(\Delta - \delta/3) \qquad (2.2)$$

Diffusion time is represented by Δ - δ/3, where δ/3 is the correction that accounts for the diffusion taking place during the time period the gradients are active[10]. The gyromagnetic ratio

(the ratio of the angular momentum of a proton and that protons magnetic field strength) of hydrogen protons (42.58 MHz/T) is represented by γ.

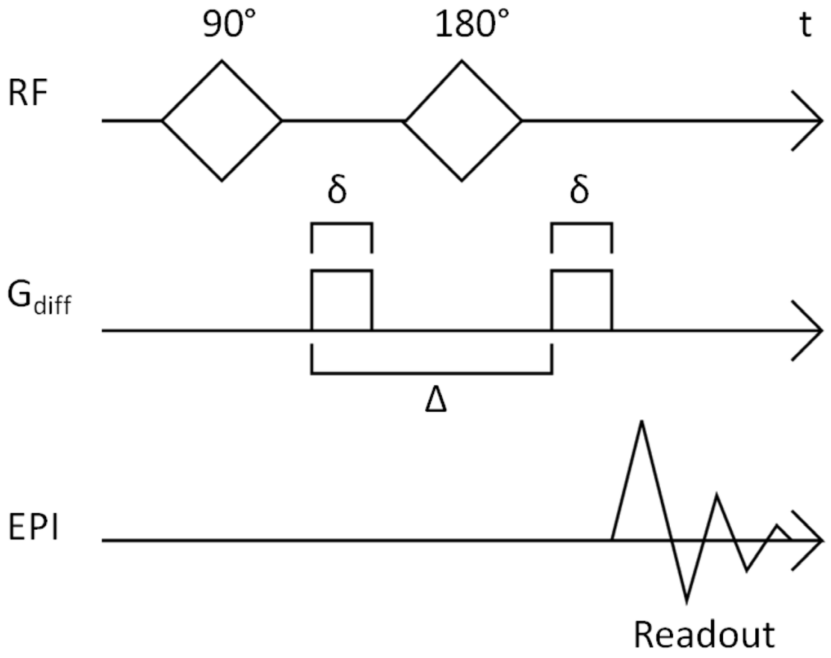

Figure 6 Pulsed Gradient Spin Echo Sequence – The basic conceptualization of diffusion sensitizing gradients applied for a time δ, with a diffusion time Δ, which can be applied along any imaging direction to sensitize the measurement of diffusion in that direction, followed by the detection of the signal.

The amount of signal available in an MR experiment using PGSE sequences sensitive to diffusion decays exponentially according to *D* and can be expressed as:

$$S/S_0 = e^{-bD} \tag{2.3}$$

Where *S* is the signal intensity acquired when the diffusion magnetic field gradients are active while S_0 represents the signal intensity of the spins obtained in the absence of any diffusion magnetic field gradients, and makes the assumption that both images are acquired with the same echo time.

3:1:3 Production of DWI Images

Typically, to begin construction of a set of DWI images, a baseline b_0 is acquired through the inactivation of diffusion sensitizing gradients. The b_0 image represents the S_0 in equation 2.4. This is followed by acquisition of images representing diffusion in the respective direction they were taken in and are commonly referred to as source images. In order to calculate a rotationally invariant measure of mean diffusion, *D* must be measured in at least three orthogonal directions. As such, source images typically represent *D* in the *x*-, *y*- and *z*- axes achieved through the activation of diffusion sensitizing gradients individually in the respective direction (*Dxx, Dyy,* and *Dzz*). Modern techniques acquire source images in 6, 12, 20 or more directions to enable characterization of anisotropy in the brain with arbitrary orientation relative to the primary gradient coil axes. The signal intensities in the respective directions (and any given combination of directions) are given by:

$$S_x = S_0 e^{-bDxx} \quad S_y = S_0 e^{-bDyy} \quad S_z = S_0 e^{-bDzz} \tag{2.4}$$

From this, the source images are combined into a final set that can be used for diagnostic purposes and can now officially be labeled as trace images, or diffusion-weighted images (**Figure 7**).

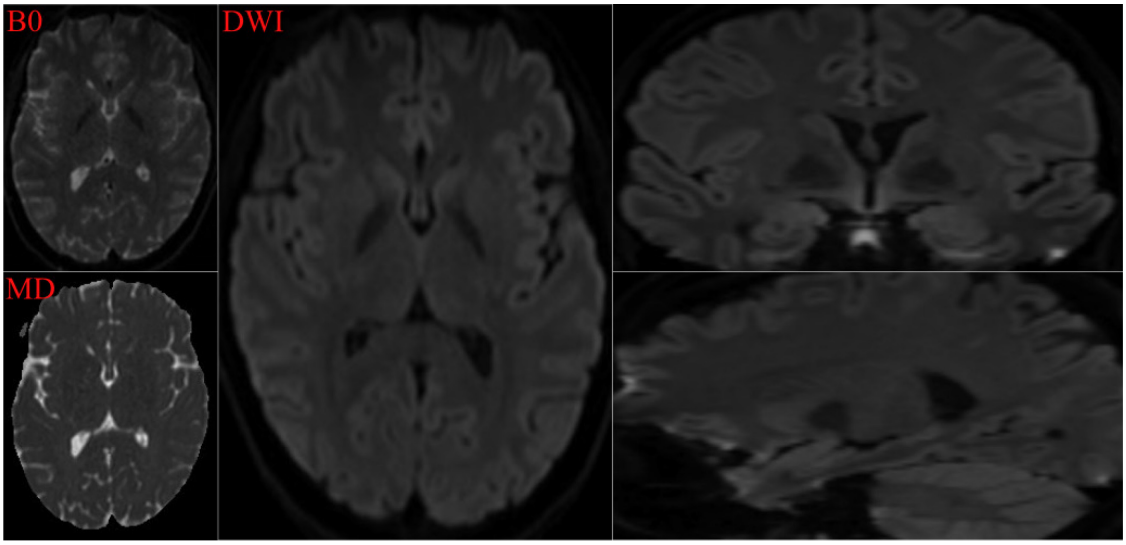

Figure 7 Construction of DWI Images – Healthy 27 year old female imaged at 3.0T. B_0 images take into account tissue signals and contrast in the absence of diffusion gradients to properly estimate the ADC, while the measurement of diffusion in 3 or more directions, enables combination and averaging to create DWI and MD maps. The DWI data was acquired using in plane resolution of 1.5 x 1.5 x 1.5 mm^3 and allows reconstruction of axially acquired images into coronal and sagittal images. Excellent tissue differentiation can be seen using high resolution (e.g. WM/GM differentiation and clarity of putamen, globus pallidus and caudate) while cortex clarity is excellent.

This is performed by matrix algebra where it is the sum of each directional element within the array. The average value is then taken to reduce multi-directionality diffusivity which represents the MD and is given by:

$$MD = (D_{xx} + D_{yy} + D_{zz})/3 \tag{2.5}$$

From equations 2.4 and 2.5, the rotationally-invariant signal intensity of the DWI images is given by:

$$S_{DWI} = \sqrt[3]{SxSySz} = S_0 e^{-b*MD} \tag{2.6}$$

Application of diffusion sensitive PGSE sequences (i.e. DWI) naturally lead to the already discussed observation that diffusion in a biological system is in fact restricted by many biological barriers. Viscosity and temperature were already known to impact diffusion, but it

seems that the third variable to consider was cellular membranes, which act as semi permeable barriers to diffusion. The first proposition to begin quantifying the degree of diffusion restriction imparted by biological barriers was made by Tanner and Stejskal, which involved varying the delay between gradient pulses[154] and using strong gradients over short periods of time (δ). The term ADC was created shortly after, and account for the fact that the "true" *D* will be reduced in biological tissues. It is the ADC that permits researchers to draw quantifiable inferences about the microstructures within biological tissues (**Figure 8**).

MD maps are useful in the identification of acute ischemic lesions, as a phenomena exists that must be taken into consideration when using DWI to identify acute infarcts known as T2-shine-through. T2 shine through is a product of T2 prolongation effects, to which DWI is susceptible to because it is largely T2 weighted due to the long echo times[155]. In contrast, the contribution of T2 relaxation is not present in the calculation of MD maps and as such, is free from the effects of this phenomenon.

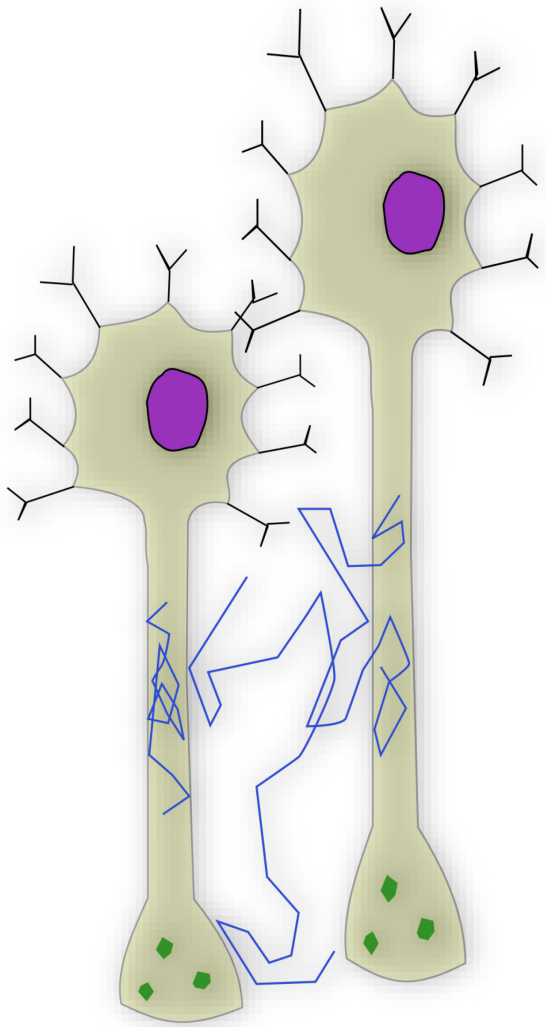

Figure 8 Apparent Diffusion of Water in a Biological System - Random movement of water is partially restricted by semi permeable membranes both intracellularly and extracellularly in a healthy neuronal environment. Intracellular organelles and the lipid bilayer prevents water from freely diffusing and results in deviation from an isotropic diffusion environment.

Application of DWI to infer physiological functions is based upon the signal detected. Tissues with high *D* are attenuated and appear hypointense on DWI (e.g. CSF) but hyperintense on MD maps. Conversely, tissues with relatively restricted diffusion appear hyperintense on DWI (e.g. stroke lesion) but hypointense on MD maps. This is relevant to studying human physiology because any pathologies that might modify diffusion of water will appear quite

obviously on DWI and MD images as changes in signal intensity (strokes, the focus of this thesis is one such pathology).

3:2 DWI Role in Pathologies

Diffusion-weighted imaging is commonly applied to study the diseased and healthy brain. But what do changes in MD allow researchers to interpret about the underlying physiology and microstructure of the brain and which disease states would DWI be most applicable to study? It is speculated that DWI success in detecting lesions in an ischemic stroke patient is owed to diffusion restriction caused by failure of sodium potassium pumps, induced by a deficit in cellular levels of adenosine tri-phosphate (ATP) that results in an influx of water, trapping it intracellularly[75]. This phenomenon is referred to as cytotoxic edema and is characterized by neurite and dendritic beading of individual cells within the brain[74, 75]. However this only explains diffusion restriction within the dendrites. Recent evidence implementing oscillating gradient spin echo diffusion techniques probes shorter diffusion times and suggests that microstructural alterations are also a product of neurite beading, causing greater reductions in MD of ischemic lesions in WM than GM[75]. Both swelling and beading prevent water molecules from diffusing as rapidly relative to normal extracellular and intracellular conditions causing signal attenuation.

Currently, DWI has become a routine examination sequence for multiple clinically relevant pathologies involving both the brain and spine[156]. Traditionally, the highest clinical value has been attributed to routine assessment of acute ischemic stroke, as tissue damage due to ischemia can be detected within minutes. But DWI has begun to have an impact in detection of other neuropathologies including intracranial infections and tumors, while demonstrating

potential to improve detection and characterization of clinically relevant lesions in multiple sclerosis patients[157]. DWI has been reported to be successful in detecting and differentiating types of lesions unique to patients that have developed toxoplasmosis following bone marrow transplantation[158], while viral encephalitis[159] and Rasmussen encephalitis[158] have similarly reported success in detecting early cytotoxic edema likely because of shared physiological mechanisms of cell degradation. These physiological conditions likely include congestion, lymphatic perivascular cuffing (i.e. leukocyte aggregation) and pathological thrombus formation which all prelude cytotoxic edema. As referred to previously, diffusion tensor imaging data can be easily acquired by increasing the number of diffusion gradient directions. This enables the study of changes to diffusion in the white matter tracts of the brain which have been associated with normal and abnormal aging, multiple sclerosis, and fetal alcohol spectrum disorder amongst many others.

DWI has become the most reliable diagnostic imaging tool in assessment of acute ischemic stroke because of its greater sensitivity over CT and is the preferred technique of evaluation in patients with minor stroke and TIA[160, 161]. The accuracy and specificity of DWI detection of acute cerebral ischemic lesions exceeds 90%[162, 163] and is becoming increasingly utilized because DWI provides a SNR contrast sufficient for imaging punctate infarcts[165] while simultaneously providing information on the age of an ischemic lesion (e.g. hyperacute and acute versus chronic)[164]. DWI has been shown to be sensitive to the detection of small infarcts very early after manifestation of clinical symptoms, with reports suggesting success within minutes of arterial occlusion[165-167], while it may take up to 6 hours to reveal infarcts on other conventional (T1,T2, and FLAIR) MRI sequences and may even exceed days to become appreciable on CT.

3:2:1 Imaging Artifacts/ Shortcomings of DWI

Optimizing the MRI acquisition for speed has consequences that most commonly come in the form of artifacts within the data, and therefore must be accounted for when conducting an MRI research study. The first major forms of artifacts arise from the drawback of in vivo imaging of live subjects. DWI pulse sequences are designed to detect molecular motion, but as one would expect when studying human brains, the person may consciously or unconsciously shift during the image acquisition period causing motion on a relatively large scale. This first major distortion caused by subject motion is known as bulk motion. Bulk motion can come in the form of spontaneous muscle twitches or conscious head movement and for obvious reasons create large distortions because of the scale of movement DWI is sensitive to. These distortions often come in the form of ghosting artifacts but are not limited to ghost artifacts, as each echo in an acquisition can be perturbed differently. Restricting patient motion is possible and commonly performed in regular routine scanning, but can become uncomfortable if too excessive.

Single-shot techniques such as echo planar imaging (EPI) do reduce motion induced artifacts because the data for each slice is acquired in a single shot, but is often accompanied by reductions in image quality in the form of motion blurring and low resolution. However, the image quality reduction through the use of EPI can be mitigated through use of parallel imaging techniques such as generalized autocallibrating parallel acquisitions[168] (GRAPPA) and was utilized in the DWI sequences used in Chapter 4 for this very reason. An additional, subtle form of motion accompanies imaging of live biological subjects that must be accounted for arises from normal physiological phenomena, such as low amplitude brain pulsations caused by breathing

and the normal cardiac rhythm[169]. A common method utilized in the literature to mitigate the effects of normal physiological functions involves timing the acquisitions of each image with the pulsation waves (e.g. 500 ms after the R wave of a normal sinus rhythm), minimizing pulsation artifacts and reducing overestimation of MD (recall MD values reflect the degree of water movement and would appear to increase in value when averaged with physiological rhythms, indicating higher than normal diffusion); cardiac gating acts to extend the acquisition time which often precludes its use clinically[170, 171]. As such, the lack of cardiac gating to account for cardiac pulsations for the work in Chapter 4 was not deemed as a limitation as the quality of images was excellent and permitted shorter scan times.

A second potential source of imaging artifacts arise from another drawback involving the EPI sequence implemented in DWI. These come in the form of magnetic field inhomogeneities. Magnetic field inhomogeneities cause artifacts that are most apparent near tissue interfaces that possess vastly different magnetic susceptibilities, such as air and tissue within para-nasal sinuses or the base of the skull. The manifestations of distortions is exacerbated at higher magnetic field strengths but can be adjusted for by implementing published methods that reduce off-resonance artifacts[172-175].

As referred to above, another potential source of artifacts comes from a phenomenon referred to as eddy currents and arises from application of the diffusion sensitizing gradients themselves. The fast alternating gradient activations generate residual magnetic fields (i.e. eddy currents) and act to adversely affect the main magnetic field by adding or subtracting from it in an uncontrolled fashion, resulting in image translations and geometric distortions. Eddy currents can be reduced by compensation of the diffusion gradients shape and using gradient shielding technologies, producing less image translations and geometric distortions. Eddy currents can also

be reduced by implementing a twice refocused, single shot EPI sequence[176], a simple modification of the Skejskal and Tanner spin echo sequence.

There are a couple of consequences to be aware of when using high strength, magnetic fields to create images of the brain. Because DWI is T2 weighted, tissue that possess long T2 decay times, permits the scenario where T2 signal can `shine through` on the DWI image and create the impression that an ischemic lesion is present. In order to combat this, MD maps must be calculated in order to confirm the presence of acute ischemic lesions as they are independent to the influence of T2 shine-through[177]. A technical drawback from increasing the magnetic field strength involves shortening of T2 values, which requires the careful maintenance of short echo times or additional T2 decay (i.e. signal loss) will occur. The next complication involves safety contra-indications to scan as it is estimated that 10% of the population is ineligible to safely enter an MRI[178]. While patients with metallic implants (e.g. cardiac pacemakers) or any other foreign metal objects that have been deemed unsafe within their bodies prevents them from safely entering MRI for obvious reasons. Despite the neuroimaging technique being free of ionizing radiation, other complications can arise and prevent them from MRI. These include claustrophobia, fear of the loud noises from gradient coil activation and physical restriction for patients that are too large to enter the small bore of the magnet. In Canada, clinical access to MRI is a substantial problem as wait times for MRI, while dependent on prioritization, range from weeks to a year and may delay or even prevent definitive treatment[179].

Despite many of the technical advances in diffusion MRI, large voxel size, large slice thickness and use of between slice gaps are still implemented in order to limit acquisition time of scanning ischemic stroke patients. As Chapter 4 will explore, the limitations imposed by acquisition parameters optimized for rapid imaging decreases the accuracy of depicting and

characterizing ischemic lesions in acute ischemic stroke and TIA. As new MR technologies and techniques emerge, it will become increasingly feasible to image ischemic stroke patients and TIA in reasonable acquisition times without having to sacrifice spatial resolution.

3:2:2 Relevant Literature to Imaging Ischemic Stroke and TIA

As described above and in the previous chapter, many imaging modalities exist to assist in the diagnostic process of ischemic stroke. MRI possess many advantages over conventional CT and perhaps the greatest interest lies in what information MRI can ascertain in TIA and minor ischemic stroke, especially when typical neuroimaging fails to detect abnormalities. There is a strong drive in research to develop improvements to MRI sequences used for clinical purposes that may lead to better treatment and understanding of diseases such as stroke.

For example, implementation of cutting-edge hardware has huge implications to the improvement of MRI sequences. One such technical advancement pertaining to DWI and PWI is implementing them at high magnetic field strengths greater than 1.5T, with clear superiority to those acquired from 1.5T scanners through the creation of additional SNR which can be "spent" increasing resolution and quality of imaging sequences or decreasing scan times[180-182]. Normally, longer scan times are required in order to increase the quality and resolution of acquisition parameters of an MRI sequence; but this is mitigated through taking advantage of scanners with a higher B_0. This is relevant to the role of diffusion imaging in stroke assessment as speed of acquisition is of utmost importance. This has revealed the potential for differences in the diagnostic utility of different strength scanners, particularly when using the combination of PWI and DWI when evaluating the mismatch principle.

It is through stronger magnetic fields that recent clinical stroke protocols have begun to moderately increase the quality of images and to achieve faster scan times, maintaining the intention of preventing delay to administration of IV t-PA[183]. The advent of complete stroke protocols that can be achieved in 6 minutes or less is testament to the benefit of stronger magnetic fields and EPI based techniques. Similarly, recall that the sensitivity to diffusion can also be improved by enhancing the peak gradient strength applied but is restricted to gradient coil the scanner is equipped with. By utilizing scanners with stronger gradient coils, the available signal for diffusion images (and other MR sequences) can be increased by decreasing TE or increasing b values[184]; however, b values greater than 1000 s/mm^2 are not used clinically.

The quality of DWI can easily be modified by adjusting the acquisition parameters. The common form used to maintain sufficient SNR is to decrease the resolution which also decreases scan time, however this is the core concept the work of this thesis argues against. One method of increasing the quality of images without decreasing resolution can be accomplished by taking additional averages directly or by increasing the number of diffusion sensitizing gradients applied (Chapter 3, which can serve to acquire diffusion tensor imaging information) as it acts to also increase SNR through the additional scans taken[181]. Ract et al[181] compared the use of two diffusion imaging sequences with the same spatial resolutions using 3 b1000 versus 6 b1000 directions at 3.0T, finding 13% more ischemic lesions predominately within the brainstem on the diffusion images with the extra scans taken through the additional diffusion sensitizing directions.

Spatial resolution, perhaps the simplest modification to the DWI sequence and the core work of this thesis, has not improved significantly in clinical trials or clinical diagnostic imaging protocols in the past 20 years (**Table 2**). While speed and quality of diffusion images have

improved, it is only recently that researchers have begun to explore improvements to the resolution of diffusion imaging in order to identify additional ischemic lesions in both acute ischemic stroke and TIA[185 - 192].

Table 2 : Common Diffusion-Weighted Imaging Parameters Utilized in Acute Ischemic Stroke and Transient Ischemic Attack

	Number of Axial Sections	Diffusion Directions	Intersection Gap (mm)	Section Thickness (mm)	Voxel Size (mm^3)	Acquisition Time (Seconds)	Magnetic Field Strength (Tesla)
K Lovblad et al 1997	20	3	0	7	27	48	1.5
A. Rovira et al 2002	15	3	1.5	5	30	25	1.5
J. Nagura et al 2003	19	3	1	5	12.4	20	1.5
Draghici H, et al 2013	-	3	1.5	4	10	126	3.0
Seeger A, et al 2014	26	3	0.5	5	4.1	52	1.5
K Nael, et al 2014	30	3	0	4	8	58	3.0
Rosso C, et al 2015	24	3	0.5	5	16	62	3.0
Jang J, et al 2016	26	3	1	5	6.1	49	3.0
Prakkamakul S, et al 2016	-	3	0	5	11.3	80	3.0
J Rosch, et al 2016	25	3	0	5	7	80	1.5

In 2011, a study looking to evaluate the success of carotid artery stenting, implemented a 6 minute, thin slice DWI (2 mm, 7 mm^3 voxels) and compared the results to a 20 s conventional

DWI (6 mm with 2 mm gap, 28 mm^3 voxels); they demonstrated 21 ischemic lesions in 7 of their 20 patients that were not seen on the conventional DWI[187]. Selectively imaging the infratentorium, a large study compared a 3 mm slice DWI (covering the infratentorium in 19 slices with an acquisition time of 89 s) to conventional 5 mm slice DWI (59 s) at 1.5T and determined that higher resolution DWI increased the sensitivity of DWI to infratentorial infarctions by 13%[190]. Unfortunately, decreasing slice thickness and voxel size while maintaining satisfactory SNR and brain coverage leads to longer scan times of these sequences[186, 187], especially when implemented at 1.5T. But accessibility to 3.0T is becoming more frequent, permitting many institutions to implement DWI with decreased slice thicknesses of 3 mm[190, 191] for routine assessment of ischemic strokes. Research looking to improve the DWI sequence has not been limited to ischemic stroke, but rather has been improved in multiple studies of other pathologies. Amongst these include high resolution DWI (2 mm slice thickness with a scan time of 136 seconds) assessment of transient global amnesia (TGA), a potential TIA mimic, to identify abnormalities that previously were not visible or thought to be associated with TGA; However, higher resolution DWI revealed permanent damage in 50% rather than 20 – 30 % of TGA patients which was speculated to have been caused by the reduced partial volume effects[192].

Both TIA patients that possess ischemic lesions after neuroimaging and those that do not are thought to arise from small minute emboli that may or may not dissolve before significant tissue damage is done. Because of these very small ischemic lesions, they may go unnoticed if spatial resolution is not high enough and as such are prime candidates to study the effect of increasing spatial resolution for diffusion imaging. This has led to interest into whether or not resolution would affect instances of identifying permanent tissue damage. Bertrand et al[186]

identified ischemic lesions in 3 of the TIA patients exclusive to higher resolution DWI sequence (3 mm slices, 6 minute scan time) but were DWI normal on conventional DWI (6 mm slice thickness, 51 second scan time). Since then, regular assessment has begun to evaluate TIA patients using thinner slice DWI. A 2013 study implemented a 2.11 minute diffusion imaging sequence that acquired 2.5 mm slices with no inters-slice gap at 3T for initial and follow up assessment of TIA patients, but no comparison to conventional DWI parameters were made to determine if these patients would have failed to demonstrate evidence of cerebrovascular tissue damage[189]. Recall that ischemic lesions identified in TIA patients alters their diagnosis, prognosis, and possibly the intervention strategies. This makes it imperative to quickly identify the potential presence of any lesions using diffusion imaging as lesions detected by DWI in TIA patients have been confirmed to reflect irreversibly damaged tissue[193]. Despite these recent improvements in resolution, they could still be insufficient to detect minute volumes of infarcted tissue arising from minute emboli causing the manifestation of transient symptoms.

Diffusion imaging can also provide quantitative measurements of the ischemic lesion, such as its volume and MD, both of which can be affected by the image resolution. Previous work evaluating the merit of increasing spatial resolution of diffusion imaging has shown significantly lower lesion volume on high resolution (10 mm^3 voxels, scan time = 256 s) (lesion volume of 2800 ± 1200 mm^3) than on low resolution (20 mm^3 voxels, scan time = 30 s) (lesion volume of 3600 ± 1300 mm^3) in addition to the drastic increase in ischemic lesion detection using higher spatial resolution DWI (122 exclusive lesions in 42 ischemic stroke patients) [185]. While Benameur et al[185] postulated that reduction in partial volume effects is the most likely cause for the absence of lesions on conventional DWI, they did not suggest that partial volume averaging affected their differences in lesion volumes using different resolutions, nor that the

difference had any significance. Accuracy of lesion volume characterization is critical, as DWI lesion volume is used in clinical trials as inclusion criteria and as a surrogate of outcomes in therapeutic trials[194-196]. Additionally, experimental evidence has shown that DWI volumes on initial assessment of minor ischemic strokes are highly indicative of the success rates of t-PA administration, with larger DWI infarcts in low to moderate NIHSS stroke patients responding better to IV t-PA than smaller DWI lesion volumes[194], creating the necessity to accurately characterize the size of infarcts identified on DWI quickly to increase the yield of thrombolytics. There is no evidence suggesting that the reduction in partial volume effects impacts the MD estimation. Despite the lack of evidence supporting resolution parameters affecting MD measurements, MD estimation has been shown to be able to assist in predicting the degree of expansion of the DWI core[197], but another more recent study suggests that MD alone cannot be used to accurately estimate response to t-PA[198]. It is possible that these measurements of MD could be affected by partial volume effects, particularly in small ischemic lesions in which signal is partially averaged out with healthy tissue, and could impact the success of utilizing MD to identify salvageable tissue and measure lesion volumes.

Various improvements have been briefly explored to enhance DWI such as magnetic field strengths stronger than 3T, modest improvements to the spatial resolution, and using more than 3 diffusion sensitizing directions. In the next chapter, we will explore implementing and improving upon such methods for the assessment of TIA and minor stroke, ideal candidates as this subset of the stroke population are most likely to possess small ischemic lesions that are missed using lower resolution DWI. By implementing diffusion imaging with acquisition parameters improved further than previous studies at 1.5T, 4.7T and 3.0T in clinically feasible times, for a cohort of minor ischemic stroke and TIA patients, we expect to demonstrate

increased lesion detection while also determining the effect that reduction in partial volume effects will have on volume and MD measurements of the lesion.

Chapter 4

High Spatial Resolution Diffusion-Weighted Imaging in Patients with Acute Ischemic Stroke

Abstract

Diffusion-weighted imaging (DWI) is considered to be the gold standard for ischemic stroke diagnosis, but is typically acquired at low spatial resolution and may be insufficient for small lesions. High spatial resolution DWI (4.7T - 1.5 x 1.5 x 1.5 mm^3 with no gap in 210 seconds; 1.5T – 1.5 x 1.5 x 2 mm^3 with no gap in 293 seconds; 3.0T – 1.5 x 1.5 x 1.5 mm^3 with no gap in 259 seconds) relative to conventional spatial resolution DWI (4.7T - 1.5 x 1.5 x 5 mm^3 with 1 mm inter-slice gaps in 252 seconds; 1.5T – 1.7 x 1.7 x 5 mm^3 with 1.5 mm inter-slice gaps in 51 seconds; 3.0T - 1.5 x 1.5 x 1.5 mm^3 with no inter-slice gap in 59 seconds) with whole brain coverage were compared for ischemic lesion detection and characterization. Transient ischemic attack (TIA, n = 19) and minor ischemic stroke (n = 29) patients were recruited for imaging on a 4.7T (n = 17), 3.0T (n = 10) and 1.5T (n = 21). The number of ischemic lesions, lesion volume and mean diffusivity (MD) values were recorded on both DWI scans. 65 ischemic lesions were identified on conventional DWI (range, 0 – 9 per patient) while an additional 29 lesions (n = 94) were only detected on high spatial resolution DWI (range, 0 – 12 per patient, $p < 0.01$). Lesion volumes on high spatial resolution DWI were 29 ± 22 % smaller with a corresponding 8.6 ± 8.3% drop in MD relative to the conventional resolution scans. Lesions seen exclusively on high resolution scans were predictably small (33 mm^3, range, 5 – 191 mm^3; MD, 0.61 ± 0.14 x 10^{-3} mm^2/s). Three of the 19 TIA patients had an ischemic lesion only on high resolution DWI while

11 were found to be DWI negative on both scans. High resolution DWI increased ischemic lesion conspicuity and detected additional ischemic lesions not seen on conventional DWI, potentially altering TIA diagnoses, suspected pathogenic mechanism and therapeutic intervention strategy.

4:1 Introduction

When evaluating ischemic stroke patients, magnetic resonance imaging (MRI) is increasingly utilized to characterize vascular related lesions within the cortex while assisting with the identification of the vascular mechanism that induced ischemia. Diffusion weighted imaging (DWI) is a specific adjunct of MRI that has permitted the early detection of acute cerebral ischemia with reported accuracies exceeding 90%[161, 163], despite routine clinical protocols being plagued by low spatial resolution and signal to noise ratios. Conventional DWI protocols for clinical purposes are typically optimized for speed of brain acquisition at the cost of spatial resolution, typically implementing voxel sizes of 20 mm^3, corresponding to 5 mm slices with an inter-slice gap. At these lower resolutions, it is not uncommon to obtain a significant number of normal appearing DWIs when evaluating transient ischemic attack (TIA) patients, limiting the efficacy of using DWI to confirm ischemic origin of the symptoms[193]. Evidence shows that TIA patients possess ischemic lesions that correspond with the manifestation of their transient clinical symptoms upon using DWI in only a third of the cases[199]. Identifying ischemic lesions quickly is essential not only to their diagnosis but also to appropriately assess their prognosis, as they are potentially at high risk for recurrent strokes[73, 99, 104, 200-204].

Small lesions associated with minor ischemic strokes and TIA are potentially going undetected if they occupy only part of a slice or volume of lost tissue. However, modest

improvements in the spatial resolution of the images have resulted in a higher prevalence of lesions associated with symptoms, which could alter a patient's management[185-192]. Performing diffusion imaging using 3.5 mm slices (1.7 x 1.7 x 3.5 mm^3 in 256 seconds) at 1.5T, Benameur et al[185] managed to detect an additional 134 lesions not seen on conventional DWIs (1.7 x 1.7 x 7 mm^3 in 30 seconds) in their 42 acute ischemic stroke patients (yielding on average 3 lesions per patient on conventional DWI and double that with 6 lesions per patient on higher spatial resolution DWI).

Modifications to the quality of diffusion imaging include acquisition by taking advantage of higher magnetic field strengths such as 3T[180-182] that can improve ischemic lesion contrast through the greater SNR available and permitting resolution to be improved without drastically increasing scan time. Similarly, increasing the number of averages or the number of diffusion directions beyond the minimum required to calculate MD maps (i.e. 3) boosts the SNR through the additional averages acquired and enhances lesion conspicuity[181,184]. High resolution imaging decreasing in partial volume averaging which could otherwise cause errors in quantitation of lesion volume and MD values.

The current study will determine if increasing the resolution can identify more ischemic lesions while improving lesion characterization in the form of more accurate lesion volume and MD estimation. While previous research has implemented DWI using 2.5 mm[191, 192] and 3 mm[190] thick slices for the assessment of ischemic stroke, this study is pushing the spatial resolution beyond other stroke studies. Here, we use 1.5 mm slices (no inter-slice gaps, voxel volume 3.4 mm^3) which are feasible using phased array radiofrequency coils, high fields, and sufficient averaging while maintaining a clinically feasible scan time (210 seconds at 4.7T, 259 seconds at 3.0T, and 293 seconds at 1.5T). High resolution DWI was compared to conventional DWI (4.7T

- 5 mm slices, 1 mm inter-slice gap, voxel volume 17 mm^3 in 252 seconds; 1.5T – 5 mm slices, 1.5 mm inter-slice gap, voxel volume 19 mm^3 in 51 seconds; 3.0T – 5 mm slices, 0 mm inter-slice gap, voxel volume 11.3 mm^3 in 59 seconds) in 48 transient ischemic attack and minor ischemic stroke patients. We hypothesized that improving the spatial resolution of diffusion imaging would result in a significant increase in the detection of ischemic lesions, with systematic differences in ischemic lesion volumes and MD values.

4:2 Materials and Methods

4:2:1 Magnetic Resonance Imaging Protocol

MRI examinations were performed using one of three separate scanners at 1.5 Tesla (Siemens Sonata), 3.0 Tesla (Siemens Prisma) and 4.7 Tesla (Varian Unity Inova) magnetic field strengths in the Peter S Allen MRI Research Centre at the University of Alberta. Conventional and high spatial resolution DWI protocols were implemented on a 4.7T Varian Inova with an 60 mT/m per axis gradient coil, 27 cm diameter birdcage radio frequency transmission coil, Pulstec 4 channel receiving coil, 3.0T Siemens Prisma with an 80 mT/m per axis gradient coil and 64 channel head coil, and a 1.5T Siemens Sonata with an 40 mT/m per axis gradient coil and an 8 channel head coil. Patients were preferentially recruited for imaging on the 4.7T, but for those who were ineligible due to more stringent screening contraindications to scanning on the 4.7T, underwent imaging on the 1.5T or 3.0T if possible in order to increase sample size. The stroke protocol acquisition time for the 4.7T was ~20 minutes and consisted of the following: conventional DWI, high resolution DWI, FLAIR, and a 2D gradient recalled echo. Some patients also underwent a 10 minute, b = 300 s/mm^2 PGSE and OGSE set of scans as part of a separate study not discussed

here[155]. The stroke protocol acquisition for the 3.0T was ~ 30 minutes and consisted of the following: conventional DWI, high resolution DWI, FLAIR, SWI, MRA and high resolution ASL. The 1.5T stroke protocol was acquired in ~ 30 min and consisted of the following: conventional DWI, high resolution DWI, T2 and T1, SWI and FLAIR. A summary of the DWI acquisition parameters for each scanner can be found in Table 3.

Table 3 : DWI Sequence Parameters

	Conventional Resolution DWI			**High Resolution DWI**		
	1.5T	**3.0T**	**4.7T**	**1.5T**	**3.0T**	**4.7T**
TR/TE, ms	2600/90	2500/51	3000/58	10800/76	8500/55	10000/60
In plane resolution, mm^3	1.7 x 1.7 x 5	1.5 x 1.5 x 5	1.7 x 1.7 x 5	1.5 x 1.5 x 1.5	1.5 x 1.5 x 1.5	1.5 x 1.5 x 1.5
Slices	19	24	19	60	80	80
Inter-slice gap, mm	1.5	0	1	0	0	0
Averages	4	1	16	6	1	4
Directions	3	12	3	3	20	3
GRAPPA	2	2	2	2	2	2
Acquisition time, s	51	59	252	293	259	210

Conventional DWI on the 4.7T was performed using single shot echo-planar imaging at a resolution of 1.7 x 1.7 mm^2 with 5 mm thick sections and 1 mm intersection gaps (17 mm^3 voxels). 16 averages were taken along three orthogonal directions, with a b value of 1000 s/mm^2 and a repetition time (TR) of 3 s and echo time (TE) 58 ms. While 16 averages for a low resolution DWI scan is not a typical parameter utilized in clinical settings, it was chosen in order

to make acquisition time somewhat equivalent to that of high resolution DWI. Whole brain coverage was achieved with 20 axial slices in 252 seconds. High resolution DWI was acquired at 1.5 x 1.5 x 1.5 = 3.4 mm^3 isotropic using 1.5 mm slices and no inter-slice gaps. A b value of 1000 s/mm^2 was used along three orthogonal directions with 4 averages in each direction and a TR of 10 s and TE of 60 ms. The entire brain was covered by 80 axial sections in 210 seconds. Parallel imaging (GRAPPA) with a rate factor of 2 was used to reduce echo time and echo train length for both protocols.

DWI parameters for the 3.0T differed slightly as higher resolutions could be obtained in similar time frames because of the stronger gradient coils. High resolution DWI parameters were acquired using a resolution of 1.5 x 1.5 x 1.5 = 3.4 mm^3 isotropic in 20 orthogonal directions with a b value of 1000 s/mm^2 and a TR of 8500 ms and TE of 55 ms. Whole brain coverage was obtained in 259 seconds by acquiring 80 axial sections with 3.4 mm^3 voxels. Conventional DWI images were obtained at a resolution of 1.5 x 1.5 x 5 mm^3 with no intersection gap along 12 directions with a b value of 1000 mm^2/s and TR of 2500 ms and TE of 51 ms, covering whole brain in 59 seconds using 24 axial sections with 11.3 mm^3 voxels, maintaining similar quality and scan time that clinical DWI achieves at 3.0T.

Both the high resolution and conventional DWI parameters on the 1.5T differed to the high resolution and conventional DWI on the 4.7T and 3.0T. The exception in regards to the high resolution DWI sequence used on the 1.5T being that 2 mm slices with 6 averages to acquire whole brain in 60 axial sections (4.5 mm^3 voxels) was used in order to maintain a satisfactory signal to noise ratio, with a TR of 10800 ms and TE of 76 ms. Conventional DWI parameters more accurately represented clinical DWI through whole brain coverage in a 51 second scan time

using 1.5 mm intersection gaps, increasing voxel size to 19 mm^3 with a TR of 2600 ms and TE of 90 ms.

4:2:2 Patients and Inclusion Criteria

Patients were eligible for entry into this study if they A) had clinical symptoms consistent with acute ischemic stroke or TIA within the first 72 hours of symptom onset, while ischemic stroke patients with symptom onset times greater than 72 hours were included for volumetric analysis and lesion identification; B) possessed no evidence of cerebral hemorrhage or previous strokes on prior scans; C) were over the age of 18 years old; D) had minor to moderate ischemic stroke severity as measured by the NIHSS (< 20); E) had no contra-indications to MRI and considered to be medically stable enough to come to the Peter S Allen MR Research Centre; and F) were able to provide informed consent (approved by the Health Research Ethics Board) to undergo both conventional DWI and high resolution DWI in the same imaging examination. Patient details will be presented in the Results section below.

4:2:3 Data Analysis

Post processing of images obtained from the 4.7T was performed in Matlab (version 2014b) using in-house developed software, developed by Corey Baron (v1B) after performing motion and eddy current correction. Post processing of images obtained from the 1.5T and 3.0T was performed using ExploreDTI (version 4.8.5) to create mean DWI and MD maps after performing motion correction. A stroke fellow directly compared the high resolution images to the conventional resolution images in order to confirm the presence of new ischemic lesions

identified by a blinded rater (H.K.). Diffusion-restricted lesion volumes were measured using Matlab in house written software Galileo (version 3.b) by manually placing regions of interest over hyperintense DWI lesions that possessed a corresponding MD hypointensity. The manually placed regions of interest were directly mapped onto the corresponding MD map. All images presented are in radiological format where the right side of an axial image corresponds to the left side of the brain.

Continuous variables with a normal distribution including differences in lesion volumes and MD between the two resolutions were compared using a 2-tailed, paired student's t test. The difference in number of lesions detected between high resolution and conventional DWIs were evaluated for significance using the Wilcoxon signed-rank test. Statistical analysis was completed using a statistical software package (IBM SPSS statistics 23). A p value ≤ 0.05 was assumed to indicate significance.

4:3 Results

In total, 48 patients were recruited to be scanned on either the 4.7T, 3.0T or 1.5T and included for analysis as listed below: 4.7T - 17 patients (15 men; mean age of 58 years; range, 26 - 76 years; mean NIHSS of 5; range, 0 – 18; ischemic stroke n = 16, TIA n = 1) between 2011 and 2015. The mean time between symptom onset and imaging was 72 hours (range, 18 – 432 hours). Four patients were accepted into the study within the subacute phase (94, 96, 144 and 432 hours).

1.5T - 21 patients (19 men; mean age of 67 years; range, 26 – 84 years; mean NIHSS of 2; range 0 -7; ischemic stroke n = 9; TIA n = 14) between 2011 and 2015. The mean time between symptom onset and imaging was 35 hours (range, 4.5 – 72 hours).

3.0T – 10 patients (6 male; mean age of 56 years; range 46 - 84 years;mean NIHSS of 2; range, 1 - 3; ischemic stroke = 6; TIA = 4) between 2015 and 2016. 6 of the 10 patients were imaged within the first 36 hours while the remaining 4 were included a month after their initial symptom manifestation.

Comparison of image quality between conventional and high resolution DWI at 3.0T and 4.7T reveals similar quality in the axial plane, while WM/GM contrast and anatomical detail is superior on high resolution scans (**Figure 9**). The higher field strength of the 4.7T and 3.0T did permit resolution to be increased further than the 1.5T protocol without sacrificing the quality of the images and is clearly depicted by Figure 9. Quality of the 1.5T high resolution was still greater than conventional images, demonstrating superior lesion conspicuity and better anatomical detail, but was found to be noisier and increased instances of ghosting artifacts were observed. Isotropic voxels readily allowed reconstruction of the diffusion images into the three planes with higher levels of quality to more effectively identify and characterize lesion patterns, demonstrating the most apparent difference in anatomical detail high spatial resolution DWI achieves over conventional DWI (**Figure 9**). Large ischemic lesions were more effectively depicted spanning the brain using these high quality coronal and sagittal planes in addition to the standard axial slices, while the additional, higher quality planes also assisted in identification of small infarctions.

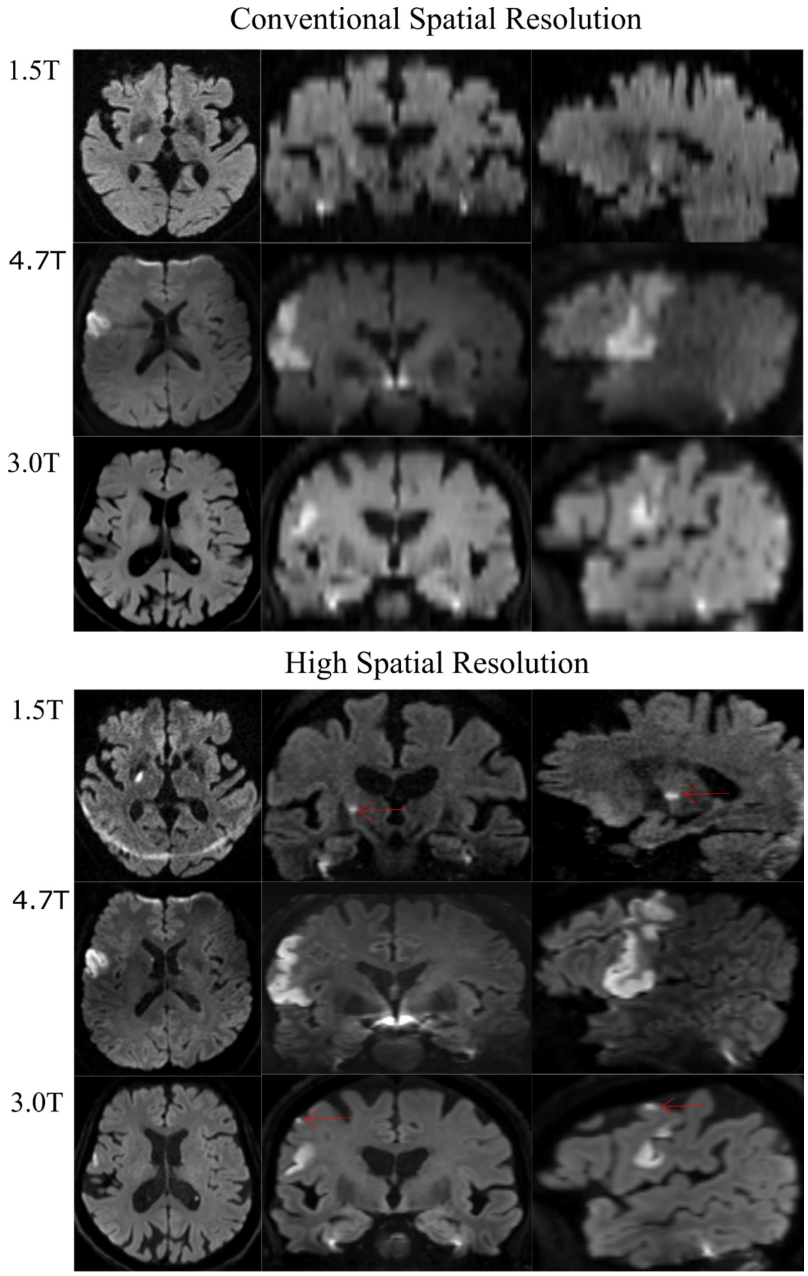

Figure 9 Conventional and High Spatial Resolution Images from Three Separate Patients Imaged at 1.5T, 4.7T and 3.0T – Comparison of axial images between conventional and high resolution DWI reveals similar quality on the 1.5T, 4.7T and 3.0T. The ghosting artifact seen on the 1.5T high resolution axial slice was a common consequence resulting from the improvement of resolution beyond those capable at 1.5T while maintaining a 3 minute scan time. Isotropic resolution permits simple and superior reconstruction of scans into axial, coronal and sagittal planes. Lesions can be easily identified in all three planes to assist in confirmation and diagnosis of ischemic lesions on high resolution DWI but are inconspicuous or obscured on conventional DWI due to differences in acquisition parameters.

The thin slices acquired using high resolution scans demonstrated superior delineation of structures within the brain and in many instances permitted the detection of ischemic lesions that were not seen on conventional diffusion images (**Figures 10 - 12**). Furthermore, lesions were much more effectively characterized across multiple thinner slices on high resolution DWI (rather than on a single slice on conventional DWI which could cause uncertainty in confirming ischemic nature of the lesion), giving a more accurate impression as to the extent of neurological tissue damage associated with the presenting symptoms (**Figures 12 - 14**). The high spatial resolution DWI also mitigates partial volume effects through reduced slice thickness which can enhance the contrast of ischemic lesions and boost the observer sensitivity to small ischemic lesions.

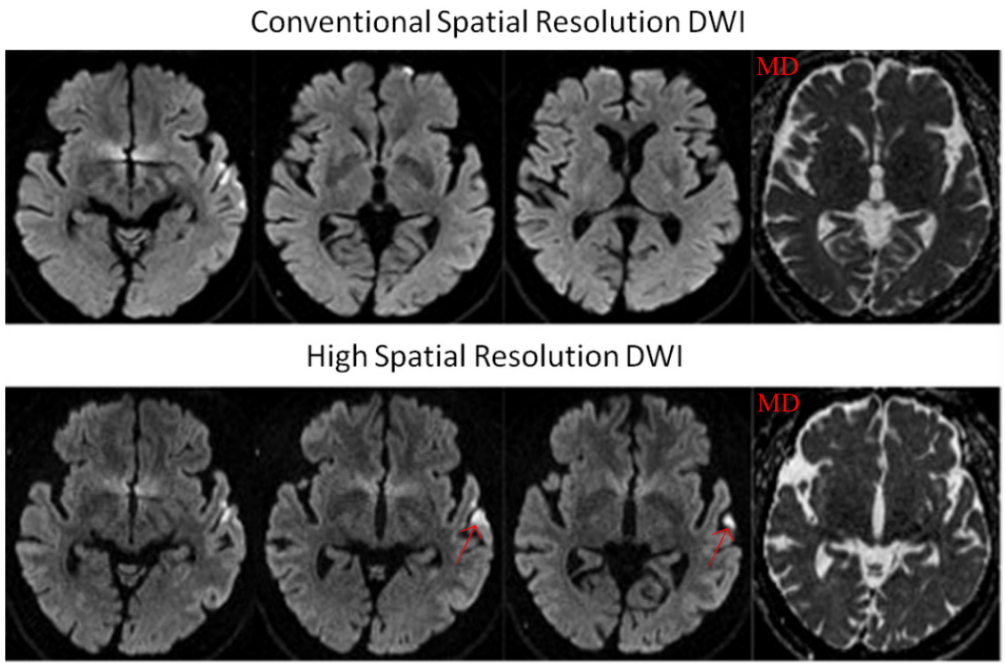

Figure 10 Superior Anatomical Detail Through Thin Slice DWI of Ischemic Stroke Imaged at 1.5T – 80 year old male diagnosed with ischemic stroke (NIHSS score = 1) presenting with mild aphasia and hemiparesis of right side of face imaged 32 hours after symptom onset. An ischemic lesion expanding superiorly through the temporal cortex was better characterized on high resolution DWI (4.5 mm^3 voxels) than on conventional DWI (19 mm^3 voxels).

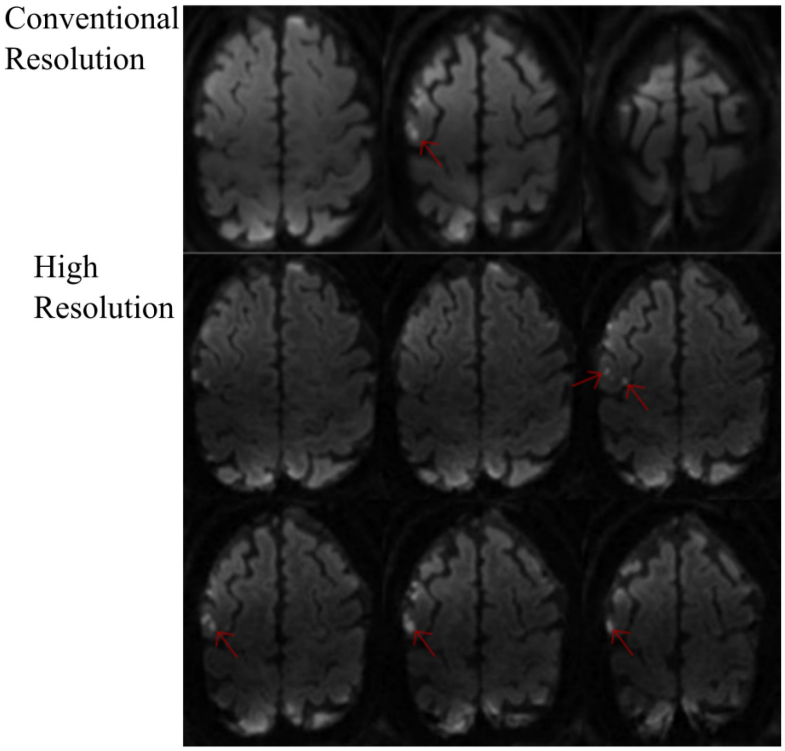

Figure 11 Conventional and High Spatial Resolution DWI in Acute Ischemic Stroke Patient Imaged at 4.7T – 53 year old male (NIHSS of 2) imaged 35 hours after symptom onset. Consecutive slices on high resolution DWI (3.4 mm^3 voxels) reveal multiple smaller lesions within the cortical regions before combining into a large lesion, but not on consecutive slices of conventional DWI (17 mm^3 voxels) where a single lesion is identified because of the better depiction of the cortex using axial slices.

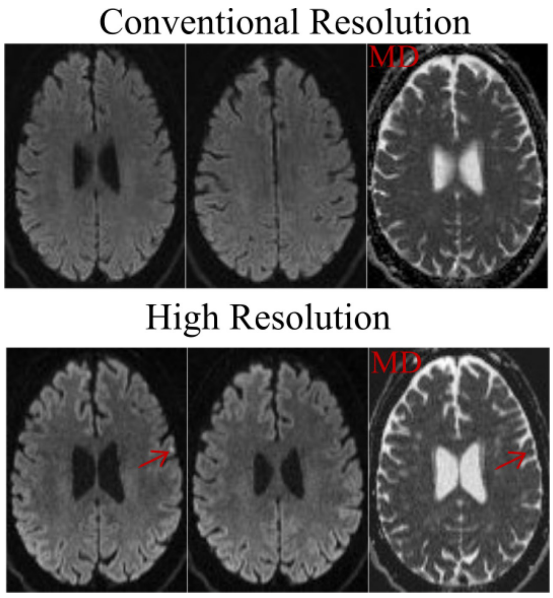

Figure 12 Superior Lesion Characterization with High Spatial Resolution in Acute Ischemic Stroke Imaged at 1.5T – 80 year old male diagnosed with minor stroke (NIHSS of 1) presenting with mild aphasia and hemiparesis of right side of face imaged 32 hours after symptom onset. Symptoms disappeared that day. High resolution images (voxel volume = 4.5 mm^3) revealed a small hyperintensity (lesion volume = 37 mm^3; MD = 0.56 x 10^{-3} mm^2/s) in the upper left cortex ipsilateral to the larger lesion below detected on both high and conventional (voxel volume = 19 mm^3) spatial resolution images.

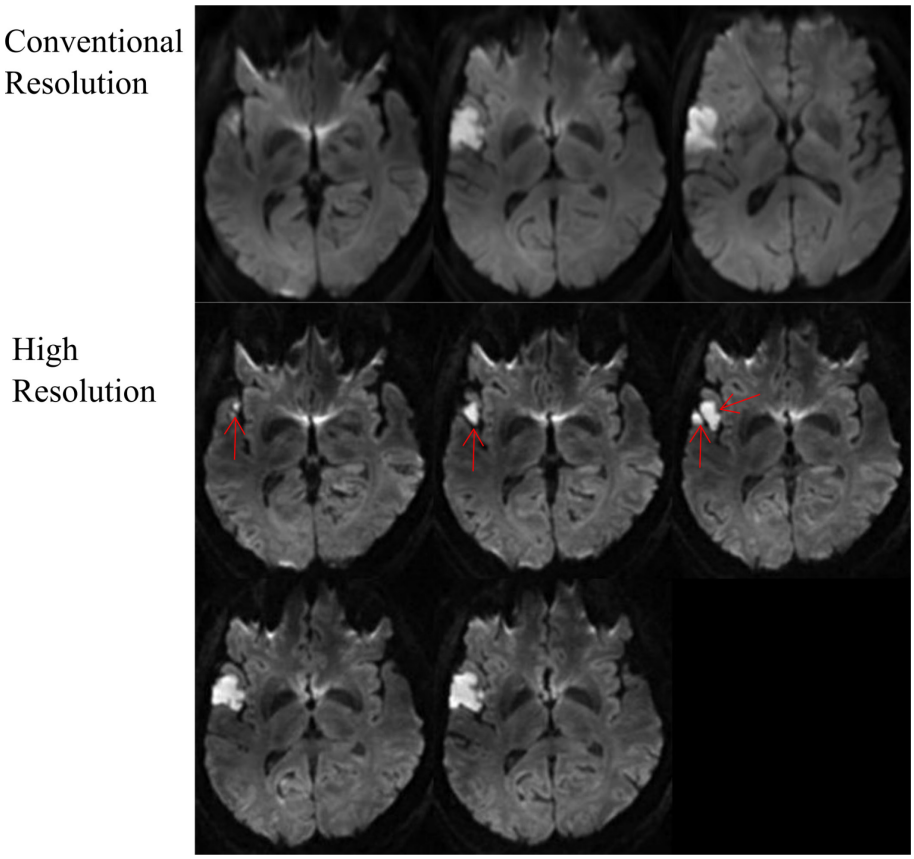

Figure 13 Conventional and High Spatial Resolution DWI in Acute Ischemic Stroke Patient Imaged at 4.7T - 56 year old male diagnosed with minor ischemic stroke (NIHSS of 3), imaged 27 hours after symptom onset, depicts a large ischemic lesion extending down into the inferior aspect of the superior temporal gyrus on high resolution DWI (voxel volume of 3.4 mm^3; lesion volume = 13,100 mm^3; MD = 0.54 x 10^{-3} mm^2/s), but can only be seen on the superior aspect of the superior temporal gyrus on conventional DWI (voxel volume of 17 mm^3 voxels; lesion volume = 13,700 mm^3; MD = 0.62 x 10^{-3} mm^2/s).

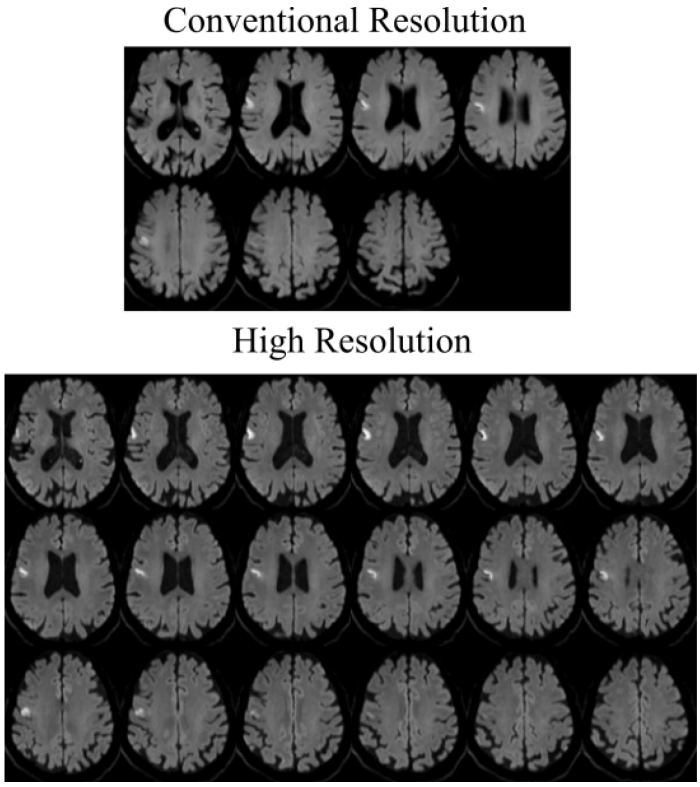

Figure 14 Conventional and High Spatial Resolution DWI in Acute Ischemic Stroke Patient Imaged at 3.0T – 80 year old male diagnosed with minor ischemic stroke (NIHSS score = 2) with moderate dysarthria and mild facial droop imaged 37 hours after symptom onset, portraying the ischemic lesion spanning 16 consecutive slices on high resolution DWI (3.4 mm^3 voxels; lesion volume = 1700 mm^3; MD = 0.56 x 10^{-3} mm^2/s), but only 5 on conventional DWI (11.3 mm^3 voxels; lesion volume = 2000 mm^3; MD = 0.64 x 10^{-3} mm^2/s).

A total of 65 discrete ischemic lesions were identified on conventional diffusion scans and 94 lesions on high resolution scans for an average of 1.5 lesions per patient on conventional DWI and 2.3 lesions per patient on high resolution DWI. ($p < 0.001$). Lesions identified on both sets of scans (n = 64) revealed a 29 ± 23% (p = 0.047) reduction in volume estimation on high resolution DWI with a corresponding reduction of MD by 8.6 ± 8.3 % (p < 0.001). A summary of the data can be found in Table 4. Every ischemic stroke patient possessed at least one ischemic lesion on conventional scans and high resolution scans, while every ischemic lesion

that was detected on conventional scans could also be identified on high resolution scans. A breakdown of the data from individual patients obtained from 4.7T, 1.5T and 3.0T and can be found in Tables 5 – 7.

Table 4 : Measurements of DWI Lesions Detected Using High and Conventional Spatial Resolution at 1.5T, 3T and 4.7T in 48 Patients with Ischemic Stroke or TIA

	Conventional Spatial Resolution DWI	High Spatial Resolution DWI	P value
Mean (median) MD of DWI lesion, $x10^{-3}$ mm^2/s	0.68 (0.66)	0.63 (0.61)	<0.001
Mean (median) MD of healthy tissue contralateral to lesion, $x10^{-3}$ mm^2/s	0.78 (0.77)	0.78 (0.78)	0.33
Mean (median) DWI lesion volume, cm^3	3.6 (0.33)	3.0 (0.21)	0.047
No. of lesions (per patient)	65 (1.5)	94 (2.3)	<0.001
No. of patients with >1 DWI lesion (%)	11 (23)	20 (43)	0.003
TIA patients with ischemic lesion (%)	5 (26)	8 (42)	0.083
Mean total volume of lesions per patient, cm^3 (median)	7.7 (1.5)	6.5 (1.2)	0.056

4.7T - 52 discrete ischemic lesions were identified on the high resolution DWI (**Figures 15 & 16**) compared to 36 on conventional DWI in our 17 patients (increase of 41%, $p < .01$), averaging to 2.9 lesions per patient (range, 1 - 8) on high resolution DWI versus 2.0 lesions per patient (range, 1 - 6) on conventional DWI. Lesions measured on high resolution DWI were found to be 29% ($p < 0.001$) smaller in volume compared against conventional DWI ischemic lesions with an associated drop of 8.7 % ($p < 0.01$) in MD.

Table 5 : Ischemic Lesions Identified on Both Scans from 4.7T Subjects (n = 17)

Patient	Age/Sex	Type (IS/TIA) & NIHSS	Lesions Low Resolution	Lesions High Resolution	Volume Low Resolution (cm^3)	Volume High Resolution (cm^3)	MD Low Resolution ($x10^{-3}$ mm^2/s)	MD High Resolution ($x10^{-3}$ mm^2/s)
1	50/M	TIA, 2	1	1	1.0	0.79	0.54	0.41
2	67/M	IS, 18	3	4	42.1	25.0	0.66	0.61
					0.38	0.22	0.80	0.71
					0.10	0.10	0.65	0.57
3	40/M	IS, 1	1	3	0.18	0.037	-	-
4	65/M	IS, 1	1	1	3.6	2.9	0.54	0.50
5	53/M	IS, 3	2	3	2.4	2.0	0.54	0.45
					0.38	0.38	0.89	0.80
6	59/M	IS, 2	4	7	13.7	13.1	0.62	0.54
					0.13	0.057	0.76	0.67
					0.067	0.032	0.74	0.53
					0.32	0.24	0.65	0.67
7	54/M	IS, 0	2	3	1.5	1.1	0.64	0.61
					0.93	0.54	0.65	0.55
8	71/F	IS, 6	1	2	0.41	0.30	0.61	0.53
9	76/M	IS, 0	1	1	0.93	0.046	0.82	0.79
10	67/M	IS	2	2	0.35	0.44	-	-
					4.5	2.0	-	-
11	25/M	IS, 4	1	1	1.7	1.3	0.58	0.58
12	58/M	IS, 3	6	8	12.2	10.7	0.63	0.61
					2.4	2.0	0.71	0.62
					0.049	0.025	0.75	0.65
					0.39	0.30	0.68	0.62
					0.36	0.25	0.67	0.63
					0.82	0.55	0.76	0.69
13	76/F	IS, 10	3	4	1.65	1.0	0.51	0.44
					0.42	0.38	0.64	0.55
					0.28	0.26	0.66	0.61
14	50/M	IS, 1	1	1	0.34	0.19	0.6	0.55
15	38/M	IS, 2	1	2	11.5	10.5	0.63	0.62
16	39/M	IS, 12	1	1	87.5	84.1	0.49	0.47
17	77/M	IS, 8	5	8	0.67	0.54	0.65	0.56
					0.60	0.46	0.67	0.68
					0.070	0.043	0.66	0.71
					0.093	0.066	0.67	0.67
					0.026	0.016	0.70	0.73
Mean			2.0	2.9	5.3	4.4	0.68	0.63

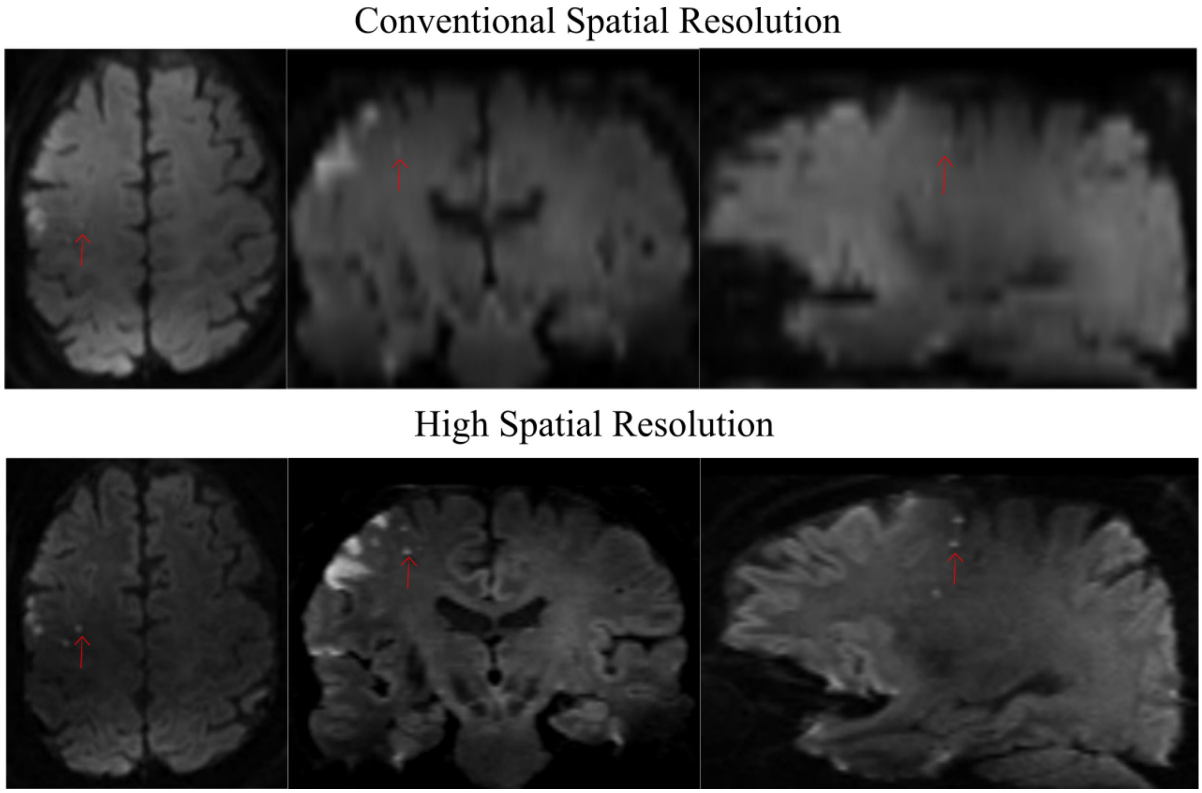

Figure 15 Small Ischemic Lesion Identification Improved Using Isotropic In-plane Resolution Imaged at 4.7T - 56 year old male diagnosed with ischemic stroke (NIHSS of 2 at time of scan) imaged 72 hours after symptom onset, demonstrates two ischemic lesions on high resolution DWI (3.4 mm^3 voxels) but would have likely been missed on conventional DWI (17 mm^3 voxels). The ischemic lesions can also be confirmed on coronal and sagittal high resolution scans but are completely absent on conventional DWI.

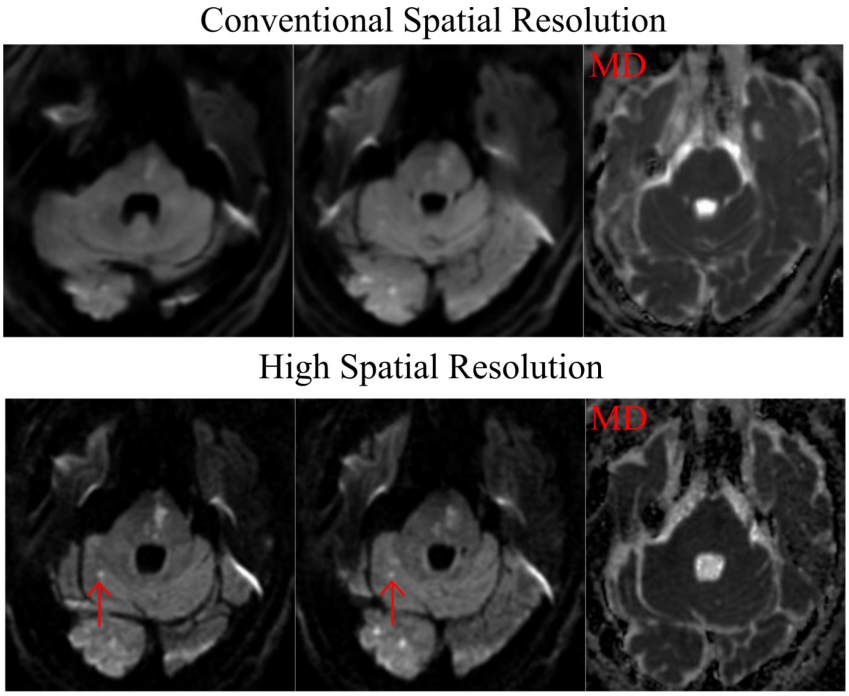

Figure 16 Superior Imaging of Small Ischemic Lesions within the Infratentorial Region Using High Spatial Resolution Imaged at 4.7T - A 77 year old man with coronary artery disease experiencing facial droop, aphasia and weakness, 48 hours after symptom onset (NIHSS of 8). High spatial resolution diffusion-weighted imaging (3.4 mm^3 voxels) reveals a small lesion (lesion volume = 16 mm^3; MD = 0.62 x 10^{-3} mm^2/s) within the cerebellum on two slices and enhanced conspicuity of the lesion within the pons. The cerebellar lesion is missed on conventional diffusion-weighted imaging (17 mm^3 voxels).

1.5T - Ischemic lesion detection increased by 49% ($p < 0.01$) on the 1.5T high resolution DWIs (37 lesions) compared against the conventional DWI (25 lesions) in our 21 patients, corresponding to 1.9 lesions per patient (range, 0 - 12) on high resolution DWI and 1.2 lesions per patient (range, 0 - 9) on conventional DWI. These lesions were also found to have a 30% decrease in volumes on high resolution DWI ($p = 0.01$) with an associated 9% drop in MD ($p = 0.02$). 4 TIA patients possessed ischemic lesions on both sets of images while 3 patients were found to have lesions exclusive to high resolution DWI.

Table 6 : Ischemic Lesions Identified on Both Scans from 1.5T Subjects (n = 9)

Patient	Age/Sex	Type (IS/TIA) NIHSS	Lesions Low Res.	Lesions High Res.	Volume Low Res. (cm^3)	Volume High Res. (cm^3)	MD Low Res. ($x10^{-3}$ mm^2/s)	MD High Res. ($x10^{-3}$ mm^2/s)
1	80/M	IS, 4	5	7	0.17	0.11	0.62	0.58
					0.67	0.54	0.67	0.64
					0.096	0.084	0.67	0.65
					0.19	0.17	0.67	0.63
					0.077	0.070	0.88	0.70
2	84/M	IS, 0	3	3	0.29	0.19	0.66	0.63
					0.096	0.093	0.69	0.78
					0.096	0.075	0.69	0.66
3	M	IS, 1	1	2	1.0	0.93	0.57	0.58
4	71/F	IS, 0	9	12	20.9	19.5	0.46	0.44
					0.084	0.037	0.75	0.57
					0.063	0.028	0.61	0.52
					0.19	0.18	0.54	0.51
					0.063	0.023	0.80	0.67
					0.084	0.056	0.52	0.50
					0.063	0.033	0.70	0.68
					0.063	0.051	0.75	0.62
					0.25	0.14	0.68	0.61
5	64/M	IS, 1	1	2	0.27	0.08	0.50	0.45
6	59/M	TIA, 0	1	3	0.077	0.03	0.75	0.58
7	59/M	IS, 2	1	1	1.5	1.0	0.54	0.52
8	74/F	TIA, 2	1	1	0.12	0.06	0.58	0.52
9	81/M	TIA, 0	1	1	0.12	0.11	0.55	0.41
Mean			1.2	1.9	1.2	1.0	0.65	0.59

3.0T - 6 ischemic stroke patients imaged on the 3.0T were found to have 2 new ischemic lesions not seen on conventional DWI (**Figure 17**). The 3 matched lesions decreased in volume by 28% on high resolution scans with a corresponding 9% reduction in MD. All four TIA patients failed to demonstrate any appreciable DWI abnormalities corresponding with their symptoms on either scan.

Table 7 : Ischemic Lesions Identified on Both Scans from 3.0T Subjects (n= 3)

Patient	Age/Sex	Lesions Low Res.	Lesions High Res.	Volume Low Res. (cm^3)	Volume High Res. (cm^3)	MD Low Res. ($x10^{-3}$ mm^2/s)	MD High Res. ($x10^{-3}$ mm^2/s)
1	F	1	1	0.062	0.06	0.67	0.63
2	84/M	1	2	2.0	1.7	0.64	0.56
3	47/M	1	1	0.10	0.036	-	-

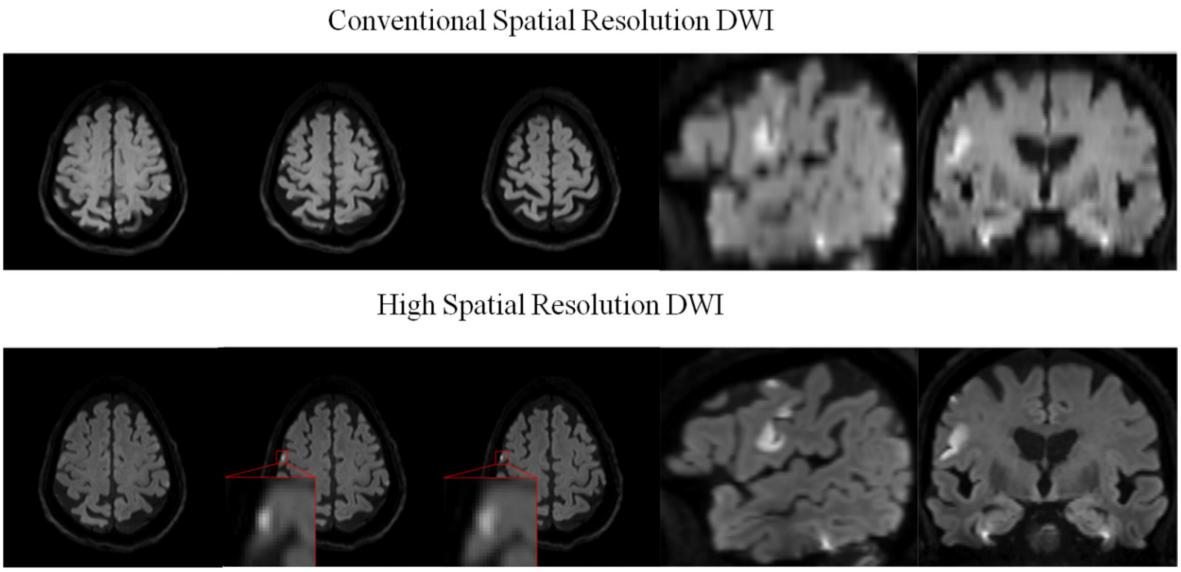

Figure 17 Conventional and High Spatial Resolution DWI in Acute Ischemic Stroke Patient Imaged at 3T – 84 year old male diagnosed with ischemic stroke (NIHSS score = 2) with moderate dysarthria and mild facial droop 37 hours after symptom onset, demonstrates a DWI lesion within the cortex on 2 slices on high spatial resolution DWI (3.4 mm^3 voxels) but is not observed on conventional DWI (11.3 mm^3 voxels). Coronal sections reveal the large ischemic lesion on both sets of images and again identifies the small ischemic lesion within the cortex on high spatial resolution DWI.

3 of the 19 TIA patients were found to have no lesions detected on conventional DWIs but were observed to possess at least one ischemic lesion on high resolution DWI (**Figures 18 - 20**). 11 of the 19 TIA patients were DWI negative on both sets of scans with the remaining 4 having an ischemic lesion identified on both scans (4.7T = 1; 1.5T = 3).

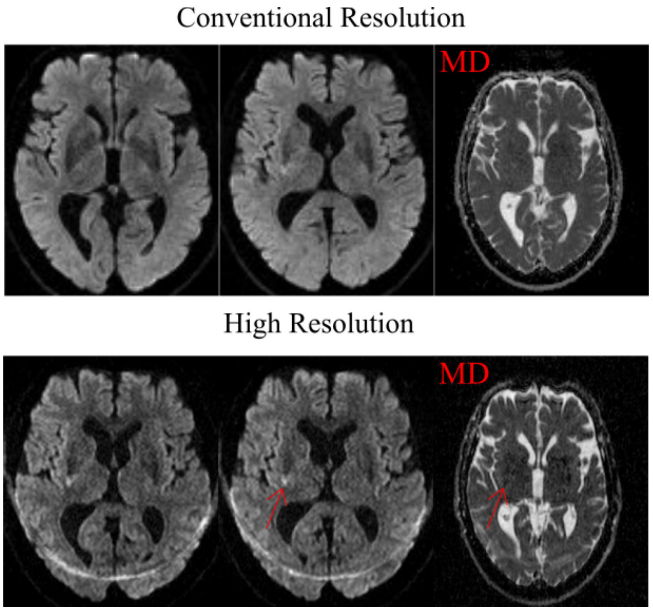

Figure 18 Conventional and High Spatial Resolution DWI of Transient Ischemic Attack Patient Imaged at 1.5T - A 73 year old male diagnosed with transient ischemic attack, experiencing slurred speech and right leg weakness imaged on the 1.5T, 4.5 hours after symptom onset (NIHSS of 3). High spatial resolution diffusion-weighted imaging (4.5 mm^3 voxels) reveals a distinct lesion within the left globus pallidus on one slice, but is not visible on conventional diffusion-weighted imaging (19 mm^3 voxels).

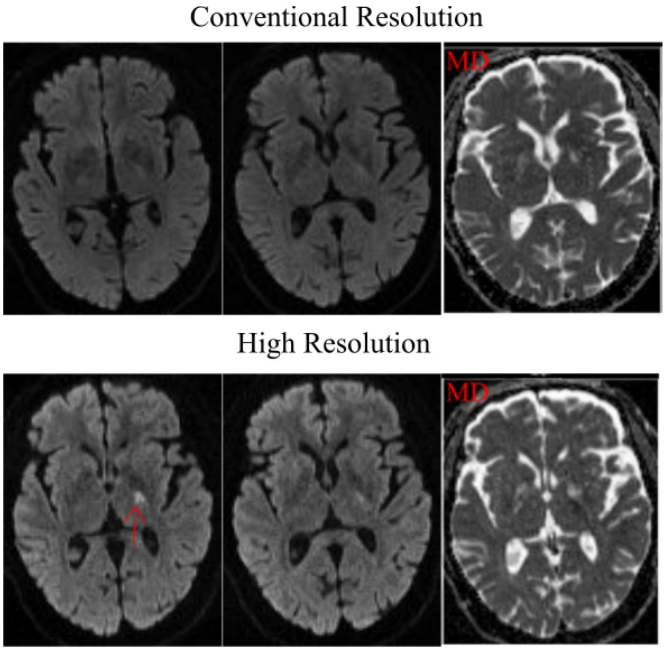

Figure 19 Identification of a Small Ischemic Lesion in a TIA Patient Using High Spatial Resolution DWI Imaged at 1.5T – Small ischemic lesion initially missed on conventional resolution DWI (19 mm^3 voxels) but was identified on two slices posterior to the right putamen on high resolution (4.5 mm^3 voxels) with a corresponding drop in MD (volume = 22 mm^3; MD = 0.57 x 10^{-3} mm^2/s).

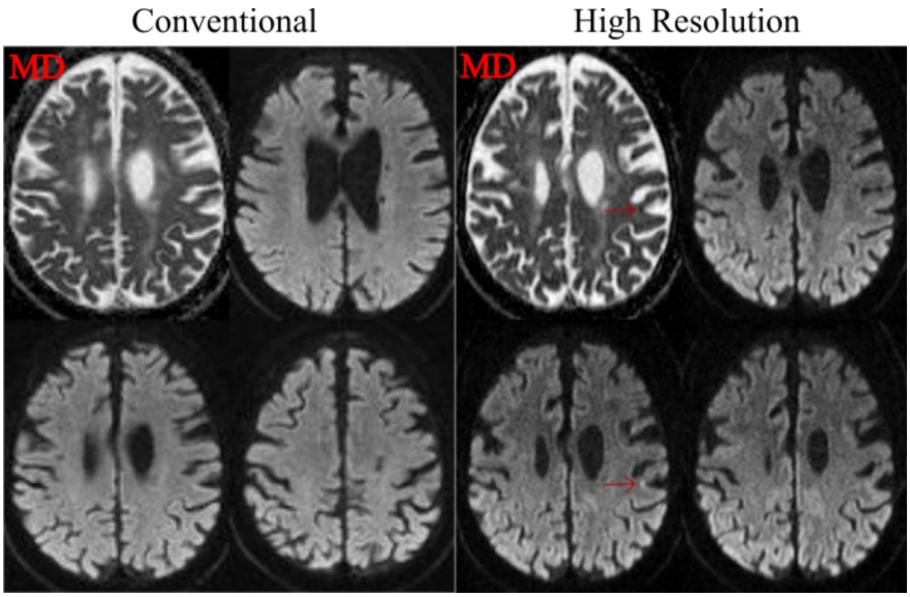

Figure 20 Conventional and High Spatial Resolution DWI of TIA Patient Imaged at 1.5T – An extremely small ischemic lesion (volume = 8 mm^3, MD =0.51 x 10^{-3} mm^2/s) can be seen on high spatial resolution DWI (4.5 mm^3 voxels) within the gray matter of the post central gyrus but not on conventional resolution DWI (19 mm^3 voxels).

In total, 20 of the 48 patients were found to possess an additional 29 ischemic lesions on high resolution DWI that were not seen on conventional DWI, with the raw data of exclusive ischemic lesions identified on high spatial resolution are summarized within Table 8. These lesions were consistently small with an average volume of 33 mm^3 (range, 5 – 191 mm^3) with an MD of 0.61 ± 0.14 x 10^{-3} mm^2/s) and were primarily located within the cortex (n = 16, 55 %) while occasionally seen within the deep white matter (n = 5), brainstem or cerebellum (n = 4), and deep gray matter nuclei (n = 4) of the brain. One instance of a lesion confirmed on conventional 1.5T DWI (volume, 230 mm^3; MD, 0.69 x 10^{-3} mm^2/s) was detected but omitted from volumetric and MD analysis on the high resolution DWI because it was partially obscured by a ghosting artifact and could not be accurately measured.

Table 8 : Exclusive Lesions Detected in Acute Ischemic Stroke and Transient Ischemic Attack (TIA) Patients Using High Resolution DWI

Scanner	Diagnosis of IS or TIA	Time to Scan, hrs	Location	Arterial Territory	Volume (cm^3)	MD ($x10^{-3}$ mm^2/s)
4.7T	IS	68	cGM	PCA	0.019	0.61
4.7T	IS	144	cGM	MCA	0.017	0.79
4.7T	IS	144	cGM	MCA	0.036	0.84
4.7T	IS	72	WM	MCA	0.014	0.57
4.7T	IS	72	cGM	MCA	0.019	0.51
4.7T	IS	72	cGM	MCA	0.015	0.74
4.7T	IS	22	cGM	PCA	0.011	0.59
4.7T	IS	24	cGM	ACA	0.016	0.77
4.7T	IS	96	WM	AChA	0.06	0.64
4.7T	IS	96	cGM	MCA	0.022	0.61
4.7T	IS	24	WM	MCA	0.034	0.74
4.7T	IS	34	cGM	MCA	0.05	0.75
4.7T	IS	45	In	SCA	0.005	0.72
4.7T	IS	45	In	SCA	0.008	0.66
4.7T	IS	45	In	SCA	0.024	0.61
4.7T	IS	35	dGM	LSA	0.043	0.8
1.5T	IS	32	cGM	MCA	0.19	0.67
1.5T	IS	32	cGM	MCA	0.014	0.49
1.5T	IS	-	cGM	MCA	0.037	0.56
1.5T	TIA	4.5	dGM	AChA	0.07	0.47
1.5T	IS	-	cGM	MCA	0.037	0.66
1.5T	IS	-	cGM	PCA	0.023	0.53
1.5T	IS	-	WM	ACA	0.17	0.61
1.5T	IS	7.5	WM	MCA	0.013	0.69
1.5T	TIA	6	dGM	LSA	0.007	0.3
1.5T	TIA	6	cGM	MCA	0.006	0.35
1.5T	TIA	-	dGM	LSA	0.022	0.54
1.5T	TIA	-	cGM	MCA	0.008	0.51
3.0T	IS	37	In	BA	0.047	0.58

ACA indicates anterior cerebral artery; AChA anterior choroidal artery; BA basilar artery; cGM cortical gray matter; dGM deep gray matter; In infratentorial; IS ischemic stroke; LSA lenticulostriate artery; MCA middle cerebral artery; MD mean diffusivity; PCA posterior cerebral artery; SCA superior cerebellar artery; TIA transient ischemic attack

4:4 Discussion

By reducing slice thickness to 1.5 mm (rather than modern protocols adopting 3 mm slices at 3.0T) to yield voxel volumes of 3.4 mm^3 while maintaining good image quality, the detection and characterization of acute ischemic lesions was improved while maintaining a reasonable acquisition time of roughly 3 - 4 minutes. A 3 - 4 minute scan time with smaller slices and voxels was adopted in order to attain satisfactory SNR and to readily fit within an acute stroke protocol, particularly, as the greatest value is for medically stable TIA and minor stroke patients that might otherwise be a diagnostic dilemma. Furthermore, high resolution isotropic acquisitions permit the depiction of ischemic lesions within three planes (sagittal, coronal and axial) that would otherwise not be feasible on conventional, thick slice acquisitions and assists in both the detection and characterization of ischemic lesions.

Our findings were consistent with previous studies that evaluated the merit to pushing resolution of diffusion imaging to 3 mm in acute stroke patients, demonstrating increased lesion detection and characterization over conventional DWI sequences[185-192]. Observation of smaller ischemic lesions on conventional resolution DWI was typically restricted to a single slice, but was consistently observed to span several slices on high resolution DWI, assisting both the detection and confirmation of hyperintensities that arise from cerebrovascular disease. A potential limitation to thin slice acquisition covering whole brain involves significantly more images and time spent assessing a single stroke patient. This could potentially limit how thin DWI can be improved to in effort to reduce time required for assessment. Increased magnetic field strength and stronger gradient coils on the 4.7T and 3T enabled a further increase in resolution because of the higher SNR ratios, producing qualitatively superior images over the 1.5T, yet were still obtained in similar acquisition times. The 3.0T also permitted the

measurement of diffusion in more than 3 directions while maintaining a scan time similar to the high resolution DWI at 4.7T. This not only increased the quality of DWI images through the additional scans, but also allowed fractional anisotropy (FA) maps to be calculated (**Figure 21**). FA maps can be used to assess how ischemic stroke directly affects tracts of the brain through retrograde and Wallerian degeneration, or indirectly through neuroplasticity in the contralateral tracts of the brain.

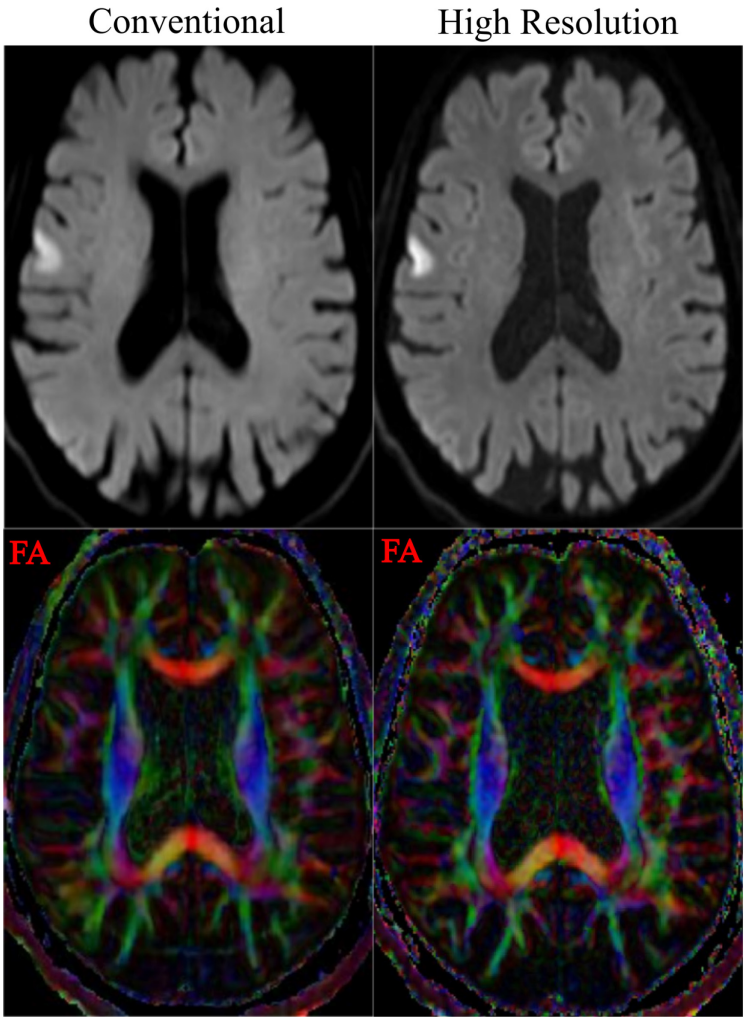

Figure 21 Conventional and High Spatial Resolution Color Fractional Anisotropy Map at 3.0T – 84 year old male diagnosed with ischemic stroke (NIHSS score = 2) with moderate dysarthria and mild facial droop 37 hours after symptom onset. By obtaining more than 3 directions such as the images from our 3.0T protocol, in addition to the calculation of MD maps, fractional anisotropy maps can be calculated, highlighting tract directions and changes in white matter anisotropy associated with ischemic stroke.

Previous literature has also demonstrated TIA patients with normal conventional DWI to have lesions on high resolution DWI[23, 186,189]. Ischemic lesions detected exclusively on high spatial resolution DWI were small and more frequently found residing within cortical GM. These can likely be explained by the presence of microemboli within small terminal branches of cortical penetrating arteries and the relative sensitivity of GM to infarction due to high metabolic demand. Specific cerebral tissues will possess varying responses to a decrease in CBF which is dependent on both the degree of collateral blood flow and metabolic demand of that tissue, possibly creating scenarios in which very small infarctions could ensue and are being masked by higher degrees of partial volume averaging on conventional DWI.

The prognostic assessment of ischemic stroke patients is at least partially based upon the specific infarct location identified using neuroimaging, as well as assists in establishing the underlying cause of the reduction in CBF[205, 206]. Furthermore, patients that demonstrate lesions within multiple territories creates an even higher risk of new DWI lesions[206]. Therefore, it becomes paramount to identify all ischemic lesions eliciting the recent neurological deficits as it potentially alters the pattern identified and may affect suspected causation, permitting initiation of more appropriate intervention strategies or alter the benefit/risk ratio of administering t-PA. High resolution DWI may not present as much merit for severe ischemic strokes, as additional time cannot be spared for these medically unstable patients and identification of additional lesions does not reduce their risk of hemorrhagic transformation following IV t-PA[207]. However, high spatial resolution DWI has promise for minor to moderate ischemic stroke and TIA through improved lesion identification and characterization to provide a more accurate assessment of their prognosis.

Volume differences of acute ischemic lesions measured using high and low resolution DWI have been previously compared in a systematic paired fashion, while differences in MD values have not been reported[185]. Yet our findings suggest that minimizing partial volume averaging of healthy adjacent tissue with diffusion restricted tissue (i.e. infarcted tissue) could be responsible for improving both volume and MD estimation when assessing DWI infarcts. Volume estimation has been shown to be one of the imaging parameters to have merit in predicting final clinical outcome [194-196,208, 209]. Likewise, minor ischemic strokes with larger DWI infarcts on initial assessment show the greatest mitigation in infarct growth when administered t-PA[194]. A 30% decrease in lesion volume estimation through accurate assessment on high resolution DWI could significantly impact the accuracy of using volume as a predictor to which minor ischemic stroke patients will respond best to t-PA and give a more consistent prediction of outcomes. Similarly, a study temporally evaluating changes in DWI lesion volume estimation between initial evaluations with a week follow up assessment, demonstrated overestimation of final infarct size when based upon the initial DWI volume assessment by 40%[210]. This could be further impacted by the increase in accuracy of volume estimation found through higher resolution DWI, possibly further increasing the importance of the temporal profile DWI volume estimation is performed in for the prediction of poststroke outcomes.

Although MD is used for the quantitative measure of the degree of bioenergetic compromise, it is not considered to be effective in predicting response to thrombolytics in ischemic stroke alone[198] and the method of MD thresholding in order to determine volume estimates of the amount of DWI infarction has sufficient doubt in its overall accuracy[211] despite only a slight overestimation (rarely more than > 10 mL) [212]. It is plausible that through accurate measurements of MD using high resolution DWI, infarcts with regions containing intermediate

MD values thought to reflect possibly salvageable tissue, could in fact be used to predict the fate of this variable tissue and the response to thrombolytics if they more accurately and consistently depicted the degree of bioenergetic compromise. Likewise, a more accurate and consistent depiction of ischemic related decreases in MD may increase MD thresholding accuracy and a subsequent increase in volume estimation accuracy using this technique. MD is also an important aid in identifying and confirming ischemic lesions over other plausible disorders causing neurological deficits with manifestations of hyperintensities on b1000 images[212]. Thus, more accurate MD values through minimized partial volume effects could also increase diagnostic accuracy when identifying and confirming small acute infarcts, especially in areas where signal averaging with CSF may cause doubt in diagnosis (e.g. infratentorium).

Detecting infarctions in TIA patients using DWI varies wildly, but typically averages to a third of diagnosed cases of TIA[100]. Detecting DWI abnormalities modifies the diagnosis of TIA to definitive acute ischemic cerebrovascular syndrome and can lead to appropriate therapeutic and preventative strategies to minimize risk of recurrence because of their negative prognostic value[73]. This includes warranting hospitalization of these patients for complete diagnostic assessment and monitoring for the development of a secondary stroke allowing rapid t-PA administration. Recent imaging studies have evaluated potential reasons for MRI negative results in TIA [189,213,214, 216, 217]. High resolution DWI managed to decrease the number of normal appearing DWI for TIA patients in our study (3 of 18 had lesions on lesions on high resolution DWI not seen on conventional DWI) but it is still not clear whether or not our high spatial resolution is sufficient, given the remaining normal appearing DWI in TIA patients within this small cohort primarily imaged at 1.5T (n = 14). The fact that resolution played a part in demonstrating additional lesions in ischemic stroke that were completely absent in conventional

scans allows us to suggest that it is not unreasonable to believe microemboli could create extremely small areas of infarction in TIA that just are simply not detectable on conventional DWI or DWI limited to 2 mm slices at 1.5T.

There remains to be many other factors that could not be ruled out by this study that could still contribute to the normal appearing DWI in TIA patients. A likely explanation for the absence of abnormalities on high resolution DWI is based upon literature demonstrating the absence of diffusion restrictions on DWI, yet identifying areas of hypoperfusion using perfusion imaging[216-218]. This possibly indicates that hypoperfusion is above the threshold required to cause energetic failure of the sodium/potassium pumps that would otherwise lead to cytotoxic edema, neurite beading and subsequent diffusion restriction, yet is sufficient enough to generate neurological deficits. It is possible that with time and inability of collateral blood flow to maintain a high enough degree of perfusion, these hypoperfused regions may progress to infarction later. It was recently demonstrated that on initial assessment using high resolution DWI that no abnormalities could be detected, yet on follow-up scans, infarcted tissue was in fact present on high resolution DWI[189] while DWI reversals have been shown to not be common in TIA[215]. No follow up imaging was performed to assess whether or not TIA patients would demonstrate a lesion after permitting time for tissue to proceed to infarction. MRI perfusion imaging techniques show promise in identifying these perfusion deficits that are insufficient enough to induce cytotoxic edema and the subsequent lack of DWI hyperintensities using high resolution acquisition parameters[86, 216,217]. Future work will focus on longitudinally attempting to identify TIA patients with perfusion deficits with and without DWI hyperintensities by combining DWI with high resolution acquisition parameters and high resolution MRI modalities that measure perfusion deficits such as ASL at 3.0T or higher.

Alternatively, these patients may not have experienced an ischemic event. TIA mimics remain to be potential diagnostic dilemmas concerning TIA when diagnostic imaging and evaluations fail to confirm or rule out a cerebrovascular accident[79]. It also remains plausible that the transient nature of symptoms indicates rapid recanalization of the occluded artery through normal physiological function and results in no permanent tissue damage in a portion of the TIA population. While monitoring of these patients outcomes and management was not performed within this study, such information would be useful to determine reoccurrence rate of transient symptoms or the occurrence of a secondary ischemic stroke following the initial event. Similarly, this may uncover evidence of alternative pathologies being responsible for the manifestation of the transient stroke like symptoms and effectively rule out TIA, explaining a portion of the DWI normal assessments.

4:5 Conclusion

In conclusion, this study supports use of higher spatial resolution diffusion-weighted imaging to assess acute ischemic stroke and transient ischemic attack patients in order to identify and characterize ischemic lesions over use of conventional, clinical DWI sequences, at the cost of increased acquisition time. We believe a moderate increase in scan time is feasible for the patients diagnosed with mild ischemic stroke and TIA in which neurological symptoms have likely diminished or resolved completely at the time of the scan and will benefit from the additional time spent to accurately assess the presence of ischemic lesions. It remains unclear if any permanent tissue damage is occurring in a large proportion of TIA patients with normal DWI, however, vascular pathology remains to be the suspected cause. Implementing high

resolution DWI clinically in conjunction with increased accessibility to higher magnetic field strengths could improve accuracy of TIA diagnoses and decrease subsequent stroke recurrences through the identification of ischemic lesions that correspond to their transient symptoms. High resolution DWI may also serve to increase the accuracy of determining an ischemic stroke patient's eligibility to receive thrombolytic therapy. Although DWI parameters are traditionally optimized for minimizing the time ischemic stroke patients remain within scanners, our results justify the additional 2 – 3 minutes spent to reduce voxel size (3.4 mm^3) and slice thickness (1.5 mm) of DWI.

Author Contributions:

Conceived and designed the experiments: Beaulieu C and Baron C. Performed the experiments: Baron C, Kate M, Gioia L, Sivakumar L, Buck B, Hafermehl K. Assisted in assessment of ischemic lesions: Kate M, Gioia L, Butcher K, Buck B. Analyzed the data: Hafermehl K. Contributed the analysis tools: Stobbe R. Wrote the paper: Hafermehl K.

Chapter 5

Concluding Remarks

Neuroimaging methods have become paramount and fundamental in the assessment of acute ischemic stroke, confirming diagnosis and predicting prognosis. Imaging, however, is not limited to detecting ischemic lesions, but also provides invaluable information on pathogenesis, the assessment of the degree of hypoperfusion, the identification of additional complications, and the understanding of the pathophysiology. Development and innovation in the field of neuroimaging, in particular MRI, will continue to pave the road to the understanding of the pathophysiology in stroke, improving patient assessment and leading to the advent of both new medications and techniques to combat the mechanisms causing neurological dysfunction in these individuals.

Diffusion-weighted imaging has solidified its position as the imaging technique to ideally assess acute ischemic stroke and transient ischemic attack. There is currently a gradual shift leading to the improvement of spatial resolution in the presently clinically trusted sequence as 3.0T MRI becomes readily available. The results presented within this work only serves to justify the decrease in slice thickness of DWI, while warranting even further improvements to spatial resolution. These improvements were further justified at higher magnetic field strengths

through the acquisition of higher quality images and shorter acquisition times when assessing minor to moderate ischemic strokes and TIA.

Further improvements in the DWI technique will only continue to serve to increase the quality and accuracy of identifying microscopic alterations in diffusion resulting from pathological mechanisms. Our study comparing conventional spatial resolution DWI to higher resolution DWI using reduced slice thickness and voxel size demonstrates decreased partial volume effects resulting in increased detection of ischemic lesions and reduced overestimation of both volume and MD measurements in acute ischemic stroke and TIA. Our observations pertaining to the enhancement of acquisition parameters for DWI in the assessment of ischemic lesions in TIA and acute ischemic stroke will serve to increase the accuracy of diagnosis, prognosis and perfusion/diffusion mismatch estimations. TIA patients continue to present with normal-appearing DWI in the majority of our patients despite reductions in voxel size and slice thickness. However, we believe that using higher magnetic field strengths, denser array radiofrequency coils, and stronger gradients on a large cohort will permit the identification of additional TIA patients who have permanent tissue damage. The three instances of TIA that had confirmation of permanent ischemic infarction on high resolution DWI not seen on conventional DWI confirms the idea that resolution does have a role to play in diffusion imaging's ability to confirm the presence of permanent vascular-related tissue damage in TIA. Small ischemic lesions may still be going undetected, but using 1.5 mm slices or pushing slice thickness to 1.0 mm because of the increased signal available at 3.0T, may identify small volumes of infarcted tissue in TIA patients. Because of the increased speed of acquisition, a large cohort of TIA patients scanned at 3.0T can consecutively be imaged using a 30 minute stroke protocol that also

incorporates FLAIR, MRA, SWI and a high resolution ASL sequence to identify hypoperfused tissue above the threshold for infarction.

As mentioned in Chapter 3, DWI is capable of detecting much more than just ischemic lesions. For this reason, application of a high spatial resolution DWI sequence could have implications for other pathologies. However, as the focus of the thesis was the application of high resolution DWI, a possible expansion of this work could be the evaluation of the connection of atrial fibrillation (AF) and TIA. A distinct characteristic of ischemic strokes caused by AF is the association of multiple tiny infarctions scattered across multiple arterial zones, as AF can result in an embolus that mechanically breaks apart into smaller emboli and sends a "shower of emboli" into the cerebrovasculature. Atrial fibrillation patients admitted into hospitals may not be demonstrating any neurological deficits, but may yet possess many small zones of silent infarctions or areas of hypoperfusion.

The MRI improvements highlighted within this thesis for the assessment of acute ischemic stroke, specifically the feasibility and merit to improve DWI resolution, may assist in understanding the underlying pathology of minor ischemic stroke and TIA if incorporated into a routine stroke protocol. The diagnostic merit could potentially be improved further when combined with MRI modalities that permit high resolution perfusion estimation for routine TIA and minor ischemic stroke assessment. As clinics procure new and advanced 3.0T scanners, resolution of diffusion imaging has begun to improve in order to detect small smaller areas of abnormalities and better depict the structure of the brain. The DWI slice thickness of 1.5 mm was thinner than previously studied but was still within clinically realistic scan times (3 – 4 minutes) for minor ischemic strokes and TIA. The advantages of high resolution DWI included the feasibility to reconstruct diffusion images into axial, sagittal and coronal planes given the

isotropic acquisition, increased volumetric and mean diffusivity assessment accuracy, and increased diagnostic accuracy through unique ischemic lesion identification.

Bibliography

1. Krueger H, Koot J, Hall RE, et al. Prevalence of Individuals Experiencing the Effects of Stroke in Canada: Trends and Projections. Stroke. 2015; 46: 2226 - 2231.
2. Public Health Agency of Canada. (2009). Tracking Heart Disease and Stroke in Canada, 2009. Retrieved from: http://www.phac-aspc.gc.ca/publicat/2009/cvd-avc/pdf/cvd-avs-2009-eng.pdf
3. Wolfe CDA. The Impact of Stroke. *British Medical Bulletin*. 2000; 56: 275-286.
4. Sheldon JJ. Blood Vessels of the Scalp and Brain. *Clinical Symposia*. 1981; 33: 1-36.
5. Marinkovic SV, Milisavljevic MM, Kovacevic MS, *et al*. Perforating Branches of the Middle Cerebral Artery. Micro-anatomy and Clinical Significance of their Intracerebral Segments. *Stroke*. 1985; 16: 1022-1029.
6. Bergman RA, Afifi AK and Miyauchi R, Circle of Willis. Illustrated Encyclopedia of Human Anatomic Variation, URL: http://www.anatomyatlases.org/AnatomicVariants/Cardiovascular/Text/Arteries/CircleofWillis.shtml.
7. Frackowiak RSJ. PET Scanning: Can it Help Resolve Management Issues in Cerebral Ischaemic Disease? *Stroke*. 1986; 17: 803-807.
8. Rutgers DR, Klijn CJ, Kappelle LJ, et al. Recurrent Stroke in Patients with Symptomatic Carotid Artery Occlusion is Associated with High-volume Flow to the Brain and Increased Collateral Circulation. *Stroke*. 2004; 35: 1345-1349.
9. Leenders KL, Perani D, Lammertsma AA, et al. Cerebral Blood Flow, Blood Volume and Oxygen Utilization. Normal Values and Effect of Age. *Brain*. 1990; 113: 27-47.

10. Blesa R, Mohr E, Miletich RS, et al. Changes in Cerebral Glucose Metabolism with Normal Aging. *European Journal of Neurology*. 1997; 4: 8-14.
11. Reed G and Devous M. South-western Internal Medicine Conference: Cerebral Blood Flow Autoregulation and Hypertension. *American Journal of Medical Science*. 1985; 289: 37-44.
12. Rothwell PM, Coull AJ, Giles MF, *et al*. Change in Stroke Incidence, Mortality, Case-Fatality, Severity and Risk Factors in Oxfordshire, UK from 1981 to 2004 (Oxford Vascular Study). *Lancet*. 2004; 363: 1925-1933.
13. Adams HP, Bendixen BH, Kappelle LJ, et al. Classification of Subtype of Acute Ischemic Stroke Definitions for Use in a Multicenter Clinical Trial. *Stroke*. 1993; 24: 35-41.
14. Tobis JM, and Azarbal B. Does Patent Foramen Ovale Promote Cryptogenic Stroke and Migraine Headache? *Cardiology*. 2005; 32: 362-365.
15. Grau AJ, Weimar C, Buggle F, et al. Risk Factors, Outcome, and Treatment in Subtypes of Ischemic Stroke. The German Stroke Data Bank. *Stroke*. 2001; 32: 2559-2566.
16. Smith E. Leukoaraiosis and stroke. *Stroke*. 2010; 41: 139-143.
17. Gorter JW. For the Stroke Prevention in Reversible Ischemia Trial (SPIRIT) and the European Atrial Fibrillation Trial (EAFT) Study Groups. *Neurology*. 1999; 53: 1319-1327.
18. Lammie GA. Hypertensive cerebral small vessel disease and stroke. *Brain Pathology.* 2002; 12:358-70.
19. French CR, Seshadri S, Destafano AL, et al. Mutation of *FOXC1* and *PITX2* induces cerebral small vessel disease. *The Journal of Clinical Investigation*. 2014; 124: 4877-4881.
20. Werner H, Marku K, Cesare F, et al. Intravenous Thrombolysis With Recombinant Tissue Plasminogen Activator for Acute Hemispheric Stroke The European Cooperative Acute Stroke Study (ECASS). *Jama*. 1995; 274: 1017- 1025.

21. Saver J, Jahan R, Levy E, et al. Solitaire flow restoration device versus the Merci Retriever in patients with acute ischaemic stroke (SWIFT): a randomised, parallel-group, non-inferiority trial. The Lancet. 2012; 380: 1241-1249.
22. Jauch E, Saver J, Adams H, et al. Guidelines for the Early Management of Patients With Acute Ischemic Stroke A Guideline for Healthcare Professionals From the American Heart Association/American Stroke Association. *Stroke*. 2013; 44: 870-947.
23. Lehmann P, Brasseur A, Saliou G, et al. Do TIAs require investigation by thin-slice high-resolution diffusion MRI with a 3T MR unit? *European Journal of Neurology.* 2008;15:62-63.
24. Touma L, Filion K, Sterlin L, et al. Stent Retrievers for the Treatment of Acute Ischemic StrokeA Systematic Review and Meta-analysis of Randomized Clinical Trials. JAMA. 2016; 73: 275-281.),
25. Hacke W, Albers G, Al-Rawi Y, et al. The Desmoteplase in Acute Ischemic Stroke Trial (DIAS). A Phase II MRI-Based 9-Hour Window Acute Stroke Thrombolysis Trial With Intravenous Desmoteplase. Stroke; 2005: 36: 66-73.
26. Feng L, Liu J, Liu Y, et al. Tirofiban combined with urokinase selective intra -arterial thrombolysis for the treatment of middle cerebral artery occlusion. Experimental and Therapeutic Medicine. 2015; 11: 1011-1016.
27. Weitz JI, Stewart RJ and Fredenburgh JC. Mechanism of Action of Plasminogen Activators. *Thrombosis and Haemostasis.* 1999; 82: 974-982.
28. Kunst MM and Schaefer PW. Ischemic stroke. *Radiol Clin N Am*. 2011; 49:1-26.
29. Nagaraja D and Karthik N. Imaging in stroke. *Medicine Update*. 2011; 214-220.

30. Aho K, et al. Cerebrovascular disease in the community: results of a WHO collaborative study. *Bull WHO*. 1980; 58: 113–130.

31. Kaplan B, Brint S, Tanabe J, et al. Temporal thresholds for neocortical infarction in rats subjected to reversible focal cerebral ischemia. Stroke. 1991; 22: 1032-1039.

32. Kidwell C, Alger J and Saver J. Beyond Mismatch. Evolving Paradigms in Imaging the Ischemic Penumbra With Multimodal Magnetic Resonance Imaging. *Stroke*. 2003; 34: 2729-2735.

33. Meijer R, Ihnenfeldt, Groot JM, et al. Prognostic factors for ambulation and activities of daily living in the subacute phase after stroke. A systematic review of the literature. *Clin Rehabil*. 2003; 17: 119 - 129.

34. Heiss WD, Kracht LW, Thiel A, et al. Penumbral probability thresholds of cortical flumazenil binding and blood flow predicting tissue outcome in patients with cerebral ischaemia. *Brain*. 2001; 124: 20-29.

35. Diener HC, Selim MH, Molina CA and Greenberg SM. Embolic Stroke, Atrial Fibrillation, and Microbleeds. Is There a Role for Anticoagulation? *Stroke*. 2016; 47: 904-907.

36. Manolio TA, Kronmal RA, Burke GL, et al. Short-term Predictors of Incident Stroke in Older Adults. The Cardiovascular Health Study. *Stroke*. 1996; 27: 1479-1486.

37. Urakhia MP, Ziegler PD, Schmitt SK, et al. Atrial fibrillation burden and short-term risk of stroke: case-crossover analysis of continuously recorded heart rhythm from cardiac electronic implanted devices. *Circ Arrhythm Electrophysiol*. 2015; 8: 1040–1047.

38. Wolf PA, Dawber TR, Thomas HE Jr, Kannel WB. Epidemiologic assessment of chronic atrial fibrillation and risk of stroke: the Framingham study. *Neurology*. 1978; 28: 973–977.

39. Kamel H, Okin PM, Elkind MSV and Iadecola C. Atrial Fibrillation and Mechanisms of Stroke. Time for a New Model. *Stroke*. 2016; 47: 895-900.

40. Lee VH, Brown Jr RD, Mandrekar JN, Mokri B. Incidence and outcome of cervical dissection; a population-based study. *Neurology*. 2006; 67 (10): 1809–1812.

41. Pantoni L. Cerebral small vessel disease: from pathogenesis and clinical characteristics to therapeutic challenges. *Neurology*. 2010; 9: 689-701.

42. Prins ND, Dijk EJV, Heijer TD, et al. Cerebral small-vessel disease and decline in information processing speed, executive function and memory. *Brain*. 2005; 128: 2034-2041.

43. Bamford JM and Warlow CP. Evolution and testing of the lacunar hypothesis. *Stroke* 1988; 19: 1074.

44. Sudlow CLM and Warlow CP. Comparable studies of the incidence of stroke and its pathological types. Results from an international collaboration. *Stroke.* 1997; 28: 491–499.

45. Astrup J, Symon L, Bhanston NM, et al. Cortical Evoked Potential and Extracellular K + and H + at Critical Levels of Brain Ischemia. *Stroke.* 1977; 8: 51 – 57.

46. Rothman SM, Olney JW Excitotoxicity and the NMDA receptors. Trends Neurosci. 1987; 10:299-302.

47. Heros R. Stroke: early pathophysiology and treatment. Stroke. 1994;25:1877-1881

48. Becker KJ. Inflammation and acute stroke. *Curr Opin Neurol*. 1998; 11: 45-49.

49. Warach S, Gaa J, Siewert B, et al. Acute Human Stroke Studied by Whole Brain Echo Planar Diffusion-weighted Magnetic Resonance Imaging. *Ann Neurol*. 1995; 37: 231-241.

50. Akpan N and Troy CM. Caspase Inhibitors Prospective Therapies for Stroke. *The Neuroscientist*. 2012: 19; 129 – 136.

51. Cuzzocrea S, Riley DP, Caputi AP and Salvemini D: Antioxidant therapy: a new pharmacological approach in shock, inflammation, and ischemia/reperfusion injury. *Pharmacol Rev*. 2001, 53: 135-159.

52. Wong Ch and Crack PJ: Modulation of neuro-inflammation and vascular response by oxidative stress following cerebral ischemia-reperfusion injury. *Curr Med Chem*. 2008, 15: 1-14. 10.2174.

53. Coyle JT and Puttfarcken P: Oxidative stress, glutamate, and neurodegenerative disorders. *Science*. 1993, 262: 689-695.

54. Lucas SM, Rothwell NJ and Gibson RM. The Role of Inflammation in CNS Injury and Disease. *Br J Pharmacol*. 2006; 147: 232-240.

55. Shih AY, Li P and Murphy TH. A small molecule inducible Nrf2-mediated antioxidant response provides effective prophylaxis against cerebral ischemia in vivo. *J Neurosci*. 2005, 25: 10321-10335.

56. Zhu Y, Yang GY, Ahlemeyer B, et al. Transforming growth factor-beta 1 increases bad phosphorylation and protects neurons against damage. *J Neurosci*. 2002, 22: 3898-3909.

57. Soriano S, Amaravadi L, Wang Y, et al. Mice deficient in fractalkine are less susceptible to cerebral ischemia-reperfusion injury. *J Neuroimmunol*. 2002, 125: 59-65.

58. Hughes PM, Allegrini PR, Rudin M, et al. Monocyte chemoattractant protein-1 deficiency is protective in a murine stroke model. *J Cereb Blood Flow Metab*. 2002, 22: 308-317.

59. Krieger DM, De Georgia MA, Abou-Chebl A, et al. Cooling for Acute Ischemic Brain Damage (COOL AID). An Open Pilot Study of Induced Hypothermia in Acute Ischemic Stroke. Stroke. 2001; 32: 1847-1854.

60. Lakhan SE, Kirchgessner A and Hofer M. Inflammatory Mechanisms in Ischemic Stroke: Therapeutic Approaches. Journal of Translation Medicine. 2009; 7: 97-108

61. Wong CH and Crack PJ. Modulation of neuro-inflammation and vascular response by oxidative stress following cerebral ischemia-reperfusion injury. *Current Medicinal Chemistry*. 2008; 15: 1-14.

62. Carden DL and Granger DN 2000. Pathophysiology of ischaemia-reperfusion injury. The *Journal of Pathology*. 2000; 190: 255–66.

63. Larrue V, Kummer RV, Müller A and Bluhmki E. Risk Factors for Severe Hemorrhagic Transformation in Ischemic Stroke Patients Treated With Recombinant Tissue Plasminogen Activator A Secondary Analysis of the European-Australasian Acute Stroke Study (ECASS II). *Stroke*. 2001; 32: 438-441.

64. Leiva-Salinas C and Wintermark M. Imaging of Ischemic Stroke. *Neuroimaging Clin N Am*. 2010; 20: 455-468.

65. Barber PA, Darby DG, Desmond PM, et al. Identification of major ischemic change. Diffusion-weighted imaging versus computed tomography. *Stroke*. 1999; 30(10):2059-2065.

66. Larrue V, Kummer R, Muller A and Bluhmki E. Risk Factors for Severe Hemorrhagic Transformation in Ischemic Stroke Patients Treated With Recombinant Tissue Plasminogen Activator A Secondary Analysis of the European-Australasian Acute Stroke Study (ECASS II). *Stroke*. 2001; 32: 438-441.

67. Latchaw RE, Yonas H, Hunter GJ, et al. Guidelines and recommendations for perfusion imaging in cerebral ischemia: A scientific statement for healthcare professionals by the writing group on perfusion imaging, from the Council on Cardiovascular Radiology of the American Heart Association. *Stroke*. 2003; 34(4):1084-1104.

68. Lell MM, Anders K, Uder M, et al. New techniques in CT angiography. *Radiographics*. 2006; 26: 45-62.

69. Lima FO, Lev MH, Silva GS, et al. Functional Contrast-enhanced CT for Evaluation of Acute Ischemic Stroke Does not Increase the Risk of Contrast-induced Nephropathy. *AJNR*. 2010; 31: 817-821.

70. Chalela JA, Kidwell CS, Nentwich LM, et al. Magnetic Resonance Imaging and Computed Tomography in Emergency Assessment of Patients with Suspected Acute Stroke: a Prospective Comparison. *The Lancet*. 2007; 369: 293-298.

71. Nael K, Khan R, Choudhary G, et al. Six-Minute Magnetic Resonance Imaging Protocol for Evaluation of Acute Ischemic Stroke Pushing the Boundaries. *Stroke*. 2014; 45: 1985-1991.

72. Moreau F, Asdaghi N, Modi J, et al. Magnetic Resonance Imaging versus Computed Tomography in Transient Ischemic Attack and Minor Stroke: The More You See the More You Know. *Cerbrovasc Dis Extra.* 2013; 3: 130-136.

73. Purroy F, Montaner J, Rovira A, Delgado P, Quintana M, A´lvarez-Sabı´n J. Higher Risk of Further Vascular Events Among Transient Ischemic Attack Patients With Diffusion-Weighted Imaging Acute Ischemic Lesions. *Stroke*. 2004; 35: 2313-2319.

74. Novikov D, Jensen J, Helpern J, and Fieremans E. Revealing mesoscopic structural universality with diffusion. *PNAS*. 2014; 111: 5088-5093.

75. Corey B, Mahesh K, Gioia L, et al. Reduction of diffusion-weighted imaging contrast of acute ischemic stroke at short diffusion times. *Stroke*. 2015; 46: 00-00.

76. Xavier AR, Qureshi AI, Kirmani JF, Yahia AM, Bakshi R. Neuroimaging of stroke: a review. *South Med J*. 2003; 96(4):367-79.

77. Zawadzki M, Atkinson D, Detrick M, et al. Fluid-Attenuated Inversion Recovery (FLAIR) for Assessment of Cerebral Infarction Initial Clinical Experience in 50 Patients. *Stroke*. 1996; 27: 1187-1191.

78. Kakar P, Charidimou A, Werring D. Cerebral microbleeds: a new dilemma in stroke medicine. *Cardiovasc Dis.* 2012; 1:22.

79. Simonsena C, Nielsenb E. Hypertensive Microbleed as a Transient Ischemic Attack Mimic. *Neurol.* 2013;5:31–33.

80. Charidimou A and Werring DJ. Cerebral Microbleeds: Detection, Mechanisms, and Clinical Challenges: What are CMBs? MRI Detection, Characteristics & Differential Diagnosis. *Future Neurology*. 2001; 6: 587-611.

81. Chalela J, Alsop D, Gonzalez-Atavales J, Maldjian J, Kasner S, Detre J. Magnetic Resonance Perfusion Imaging in Acute Ischemic Stroke Using Continuous Arterial Spin Labeling. *Stroke*. 2000;31:680-687.

82. Schellinger P, Fiebach J, Hacke W. Imaging-Based Decision Making in Thrombolytic Therapy for Ischemic Stroke Present Status. *Stroke*. 2003;34:575-583.

83. Reid E, Graham D, Lopez-Gonzalez MR, Holmes W, Macrae IM and McCabe C. Penumbra detection using PWI/DWI mismatch MRI in a rat stroke model with and without comorbidity: comparison of methods. *Journal of Cerebral Blood Flow & Metabolism.* 2012; 32: 1765–1777.

84. Warach S. Measurement of the Ischemic Penumbra with MRI: It's About Time. *Stroke*. 2003; 34: 2533-2534.

85. Holdsworth S and Bammer R. Magnetic Resonance Imaging Techniques: fMRI, DWI, and PWI. Semin Neurol. 2008; 28: 395-406.

86. Wang D, Alger JR, Qiao JX, et al. The Value of Arterial Spin-Labeled Perfusion Imaging in Acute Ischemic Stroke-comparison with Dynamic Susceptibility Contrast Enhanced MRI. *Stroke*. 2012; 43: 1018-1024.

87. Hill MD, Yiannakoulias N, Jeerakathil T, Tu JV, Svenson LW, Schop-flocher DP. The high risk of stroke immediately after transient ischemic attack. Neurology. 2004; 62: 2015–2020.

88. Sorensen AG and Ay H. Transient Ischemic Attack Definition, Diagnosis and Risk Stratification. *Neuroimaging Clin N Am*. 2011; 21: 303-313.

89. Rothwell PM, Warlow CP. Timing of transient ischaemic attacks preceding ischaemic stroke. *Neurology*. 2005; 64: 817–820.

90. Lloyd-Jones D, Adams RJ, Brown TM, et al. Heart disease and stroke statistics--2010 update: a report from the American Heart Association. *Circulation*. 2010; 121:46-215.

91. Nadarajan V, Perry RJ, Johnson J and Werring DJ. Transient ischaemic attacks: mimics and chameleons. *Pract Neurol*. 2014; 14: 23-31.

92. WHO MONICA Project Principal Investigators. The World Health Organization MONICA Project (monitoring trends and determinants in cardiovascular disease): a major international collaboration. *J Clin Epidemiol.* 1988; 41:105-14.

93. Ay H, Oliveira-Filho J, Buonanno FS, et al. "Footprints" of Transient Ischemic Attacks: a Diffusion-weighted MRI Study. *Cerbrovasc Dis*. 2002; 14: 177-186.

94. Kidwell CS, Alger JR, Di Salle F, et al. Diffusion MRI in Patients with Transient Ischemic Attacks. *Stroke*. 1999; 30: 1174-1180.

95. Levy DE. How Transient are Transient Ischemic Attacks? *Neurology*. 1988; 38: 674-677.

96. Koudstaal PJ, Gerritsma JG and van Gijn J. Clinical disagreement on the diagnosis of transient ischemic attack: is the patient or the doctor to blame? *Stroke*. 1989;20:300.

97. Ferro JM, Falcão I, Rodrigues G, et al. Stroke-trained neurologists have a fair amount of disagreement when diagnosis TIA - Diagnosis of transient ischemic attack by the non-neurologist. A validation study. *Stroke*. 1996; 27(12):2225-2229.

98. Castle J, Mlynash M, Lee K, et al. Agreement regarding diagnosis of transient ischemic attack fairly low among stroke-trained neurologists. *Stroke*. 2010;41:1367-1370.

99. Giles M, Rothwell P. Risk of stroke early after transient ischaemic attack: a systematic review and meta-analysis. *Neurol.* 2007; 6: 1063–1072.

100. Crisostomo RA, Garcia MM and Tong DC. Detection of diffusion-weighted MRI abnormalities in patients with transient ischemic attack: correlation with clinical characteristics. *Stroke.* 2003; 34(4):932-937.

101. Albers GW, Caplan LR, Easton D, et al. Transient Ischemic Attack-Proposal for a New Definition. *N Engl J Med*. 2002; 347: 1713-1716.

102. Easton JD, Saver JL, Albers GW, et al. Definition and evaluation of transient ischemic attack: a scientific statement for healthcare professionals from the American Heart Association/American Stroke Association Stroke Council; Council on Cardiovascular Surgery and Anesthesia; Council on Cardiovascular Radiology and Intervention; Council on Cardiovascular Nursing; and the Interdisciplinary Council on Peripheral Vascular Disease. *Stroke.* 2009; 40: 2276–2293.

103. Ovbiagele B, Kidwell CS, and Saver JL. Epidemiological Impact in the United States of a Tissue-based Definition of Transient Ischemic Attack. *Stroke*. 2003; 60: 1429-1434.

104. Coull AJ, Lovett JK, Rothwell PM. Population based study of early risk of stroke after transient ischaemic attack or minor stroke: implications for public education and organization of services**.** *BMJ.* 2004; 328: 326.

105. Coutts SB, Hill MD, Campos CR, et al. Recurrent Events in Transient Ischemic Attack and Minor Stroke. What Events are Happening and to Which Patients? *Stroke*. 2008; 39: 2461-2466.

106. Rothwell PM, Giles MF, Chandratheva A, et al. Effect of urgent treatment of transient ischaemic attack and minor stroke on early recurrent stroke (EXPRESS study): a prospective population-based sequential comparison [published correction appears in Lancet. 2008;371(9610):386]. *Lancet*. 2007; 37: 1432-1442.

107. Ay H and Koroshetz WJ. Transient Ischemic Attack: Are There Different Types or Classes? Risk of Stroke and Treatment Options. *Current Treatment Options in Cardiovascular Medicine*. 2006; 8: 193-200.

108. Ay H, Koroshetz WJ, Benner T, et al. Transient Ischemic Attack with Infarction: A Unique Syndrome? *Ann Neurol*. 2005; 57: 679-686.

109. Verro P, Gorelick PB, Nguyen D. Aspirin plus dipyridamole versus aspirin for prevention of vascular events after stroke or TIA: a meta-analysis. *Stroke*. 2008;39(4):1358-1363.

110. Donan GA, O'Malley HM M, Quang L, Hurley S and Bladin PF. The capsular warning syndrome. *Neurology.* 1993; 43:957–962.

111. Saposnik G and Caplan LR. Pontine warning syndrome. *Arch Neurol.* 2008; 65:1375–1377.

112. Vivanco-Hidalgo RM, Rodriguez-Campello A, Ois A, Cucurella G, Pont-Sunyer C, Gomis M, Cuadrado-Godia E, Roquer J: Thrombolysis in capsular warning syndrome. *Cerbrovasc Dis*. 2008; 25:508–510.

113. Lee J, Albers GW, Marks MP, Lansberg MG: Capsular warning syndrome caused by middle cerebral artery stenosis. *J Neurol Sci*. 2010; 296: 115–120.

114. Herve D, Gautier-Bertrand M, Labreuche J and Amarenco P. Predictive values of lacunar transient ischemic attacks. *Stroke*. 2004; 35:1430–1435.

115. Tomasello F, Mariani F, Fieschi C, et al. Assessment of inter-observer differences in the Italian multicenter study on reversible cerebral ischemia. *Stroke* 1982; 13: 32.

116. Kraaijeveld CL, van Gijn J, Schouten HJ, et al. Interobserver agreement for the diagnosis of transient ischemic attacks. *Stroke*.1984;15:723.

117. Devere TR, Trotter JL and Cross AH. Acute aphasia in multiple sclerosis. *Arch Neurol* 2000; 57: 1207–1209.

118. Lacour A, De Seze J, Revenco E, et al. Acute aphasia in multiple sclerosis: a multi center study of 22 patients. *Neurology.* 2004; 62: 974–977.

119. Cowan J, Ormerod IE and Rudge P. Hemiparetic multiple sclerosis. *J Neurol Neurosurg Psychiatry.* 1990; 53: 675–680.

120. Rosso C, Remy P, Creagne A, et al. Diffusion-Weighted MR Imaging Characteristics of an Acute Stroke-like Form of Multiple Sclerosis. *Am J Neuroradiol*. 2006; 27: 1006-1008.

121. Gass A, Niendorf T and Hirsch JG. Acute and chronic changes of the apparent diffusion coefficient in neurological disorders-biophysical mechanisms and possible underlying histopathology. *J Neurol Sci.* 2001; 186: 15–23.

122. Putnam TJ. The pathogenesis of multiple sclerosis: a possible vascular factor. *N Engl J Med.* 1933; 209: 786–790.

123. Wakefield AJ, More LJ, Difford J, et al. Immunohistochemical study of vascular injury in acute multiple sclerosis. *J Clin Pathol.* 1994; 47: 129–133.

124. McDonald WI, Compston A, Edan G, et al. Recommended diagnostic criteria for multiple sclerosis: guidelines from the International Panel on the Diagnosis of Multiple Sclerosis. *Ann Neurol.* 2001; 50: 121–127.

125. Horstmann S, Mohlenbruch M, Wegele C, et al. Prevalence of Atrial Fibrillation and Association of Previous Antithrombotic Treatment in Patients with Cerebral Microbleeds. *European Journal of Neurology*. 2015; 22: 1355-1362.

126. Simonsen CZ and Nielsen E. Hypertensive Microbleed as a Transient Ischemic Attack Mimic. *Case Rep Neurol*. 2013; 5: 31-33.

127. Watanabe A and Kobashi T. Lateral gaze disturbance due to cerebral microbleed in the medial lemniscus in the mid-pons region: a case report. *Neuroradiology.* 2005; 47: 908–911.

128. Kakar P, Charidimou A and Werring DJ. Cerebral microbleeds: a new dilemma in stroke medicine. *J R Soc MedCardiovasc Dis*. 2012; 1: 22-36.

129. Kidwell CS, Saver JL, Villablanca JP, et al. Magnetic Resonance Imaging Detection of Microbleeds before Thrombolysis. An Emerging Application. *Stroke*. 2002; 33: 95-98.

130. Lee SH, Kang BS, Kim N and Roh JK. Does Microbleed Predict Haemorrhagic Transformation after Acute Atherothrombotic or Cardioembolic Stroke? *J Neurol Neurosurg Psychiatry*. 2008; 79: 913-916.

131. Dennis M and Warlow C. Migraine Aura without Headache: Transient Ischaemic Attack or not. *Journal of Neurology, Neurosurgery, and Psychiatry*. 1992; 55: 437-440.

132. Simmons BB, Cirignano B and Gadegbeku AB. Transient Ischemic Attack: Part I. Diagnosis and Evaluation. *Indian Journal of Clinical Practice*. 2014; 25: 407- 411.

133. Gelfand JM, Wintermark M and Josephson SA. Cerebral Perfusion-CT Patterns Following Seizure. *Eur J Neurol*. 2010; 17: 594-601.

134. Kosior RK, Wright CJ, Kosior JC, et al. 3-Tesla versus 1.5-Tesla magnetic resonance diffusion and perfusion imaging in hyperacute ischemic stroke. *Cerebrovasc Dis.* 2007; 24: 361-368.

135. Douek P, Turner R, Pekar J, Patronas N and Le Bihan D. MR color mapping of myelin fiber orientation. *Journal of Computer Assisted Tomography*. 1991; 923-929.

136. Gray H (1918) revised by Warren H. Lewis (2000). *Gray's Anatomy* (20th ed.) Philadelphia. Lea and Febiger.

137. Tang Y, Nyengaard JR, Pakkenberg B and Gundersen HJ. Age induced white matter changes in the human brain: a sterological investigation. *Neurobiol Aging*. 1997; 609-615.

138. Moseley ME, Cohen Y, Kucharczyk J, et al. Diffusion-weighted MR imaging of anisotropic water diffusion in cat central nervous system. *Radiology*. 1990; 176(2): 439-45.

139. Beaulieu C and Allen PS. Determinants of anisotropic water diffusion in nerves. *Magnetic Resonance in Medicine*. 1994; 31 (4); 394-400.

140. Wimberger DM, Roberts TP, Barkovich AJ, Prayer LM, MOseley ME and Kucharczyk J Identification of premyelination by diffusion-weighted MRI. *J Comput Assist Tomogr*. 1995; 19(1): 28-33.

141. Gulani V, WEbb AG, Duncan ID and Lauterbur PC Apparent diffusion tensor measurements in myelin-deficient rat spinal cords. *Magn Reson Med*. 2001; 45(2); 191-195.

142. Helenius J, Soinne L, Perkiö J, et-al. Diffusion-weighted MR imaging in normal human brains in various age groups. *AJNR Am J Neuroradiol*. 2002;23 (2):194-199.

143. Annet L, Duprez T, Grandin C, et-al. Apparent diffusion coefficient measurements within intracranial epidermoid cysts in six patients. *Neuroradiology*. 2002;44 (4): 326-328.

144. Hilario A, Ramos A, Perez-Nuñez A, et-al. The added value of apparent diffusion coefficient to cerebral blood volume in the preoperative grading of diffuse gliomas. *AJNR Am J Neuroradiol*. 2012;33 (4): 701-707.

145. Hahn EL. Spin Echoes. *Physical Review.* 1950; 80: 580-594

146. Carr HY and Purcell EM. Effects of Diffusion on Free Precession in Nuclear Magnetic Resonance Experiments. *Physical Review*. 1954; 94: 630-638.

147. Stejskal EO and Tanner JE. Spin Diffusion Measurements: Spin Echoes in the Presence of a Time-Dependent Field Gradient. *The Journal of Chemical Physics*. 1965; 42: 288-292.

148. Lauterbur PC. Image Formation by Induced Local Interactions: Examples of Employing Nuclear Magnetic Resonance. *Nature.* 1973; 242:190-191.

149. Lauterbur PC. Magnetic Resonance Zeumatography. *Pure and Applied Chemistry*. 1974; 40:149-157.

150. Le Bihan D, Breton E, Lallemand D, et al. MR imaging of intravoxel incoherent motions: application to diffusion and perfusion in neurologic disorders. *Radiology*. 1986; 161(2):401-407.

151. Stehling MK, Turner R and Mansfield P. Echo-planar imaging: magnetic resonance imaging in a fraction of a second. *Science*. 1991; 254 (5028):43-50.

152. Turner R, Le Bihan D, Maier J, et al. Echo-planar imaging of intra voxel incoherent motion. *Radiology*. 1990; 177(2): 407-14.

153. Hagmann P, Jonasson L, Maeder P, et al. Understanding Diffusion MR Imaging Techniques: From Scalar Diffusion-weighted Imaging to Diffusion Tensor Imaging and Beyond. *RadioGraphics*. 2006; 26: 205-223.

154. Tanner JE and Stejskal EO. Restricted Self-Diffusion of Protons in Colloidal Systems by the Pulsed-Gradient, Spin-Echo Method. *Journal of Chemical Physics*. 1968; 49:1768-1777.

155. Provenzale JM and Sorensen AG. Diffusion-weighted MR imaging in acute stroke: theoretical considerations and clinical applications. *Am J Roentgenol*. 1999; 173: 1459-67.

156. Le Bihan D, Turner R, Douek P, Patronas N. Diffusion MR imaging: clinical applications. *Am. J. Roentgenol.*1992; 159(3): 591–599.

157. Michael H. Lev. Diffusion-weighted MR Imaging of Multiple Sclerosis: Added Clinical Value or ‘‘Just Another Pretty Face?’’. *AJNR.* 2000; 21: 805-808.

158. Mueller-Mang C, Mang TG, Kalhs P, Thurnher MM. Imaging characteristics of toxoplasmosis encephalitis after bone marrow transplantation: report of two cases and review of the literature. *Neuroradiology.* 2006; 48(2): 84–89.

159. Tsuchiya K, Katase S, Yoshino A, Hachiya J. Diffusion-weighted MR imaging of encephalitis. *Am. J. Roentgenol.* 1999*;* 173(4): 1097–1099.

160. National Institute for Health and Clinical Excellence (NICE). Stroke. The diagnosis and acute management of stroke and transient ischaemic attacks. CG68, 1–37. London, UK: National Institute for Health and Clinical Excellence, 2008.

161. Gonzàlez RG, Schaefer PW, Buonanno FS, et al. Diffusion-weighted MR Imaging: Diagnostic Accuracy in Patients Imaged within 6 Hours of Stroke Symptom Onset. *Radiology.* 1999;210:155-162.

162. Marks MP, Crespigny A, Lentz D, et al. Acute and Chronic Stroke: Navigated Spin-Echo Diffusion-Weighted MR Imaging. *Radiology*. 1996; 199:403-408.

163. Warach S, Dashe JF and Edelman RR. Clinical Outcome in Ischemic Stroke Predicted by Early Diffusion-Weighted and Perfusion Magnetic Resonance Imaging: A Preliminary Analysis. *Radiology.* 1996;16:53-59.

164. Gass A, Ay H, Szabo K and Koroshetz WJ. Diffusion-Weighted MRI for the "Small Stuff": the Details of Acute Cerebral Ischaemia. *Neurology*. 2004; 3:39-45.

165. Davis D, Ulatowski J, Eleff S, et al. Rapid monitoring of changes in water diffusion coefficients during reversible ischemia in cat and rat brain. *Magn Reson Med*. 1994;31:454 – 460.

166. Pierpaoli C, Alger JR, Righini A, et al. High temporal resolution diffusion MRI of global cerebral ischemia and reperfusion. *J Cereb Blood Flow Metab*. 1996; 16: 892–905.

167. Li F, Han S, Tatlisumak T, et al. A new method to improve in-bore middle cerebral artery occlusion in rats: demonstration with diffusion and perfusion-weighted imaging. *Stroke*. 1998; 29: 1715–1720.

168. Skare S, Newbould RD, Clayton DB, Albers GW, Nagle S, and Bammer R. Clinical multishot DW-EPI through parallel imaging with considerations of susceptibility, motion, and noise. *Magnetic Resonance in Medicine.* 2007; 57:881-890.

169. Wirestam R, Greitz D, Thomsen C, Brokstedt S, Olsson MB and Stahlber F. Theoretical and Experimental Evaulation of Phase-dispersion Effects Caused by Brain Motion in Diffusion and Perfusion MR Imaging. *J Magn Reson Imaging*. 1996; 6:348-355.

170. Skare S and Anderssson JL. On the Effects of Gating in Diffusion Imaging of the Brain using Single Shot EPI. *Magn Reson Imaging.* 2001: 19; 1125-1128.

171. Brokstedt S, Borg M, Geijer B, Wirestam R, Thomsen C, Holtas S and Stahlberg F. Triggering in Quantitative Diffusion Imaging with Single-shot EPI. *Acta Radiol*. 1999; 40: 263-269.

172. Weiskope N, Klose U, Birbaumer N and Mathiak K. Single-shot Compensation of Image Distortions and BOLD Contraset Optimization Using Multi-echo EPI for Real-time fMRI. *Neuroimage*. 2005; 24: 1068-1079.

173. Jezzard P and Balaban RS. Correction for Geometric Distortion in Echo Planar Images from B0 Field Variations. *Magn Reson Med*. 1995; 34: 65-73.

174. Reber PJ, Wong EC, Buxton RB and Frank LR. Correction of Off Resonance Related Distortion in Echo-planar Imaging using EPI-based Field Maps. *Magn Reson Med.* 1998; 39: 328-330.

175. Zeng H, Gatenby JC, Zhao Y and Gore JC. New Approach for Correcting Distortions in Echo Planar Imaging. *Magn Reson Med*. 2004; 52: 1373-1378. 87-90.

176. Reese TG, Heid O, Weisskoff RM and Wedeen VJ. Reduction of Eddy-current-induced Distortion in Diffusion MRI using a Twice-refocused Spin Echo. *Magn Reson Med*. 2003; 49: 177- 182.

177. Burdette JH, Elster AD, and Ricci PE. Acute Cerebral Infarction: Quantification of Spin-Density and T2 Shine-through Phenomena on Diffusion-weighted MR Images. *Radiology*. 1999; 212: 333-339.

178. Ay H, Arsava EM, Johnston SC, et al. Clinical and Imaging Based Prediction of Stroke Risk After TIA: The CIP Model. *Stroke*. 2009;40 : 181-186.

179. Emery DJ, Forster AJ, Shojani KJ, et al. Management of MRI Wait Lists in Canada. *Healthcare Policy*. 2009; 4: 76-86.

180. Kosior RK, Wright CJ, Kosior JC, et al. 3-Tesla versus 1.5-Tesla magnetic resonance diffusion and perfusion imaging in hyperacute ischemic stroke. *Cerebrovasc Dis.* 2007; 24: 361-368.

181. Ract I, JC Ferre, T Ronziere, et al. Improving detection of ischemic lesions at 3 Tesla with optimized diffusion-weighted magnetic resonance imaging. *Journal of Neuroradiology*. 2014; 41- 45-51.

182. Kuhl Ck, Textor J, Gieseke J, et al. Acute and Subacute Ischemic Stroke at High-Field-Strength (3.0-T) Diffusion-weighted MR Imaging: Intraindividual Comparative Study. *Radiology.* 2005; 234: 509-516.

183. Jauch EC, Saver JL, Adams HP et al; American Heart Association Stroke Council; Council on Cardiovascular Nursing; Council on Peripheral Vascular Disease; Council on Clinical Cardiology. Guidelines for the early management of patients with acute ischemic stroke: a guideline for healthcare professionals from the American Heart Association/American Stroke Association. Stroke. 2013; 44: 870–947.

184. Cihangiroglu M, Citci B, Kliickesmez O, et al. The utility of high b-value DWI in evaluation of ischemic stroke at 3 T. *European Journal of Radiology.* 2011: 78; 75–81

185. Benameur K, Bykowski J.L, Luby M, Warach S, Latour L.L. Higher Prevalence of Cortical Lesions Observed in Patients with Acute Stroke Using High Resolution Diffusion-Weighted Imaging. *Am J Neuroradiol.* 2006; 27:1987-1989.

186. Bertrand A, Oppenheim C, Lamy C, et al. Comparison of Optimized and Standard Diffusion Weighted Imaging at 1.5T for the Detection of Acute Lesions in Patients with Transient Ischemic Attack. *Am J Neuroradiol.* 2008;29:363-365.

187. Yamatogi S, Furukawa M, Iida E, et al. Evaluation of small ischemic lesions after carotid artery stenting: the usefulness of thin-slice diffusion-weighted MR imaging. *Neuroradiology*. 2011; 53: 255- 260.

188. Sorimachi T, Ito Y, Morita K, et al. Thin-section Diffusion-Weighted Imaging of the Infratentorium in Patients with Acute Cerebral Ischemia Without Apparent Lesion on Conventional Diffusion-Weighted Imaging. *Neurol Med Chir.* 2008; 48: 108-113.

189. Hotter B, Kufner A, Malzahn U, et al. Validity of Negative High-Resolution Diffusion-Weighted Imaging in Transient Acute Cerebrovascular Events. *Stroke*. 2013; 44: 2598-2600.

190. Entwisle T, Perchyonok Y and Fitt G. Thin section magnetic resonance diffusion-weighted imaging in the detection of acute infratentorial stroke. J Med Imaging and Radiat Oncol. doi: 10.1111/1754-9485.12490.

191. Albach F, Brunecker P, Usnich T, et al. Complete Early Reversal of Diffusion-Weighted Imaging Hyperintensities After Ischemic Stroke Is Mainly Limited to Small Embolic Lesions. Stroke; 2013: 44:1043-1048.

192. Choi BS, Kim JH, Jung C and Kim SY. High-Resolution Diffusion-Weighted Imaging Increases Lesion Detectability in Patients with Transient Global Amnesia. *AJNR*. 2012. 1771-1774.

193. Oppenheim C, Lamy C, Touze E, et al. Do transient ischemic attacks with diffusion weighted imaging abnormalities correspond to brain infarctions? *American Journal of Neuroradiology* 2006; 27: 1782– 1787.

194. Villringer K, Grittner U, Schaafs LA, et al. (2014) IV t-PA Influences Infarct Volume in Minor Stroke: A Pilot Study. *PLoS ONE* 9(10): e110477. doi:10.1371/journal.pone.0110477.

195. Zaidi SF, Aghaebrahim A, Urra X, et al. Final Infarct Volume Is a Stronger Predictor of Outcome Than Recanalization in Patients With Proximal Middle Cerebral Artery Occlusion Treated With Endovascular Therapy. *Stroke.* 2012;43:3238-3244.

196. Thijs VN, Lansberg MG, Beaulieu C, Marks MP, Moseley ME and Albers GW. Is early ischemic lesion volume on diffusion-weighted imaging an independent predictor of stroke outcome? A multivariable analysis. *Stroke*. 2000;11:2597-602.

197. Oppenheim C, Grandin C, Samson Y, et al. Is there an apparent diffusion coefficient threshold in predicting tissue viability in hyperacute stroke? *Stroke*. 2001; 32: 2486–2491.

198. Loh PS, Butcher K, Parsons M, et al. Apparent Diffusion Coefficient Thresholds Do Not Predict the Response to Acute Stroke Thrombolysis. *Stroke.* 2005;36:2626-2631.

199. Brazzelli M, Chappell FM, Miranada H, et al. Diffusion-Weighted Imaging and Diagnosis of Transient Ischemic Attack. *Ann Neurol.* 2014;75:67-76.

200. Coull AJ, Lovett JK, Rothwell PM. Population based study of early risk of stroke after transient ischaemic attack or minor stroke: implications for public education and organization of services**.** *BMJ.* 2004; 328: 326.

201. Eliasziw M, Kennedy J, Hill MD, et al. North Am Symptomatic Carotid Endarterectomy Trial Group. Early risk of stroke after a transient ischemic attack in patients with internal carotid artery disease. *CMAJ.* 2004;170: 1105–1109.

202. Hill MD, Yiannakoulias N, Jeerakathil T, et al. The high risk of stroke immediately after transient ischemic attack: a population-based study. *Neurology.* 2004;62:2015–2020.

203. Friedman GD, Wilson WS, Mosier JM, Colandrea MA, Nichaman MZ. Transient ischemic attacks in a community. *JAMA*. 1969;210:1428–1434.

204. Johnston SC, Gress DR, Browner WS, et al. Short-term prognosis after emergency department diagnosis of TIA. *JAMA.* 2000;284: 2901–2906.

205. Bang Oy, Lee Ph, Heo KG, et al. Specific DWI lesion patterns predict prognosis after acute ischaemic stroke within the MCA territory. *J Neurol Neurosurg Psychiatry.* 2005;76:1222-1228.

206. Kang DW, Chu K, Ko KB, et al. Lesion patterns and mechanism of ischemia in internal carotid artery disease. *Arch Neurol.* 2002;59:1577-1582.

207. Lansberg M, Thijs V, Bammer R, et al. Risk Factors of Symptomatic Intracerebral Hemorrhage After tPA Therapy for Acute Stroke. *Stroke*. 2007: 38(8): 2275–2278.

208. Yoo AJ, Verduzco LA, Schaefer PW, et al. MRI-based selection for intra-arterial stroke therapy: value of pretreatment diffusion-weighted imaging lesion volume in selecting patients with acute stroke who will benefit from early recanalization. *Stroke* 2009;40:2046-2054.

209. Parsons MW, Christensen S, Levi CR, et al. Pretreatment diffusion- and perfusion-MR lesion volumes have a crucial influence on clinical response to stroke thrombolysis. *J Cereb Blood Flow Metab.* 2010;30:1214-1225.

210. Kate M, Riaz P, Gioia L, et al. Dynamic Evolution of Diffusion-Weighted Imaging Lesions in Patients With Minor Ischemic Stroke. *Stroke*. 2015; 46: 2318-2321.

211. Thomas R, Lymer G, Armitage P, et al. Apparent Diffusion Coefficient Thresholds and Diffusion Lesion Volume in Acute Stroke. *Journal of Stroke and Cerebrovascular Diseases.* 2013; 22: 906-909.

212. Latchaw RE, Alberts MJ, Lev MH, et al. Recommendations for imaging acute ischemic stroke. A scientific statement from the American heart association. *Stroke*. 2007; 40: 3646-3678.

213. Birenbaum D, Bancroft L, Felsberg G. Imaging in Acute Stroke. *West J Emerg Med* 2011; 12: 67-76.

214. Mlynash M, Olivot J.M, Tong D.C, et al. Yield of Combined Perfusion and Diffusion MR Imaging in Hemispheric TIA. *Neurology.* 2009;72:1127-1133.

215. Hacke W, Albers G, Al-Rawi Y, et al. The desmoteplase in acute ischemic stroke trial (DIAS): A phase II MRI-based 9-hour window acute stroke thrombolysis trial with intravenous desmoteplase. *Stroke*. 2005;36:66–73. [PubMed: 15569863].

216. Asdaghi N, Campbell B.C.V, Butcher K, et al. DWI reversal is associated with small infarct volume in patients with TIA and minor stroke. *AJNR Am J Neuroradiol*. 2014; 35:660–66.

217. Albers G, Thijs V, Wechsler L, et al. Magnetic resonance imaging profiles predict clinical response to early reperfusion: the diffusion and perfusion imaging evaluation for understanding stroke evolution (DEFUSE) study. *Annals of Neurology.* 2006;60:508-517.

218. Qiao X.J, Salamon N, Wang D.J.J, et al. Perfusion Deficits Detected by Arterial Spin-Labeling in Patients with TIA with Negative Diffusion and Vascular Imaging. *Am J Neuroradiol.* 2013;34:2125-2130.

219. Sylaja PN, Coutts SB, A Krol,, et al. When to expect negative diffusion-weighted images in stroke and transient ischemic attack. *Stroke*. 2008; 39; 1898-1900.